" I hereby declare that I have read through the report entitle Development and Vibration Analysis of Go-Kart System and found that it has comply the partial fulfillment for a warding the degree of Bachelor of Mechatronics Engineering "

Signature : ....

Supervisor's Name : ....

Date : ....

DEVELOPMENT AND VIBRATION ANALYSIS OF GO-KART SYSTEM

LIM SEONG CHUAN

A Report Is Submitted In Partial Fulfillment Of The Requirements For The Degree Of Bachelor Of Mechatronics Engineering

Faculty of Electrical Engineering
UNIVERSITI TEKNIKAL MALAYSIA MELAKA

2014

I declare that this report entitle Development and Vibration Analysis of Go-Kart System is the result of my own research except as cited in the reference. This report has not been accepted for any degree and is not concurrently submitted in candidature of any other degree.

Signature : ....

Name : ....

Date : ....

To my beloved mother and father

ACKNOWLEDGEMENT

In preparing this report, I would like to gratefully and sincerely thank my supervisor, Mr. Zamzuri Bin Ab. Rashid for his guidance during my final year project. His supervision and advices provide a well encouragement motivation for me in completing my final year project. His suggestion and critics are also well appreciated. Without his guidance and support, the project would not have been same as presented here.

Besides that, I would like to express my gratitude towards my faculty which is Faculty of Electrical Engineering of Universiti Teknikal Malaysia Melaka for providing funding to the project as well as providing place and equipments in completing the project. I would like to thank all the lecturers and technicians for their valuable suggestions and opinions in helping to complete the project.

Furthermore, my fellow friends in Universiti Teknikal Malaysia Melaka especially the member in the same team in developing Go-Kart system for providing support and useful information at various occasions in completing my final year project. Their helps and assistance in developing the project is highly appreciated.

Lastly, I would like to thank both my parents in supporting me all the time during my study in university level as well as providing continuous support and motivation during the completion of my project.

ABSTRACT

This project highlights the development and vibration analysis of a go-kart chassis. A chassis is developed and proved to have a strong structure and minimized vibration which fulfilled the requirements from Formula UniMAP 2013 and Shell Eco-Marathon competitions. First, this project is concentrating on determining the static stress and strain concentrated on the chassis structure as well as determining the resultant displacement of the chassis frame with applied load exerted on the chassis. This is vital because the chassis acts as the main frame of the vehicle that subjected to stress, strain and vibration during the vehicle moved. Second, this project is also focussing on the obtaining the vibration experienced by the chassis body. In this report, the results obtained from the static test conducted on the basic chassis frame structure designed by using Solidworks software are presented as well as the fabricated basic chassis frame structure. The three dimensional modelling chassis frame structure is designed using Solidworks software and the static test is conducted in the simulation environment of the Solidworks software as well. The fabrication of the basic chassis frame structure is fabricated using the selected material which is the 25mm x 25mm square mild steel tube with the thickness of 1.6mm and the method of welding is used in developing the chassis. The developed chassis frame structure is able to withstand the applied load with a satisfactory factor of safety (FOS). Furthermore, the vibration testing of the chassis is done using Inertial Measurement Unit (IMU). The vibration on the chassis is determined from experiment during free gear and first gear. The results obtained through the vibration test are sent to MATLAB software for graph plotting and is analyzed.

ABSTRAK

Projek ini menyerlahkan penghasilan dan analisis getaran terhadap casis go-kart. Casis ini dihasilkan dan dibuktikan bahawa mempunyai struktur yang kuat dan dapat mengurangkan getaran serta memenuhi spesifikasi daripada pertandingan Formula UniMAP 2013 dan Shell Eco-Marathon. Pertama, projek ini menumpukan perhatian terhadap menentukan tekanan statik yang tertumpu pada struktur casis tersebut serta anjakan yang berlaku terhadap casis apabila muatan diaplikasikan ke atas casis tersebut. Ini adalah sangat penting disebabkan casis merupakan frame yang penting dalam kenderaan yang dikenakan tekanan dan getaran semase kenderaan itu bergerak. Kedua, projek ini menumpukan perhatian untuk mendapatkan getaran yang dialami oleh casis. Dalam repot ini, keputusan daripada ujian statik yang dijalankan ke atas frame casis yang dicipta melalui perisian Solidworks dan fabrikasi frame casis tersebut akan dibentangkan. Model tiga dimensi casis tersebut akan dicipta menggunakan perisian Solidworks dan ujian statik terhadap casis itu juga akan dijalankan menggunakan perisian Solidworks. Fabrikasi frame casis itu menggunakan bahan-bahan yang dipilih iaitu tiub persegi keluli yang mempunyai dimensi 25mm x25mm serta mempunyai ketebalan 1.6mm dengan menggunakan kaedah kimpalan. Casis yang dihasilkan itu dapat menahan muatan yang diaplikasikan ke atas casis itu dengan magnitud faktor keselamatan yang memuaskan. Seterusnya, ujian getaran terhadap casis yang dihasilkan itu akan dijalankan menggunakan Inertial Measurement Unit (IMU). Ujian itu akan dijalankan semasa engin berada pada gear free dan gear pertama. Dapatan daripada ujian tersebut akan dihantar ke perisian MATLAB untuk mendapatkan graf getaran dan analisa mengenai getaran dijalankan.

TABLE OF CONTENTS

LIST OF TABLES

LIST OF FIGURES

LIST OF APPENDICES

CHAPTER 1

INTRODUCTION

1.1 Introduction

Chassis acts as the main frame of the body structure of the vehicle. It is one of the most important part to be considered when designing a vehicle. Chassis is defined as the lower part of a vehicle which includes the wheels, frame, driveline, engine and suspensions. There are 3 types of chassis structure which is the ladder chassis frame, space frame chassis and monocoque chassis.

Elements that always been considered during the design of the chassis structure is such as the strength and the stiffness of the chassis. Chassis built for vehicle has to be strong because it tends to be subjected to static stress, strain and also vibration due to various dynamic excitation. Static analysis of the chassis structure is important in determining the safety of the chassis structure. Besides that, vibration on the chassis could affect the comfort during ride, the stability of the whole vehicle as well as the safety of the vehicle. Besides that, vibration can also caused high stress concentration at certain part of the structure, fatigue on the structure and loose in the joints of the structure. Therefore, the vibration analysis is vital to be done on the chassis, ensuring the safety and the stability of the vehicle.

This project is about developing a go-kart chassis according to specifications as well as performing static analysis and vibration analysis on the chassis developed. The dimension of the chassis is according the specifications of two racing competition which is the Formula UniMAP 2013 and the Shell Eco Marathon. The design of the chassis will utilize the space frame chassis type and the material chosen is 25mm x 25mm square mild steel tube with the thickness of 1.6mm and also 2.0mm thickness mild steel plate. The square mild steel tube and plate are cut into desired dimensions and welded using 2.5mm thickness welding rod to form the space frame chassis. The fasteners used in connecting other parts such as bearing and absorber are M10 mild steel bolts and nuts with washers.

Before the process of developing the chassis been started, a three dimensional modeling of the chassis is drawn using Solidworks software in order to perform finite element analysis on the designed chassis structure. Materials used in constructing the whole chassis structure is also been identified and assigned in the software to increase the accuracy of the result. Static analysis is done on the modeling of the chassis using the simulation functions in Solidworks software to determine the distribution of static stress on the structure and the displacement of the structure after the load force is added into the simulation. The safety factor for the chassis can also be calculated after the analysis.

After the fabrication of the chassis is completed, the vibration test will be done physically using 5 degrees of freedom Inertia Measurement Unit (IMU) sensor and aided with programming codes. The accelerometers in the IMU sensor are the main components that been used to detect the vibration along the three axes which are x-axis, y-axis and z-axis. The aided programming code is uploaded to an Arduino Uno board in order to extract the data obtained from the accelerometer of the IMU sensor. The data obtained from the vibration test is analyzed and graph is plotted in MATLAB software in order to illustrated the vibration of the chassis structure at different point on the chassis.

1.2 Problem Statement

The project concentrates on the static stress and strain distribution on the chassis structure when the vehicle is in static condition and the vibration experienced by the developed chassis structure when the vehicle is in static and mobile. Firstly, the project concerns in developing a chassis structure that has minimum vibration where the vibration of the racing car could cause decreases in efficiency of the racing car. Due to the road condition and many others external factors, chassis of a go-kart need to withstand vibration of the components of the racing car such as engine. Due to several constraints, the project will focus on obtaining and analyzing the vibration experienced by the chassis structure.

Secondly, the project focuses on how to perform vibration test on the chassis designed using IMU sensor with aided programming code uploaded to Arduino Uno board to determine the vibration because vibration is hard to measure using hand held equipment such as vibration meter due to human error. With the aided of the IMU sensor, data can be obtained easily as well as be able to transfer the data into computer, The data obtained can also be analyzed and recorded easily. Furthermore, human errors can be eliminated and the accuracy of the data obtained can be increased.

Thirdly, determining the static stress and strain concentrated at certain point on the chassis structure and determining the displacement of the structure of the chassis could increase the performance of the go-kart and increase the safety of the driver of that particular vehicle. In the end of the project, the chassis designed will be a chassis structure that able to withstand the load with a satisfactory safety factor.

1.3 Objective

The objectives of this final year project are stated as follows:

1. To develop a chassis structure according to specifications.
2. To identify and analyze the static stress, strain and vibration on the chassis designed.

1.4 Scope

The scope of the project are stated as follows:

1. Design the chassis of a go-kart using Solidworks software that suitable for competitions.
2. Develop the chassis design using suitable materials that fulfill the requirements in the competitions.
3. Undergone stimulation using Solidworks software to perform static test on the chassis design.
4. Perform vibration test using IMU sensor and Arduino programming code on the chassis design physically.

1.5 Report Outline

The main body of the project is arranged according to consecutive chapters. The report consists of 5 chapters such as:

i. Chapter 1: Introduction

The first chapter identifies the problem statement of the project, defines the objectives of the project and limits the scope for the project.

ii. Chapter 2: Literature Review

This chapter discusses about the studies done by other researchers that related to the project. The background of the theory and method used in conducting experiments are included in this chapter.

iii. Chapter 3: Methodology

This chapter describes all the techniques used in performing experiments. The flowcharts and block diagrams of the project is also included in this chapter to illustrate the methodology of the project.

iv. Chapter 4: Result And Discussion

This chapter explains about the outcomes of the project. Visual representation such as figure, table, graph and chart are shown in this chapter. The interpretation of the data obtained during experiments is also included. Furthermore, the analysis and discussion regarding the outcome of the project are also provided in this chapter.

v. Conclusion And Recommendation

This chapter explained about the summary of the entire project includes the method in conducting experiments used, the results obtained from the experiments and the conclusion of the entire project. Recommendations for future works is also included in the chapter

CHAPTER 2

LITERATURE REVIEW

2.1 Introduction

The previous chapter explained about the introduction of the project and stated the problem statement of the project. Besides that, the objectives and scope of the project are also defined in order to set the project at the correct path. In this chapter, the literature and past studies related to the chassis design and analysis is studied and the knowledge related to the chassis design is summarized.

2.2 Chassis design

Chassis of the vehicles is the frame work that are used to support the body and all the parts of a vehicle. Chassis played a vital role in vehicles for example cars, trucks, SUV, sports car and also racing car. The design of the chassis of the vehicle has different kind of structure. For instance, the honeycomb sandwich panel monocoque chassis, the ladder chassis frame and the tube space frame structure. In this project. A chassis structure chosen is the tube space frame structure and it is needed to be produced to have a stable and strong structure.

There are researchers in [1] stated that the design of the chassis is combining the factors of performance and safety. Performance which is the torsion stiffness of the chassis that directly affects the cornering behavior of the vehicle. Safety of the chassis design is also determined by the absorbing capabilities of the structure. In manufacturing the low cost vehicle chassis using the low-carbon steel tubes, steel tubes are cut and welded to form the structure of the chassis. This method of fabrication is stated as the technologies used in the late fifties and the early sixties. Apart from that, the usage of aluminium in vehicle design could reduce the weight of the vehicle while maintaining the performance and safety of the vehicle. Hirsch [2] pointed out the full usage of aluminium on the car body could reduce the weight of the body approximately 30-40%. Aluminium solutions were already established in AUDI A8 cars by having aluminium chassis, power train, bumpers and car body.

Based on [3], the important variables in vehicle engineering includes the vehicle centre of gravity, body (sprung-mass) centre of gravity and also axle (unsprung mass) centre of gravity. The distance of vehicle centre of gravity and the distance of body centre of gravity from the front or rear axle as well as the height above the ground are crucial for:

i. Braking and acceleration capability
ii. Determining climbing ability
iii. Designing brake system
iv. Designing body centre of gravity and aspects of vibration stability
v. Driving stability
vi. Determining mass moment of inertia

They also stated that low centre of gravity could also contributed in fewer driving dynamic problems and increased the performance of the vehicle [3, pp. 386-388].

Moreover, the torsional stiffness of a vehicle is an important element in producing a safe vehicle. When the vehicle is in motion and steering force is exerted on the chassis, the chassis will experience twist stress. Therefore, the studies on vehicle torsional stiffness has to be done to ensure the vehicle handling performance. In [4], it is stated that chassis of a vehicle has 2 roll degree of freedoms, roll angle and roll angular velocity of sprung mass centre. The torsional stiffness of the vehicle could affect the roll angle of the vehicle after a analysis on the chassis to determine the influence of torsional stiffness on the roll angle at the suspension of the vehicle.

Based on the reviewed researches, there are few characteristics of a chassis of a vehicle need which is the strong structure, using light but strong material, could withstand several types of stress and vibration. Besides it also able to withstand a range of applied load and the importance of torsional stiffness on chassis design. Therefore, this project will mainly focus on these few criteria and develop a race car chassis.

2.3 Dynamic analysis

For every chassis designed, several tests will be done on the chassis in order to justify the functionality of the chassis. For example, dynamic analysis is the one of the common test done on the chassis design. Nowadays, there is simulation function in the CAD software that enables the users to test their chassis design using the software after the modeling process. In this project, the chassis designed need to be analyzed dynamically to determine the stability of the structure using simulation function in CAD software.

Next, in [5], the authors stated that when a vehicle travels along the road, the chassis of the vehicle is excited by the dynamic force caused by external issue such as the road condition and also internal issue such as engine and transmission. Based on the analysis done by [5], the result is based on the first 30 frequency modes. The chassis maximum displacement in x, y and z direction is determined as well as the natural frequencies from the modal analysis. There are groups of researchers performed analysis on their designed chassis using Modal Analysis in ANSYS software after modeling of the 3 dimensional chassis design is completed [5, 6, 7]. The dynamic analysis is done to determine whether the natural frequency of the chassis is in the suitable range.

Furthermore, [6] performed vibration analysis on a vehicle frame and stated that the natural frequency of the structure coincides with the frequency from forced vibration can caused resonance which could leads to failure to the structure. Besides that, the analysis done by [7] is to determine the frequency in different mode. During the analysis, a few assumptions had to be made such as damping is ignored and any applied load is ignored. In the result, the natural frequency in each mode is determined. From an analysis done in China, the experimental modal was the chassis of a Land-wind X6. During the analysis, the system is supported by 2 plat tires, a 16-channel data acquisition system, a data analysis system, 16 accelerometer that act as sensors and a input hammer. 48 different points at the chassis are determined as the test points of the analysis and the points are selected mostly at the front or rear of the chassis. The analysis successfully outcome the frequency response of the chassis [8].

From all the literature reviewed, vibration in the vehicle contributes losses to the performance of the vehicle. Vibration of the chassis of the vehicle can be reduced by installing suitable suspension to the chassis structure which could absorb the shock from external factor such as bumpy road. In this project, dynamic analysis on the chassis will be done is the vibration analysis software. Before the analysis is done, the modeling of the 3 dimensional chassis design will be prepared in Solidworks software. Furthermore, finite element analysis (FEA) will be conducted to find the stable chassis structure and the vibration analysis will be done physically using sensors and the data obtained will be transferred to computer to be further analyzed and compared.

2.4 Static analysis

Static analysis is an analysis on chassis which determine the static stress and strain that acts on the structure and determine the forces distribution all over the structure of the chassis. Besides that, it is also includes the determination of static displacement of the structure after load is added to the structure. Static analysis can be done using CAD software where for Solidworks software, static test could aid us in finding the Von Mises Stress, strain and maximum displacement of the structure when load is applied to the structure. This also could help us in determining the safety factor on the chassis structure designed.

A group of researchers performed static test on the chassis created by using the ALGOR Fempro software to determine the Stress Von Misses of the chassis. Simulation in the software showed the distribution of the stress clearly on the three dimensional modeling of the chassis structure when forces or load was added to the model [9]. Not only that, the bending of the structure can be easily seen in the software. Besides that, simulation is also can be done using ANSYS software after obtaining the 3 dimensional modeling of the chassis. Based on the structural analysis using ANSYS performed by [10] found that the loading and boundary condition of were set before element and nodes is determined and set. A finer meshing was applied in order to obtain a more accurate result especially at the region having the highest stress.

Furthermore, [11] designed and manufactured an aluminium honeycomb sandwich panels and performed finite element analysis (FEA) to gain more understanding on the structure designed. For the chassis designed, the maximum von Mises stress was obtained and yield load of the structure was calculated. These researchers also compared the yield load can be sustained by both monocoque design and space frame design. Furthermore, chassis frame of race car is produced in UTeM for Formula Varsity 2012 competition. The designed chassis was tested using CATIA V5 R20 software to determine the Von Mises Stress at the structure developed with applied load of 6000N which is 3 times the maximum weight of the chassis structure only. Based on the value obtained, the safety factor is calculated at the location where the simulation showed red spot on the stress contour [12].

In static analysis, stress or Von Mises Stress experienced by the structure is one of the most vital aspect in determining the strength of the structure of a chassis. Besides that, the displacement of the structure from the original structure can be illustrated using the simulation from the CAD software. Lastly, the factor of safety (FOS) of the chassis design can also be determined and modification can be done on the chassis to improve the design of the chassis in order to increase the performance and the safety of the vehicle. In this project, the static test will determine the Von Mises Stress acting on the chassis structure, the displacement of the structure after load is applied and also the factor of safety (FOS) of the chassis. The static test will be performed using the Solidworks software and the result obtained will be analyzed. Lastly, the chassis design will be developed using the materials selected.

2.5 Formula UniMAP 2013

The chassis design is developed to fulfill the requirements from the competition Formula UniMAP 2013 in Universiti Malaysia Perlis (UniMAP). The following Table 2.1 is the chassis requirements extracted from the technical requirements provided [13].

Table 2.1: Specification Of Chassis From Formula Unimap 2013

Specification	Description
Number of seat	1
Material	Titanium or carbon fibre are strictly prohibited from the car design. The use of fire-resistant composite based on fiberglass are allowed
Overall height	Maximum of 900mm from the ground
Overall width	Maximum 1500mm with steered wheels in straight position

Wheelbase	Minimum of 1600mm
Ground clearance	Minimum of 50mm with driver on board seated normally
Overall body width	Should not exceed the overall width of the car
Minimum weight	140kg without fuel
Cockpit opening	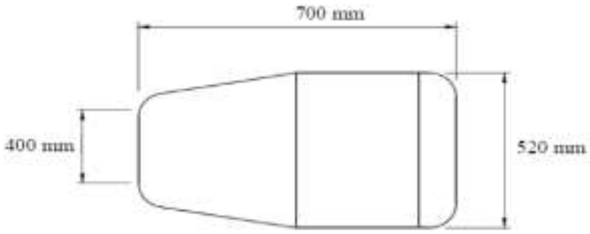
Wheel dimension	Diameter: 300mm-325mm Width: minimum of 100mm and maximum of 163mm

2.6 Shell Eco-Marathon

The chassis designed is based on the requirements from the Shell Eco-Marathon official rules 2013 for prototype group. The requirements for the vehicles designed is extracted and tabulated in the Table 2.2 below [14].

Table 2.2: Specification Of Chassis From Shell Eco-Marathon

Specification	**Description**
Number of seat	1
Material	Titanium or carbon fibre are strictly prohibited from the car design. The use of fire-resistant composite based on fiberglass are allowed
Overall height	Maximum of 1000mm and less than 1.25 times the maximum track width between two outermost wheels
Track width	Minimum of 500mm measured between midpoints where the tires touched the ground
Overall width	Maximum 1300mm
Wheelbase	Minimum of 1000mm
Overall length	Maximum of 3500mm
Maximum weight	140kg without driver

2.7 Inertia Measurement Unit (IMU)

The sensor used in this project in order to obtain the vibration of the chassis structure developed is 5 degrees of freedom Inertia Measurement Unit (IMU). The IMU consists of ADXL335 accelerometer ICs that measure movement in 3 axes which are x-axis, y-axis and z-axis [15]. The accelerometer is used to obtain the vibration experienced by the chassis into data that can be interpreted using computers. The 5DOF IMU used is as shown in the Figure 2.1 below.

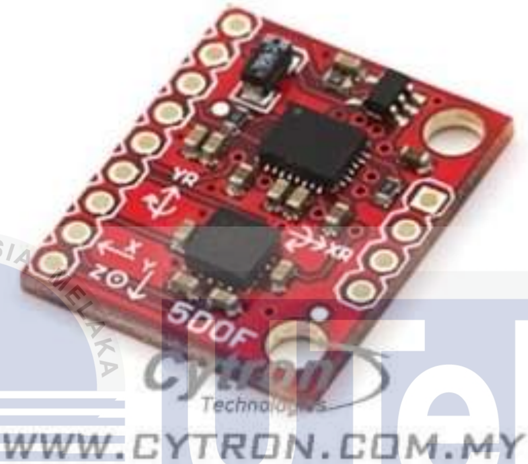

Figure 2.1: 5 Degrees Of Freedom IMU

2.8 Butterworth Low Pass Filter In MATLAB Software

Filter is used during signal processing to remove the unwanted noise frequencies from the signal obtained from sensor. However, MATLAB filter also can be applied to the data obtained that analyzed in MATLAB software in order to act as a smoothing device onto the data obtained. The purpose of using MATLAB filter is to remove the noise frequencies in the data obtained that could be affecting the accuracy of the data.

Butterworth filter is one of the available filters in MATLAB software. There are low pass, high pass, bandpass and also band stop filter available in Butterworth filter in MATLAB software [16]. Based on [17], the analog low pass filter is useful in preventing high frequency noise from affecting the signal. This can be ensured that the plotted graph from the obtained data can be clearly seen and can be analyzed easily.

Therefore in data analyzing process after the vibration test done on the chassis structure, the data is processed using MATLAB software with the aid of the Butterworth low pass filter as the smoothing agent. The use of this MATLAB filter could help to smooth the plotted graph from the data obtained and can be analyzed easily.

2.9 Summary

The literature reviews studied related to material used in developing a chassis and method in performing vibration test can be summarized into table 2.3 and 2.4 below.

Table 2.3: Material Used In Developing Chassis

	[1]	[2]
Material used	Low Carbon Steel	Aluminium
Weight	Light	Lighter than Low Carbon Steel
Strength	Hard	Hard
Price	Cheap	Moderate
Ease of Welding	Easy	Hard

Table 2.4: Method In Performing Dynamic Analysis

	[5,6,7]	[8]
Method used	ANSYS CAD software	Used sensors to perform experiment
Sensors used	None	Accelerometers
Result accuracy	High (errors can be minimized or ignored)	Moderate (many errors could happened during experiment)
Price	Cheap	Moderate
Testing Points	None	Random or fixed points around the chassis surface
Ease of performing experiment	Easy	Hard

In this chapter, the studies about the chassis design, material used to construct a chassis and a few tests that conducted on the chassis are studied. The literatures studied included the static test conducted and the vibration test conducted on the previous studies. The same tests is going to test on the developed chassis. Besides that, the requirements that Formula UniMAP and Shell Eco-Marathon competition are studied and summarized.

CHAPTER 3

METHODOLOGY

3.1 Introduction

In the previous chapter discussed about the literature reviewed from previous studies and experiments done by researchers related to the project. This chapter is explained about the methodology of conducting the experiments throughout the project. The flow charts of the processes in the project is also illustrated by using flow charts and block diagrams.

3.2 Project Flow Chart

The flow chart of the whole project is as follows:

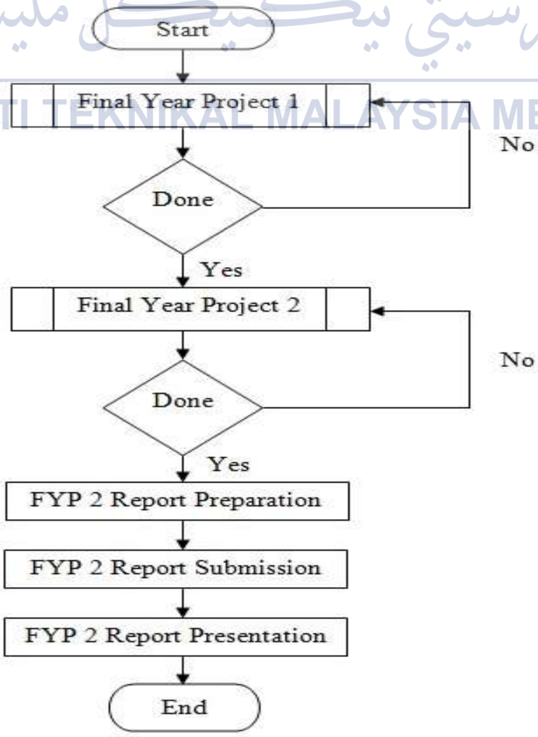

Figure 3.1: Flow Chart Of Whole Project

3.2.1 Final Year Project 1 Flow Chart

The flow chart of the final year project 1 is as follows:

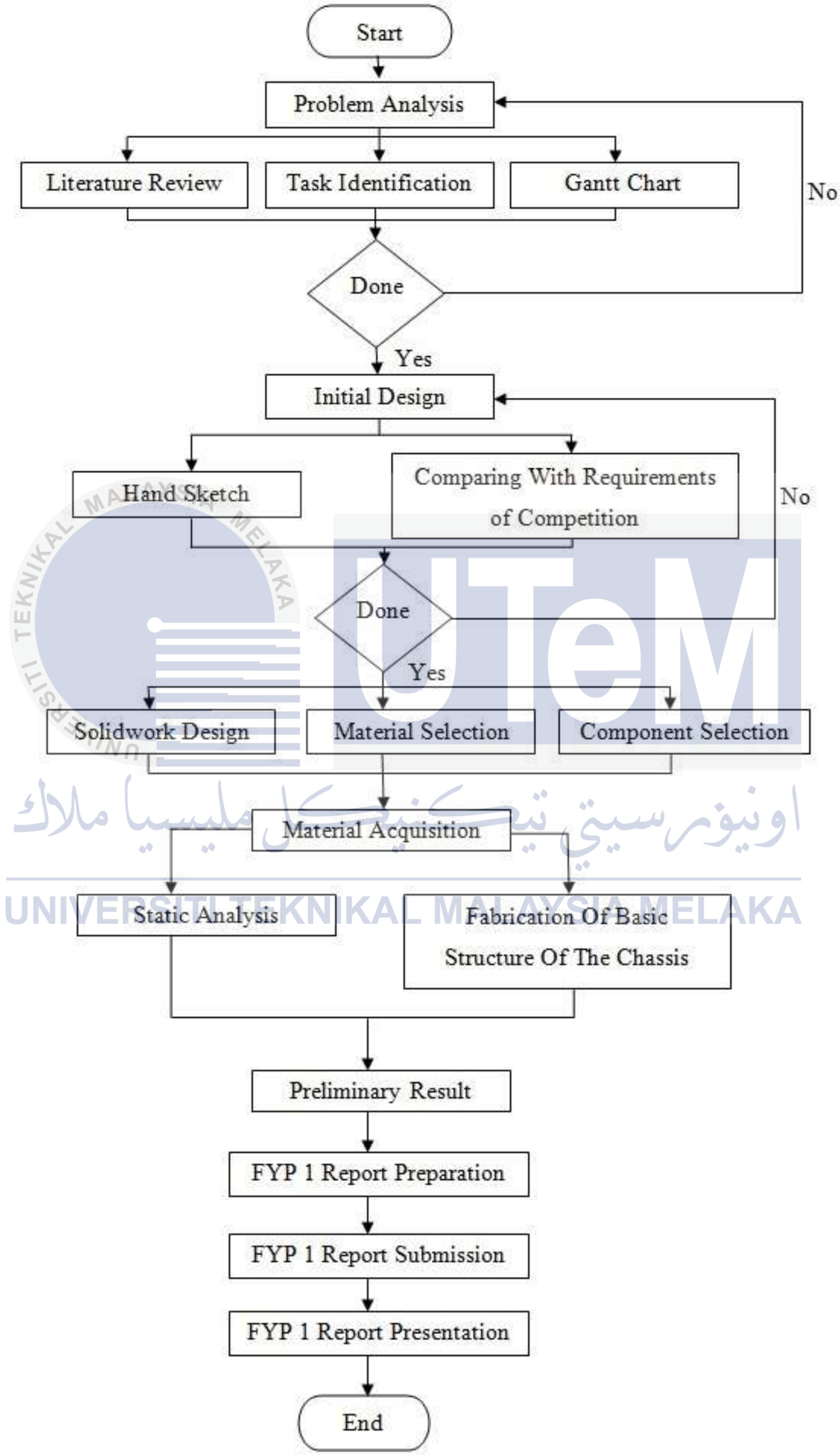

Figure 3.2: Flow Chart Of Final Year Project 1

3.2.2 Final Year Project 2 Flow Chart

The flow chart of the final year project 2 is as follows:

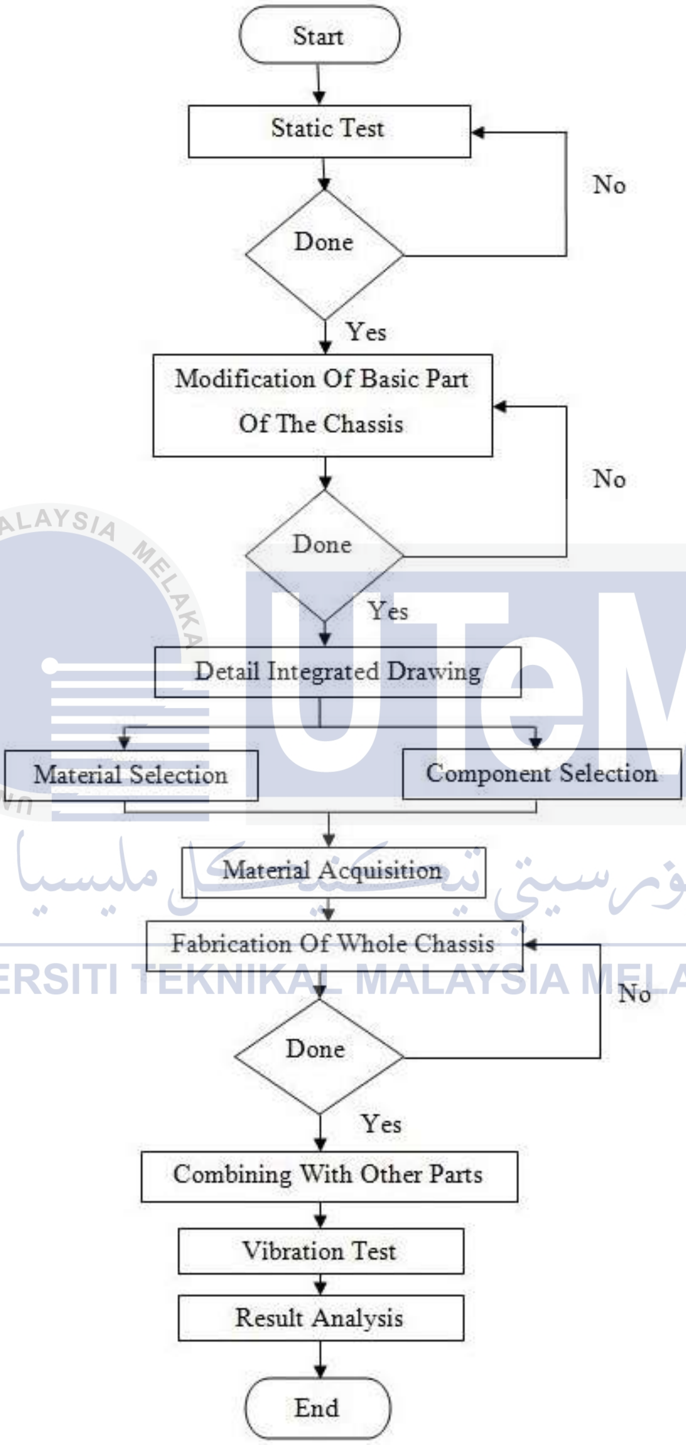

Figure 3.3: Flow Chart Of Final Year Project 2

The flow chart of the whole project is shown in Figure 3.1. From the beginning of the project, there is the start of the final year project 1 where the flow chart of final year project 1 is shown in Figure 3.2. After the completion of final year project, there is the start of the final year project 2 where the flow chart of the final year project 2 is shown in the Figure 3.3. The final year project 2 is started only when the final year project 1 is completed. After the completion of final year project 2, there is the start for the final year project 2 report preparation. During this stage, the report consists of 5 chapters is produced and all the result obtained from the experiments conducted during final year project 1 and final year project 2 are written in the report. Then, the report will be submitted to the panel of final year project of Universiti Teknikal Malaysia Melaka for evaluation. After the submission of the final year project report, a presentation is conducted to present the outcomes from both final year project 1 and final year project 2.

The flow chart of final year project 1 is shown in Figure 3.2. From the beginning of the final year project 1, the final year project title is registered and the problem of the title is analyzed. The process followed by reviewing literatures, identifying the task to be completed in order to complete the project and preparing Gantt chart to estimate the duration for the project. After the tasks in the previous stage is completed, the initial design of the chassis structure is prepared. The design of the chassis is performed using sketches and the sketches is done based on the requirements of both Formula UniMAP 2013 competition and the Shell Eco-Marathon competition. Then, the process continued by preparing three dimensional drawing using Solidworks software as well as selecting materials and components needed in developing the chassis structure. After all the materials is acquainted, the static analysis on the structure drawn in Solidworks software is simulated using the simulation function in the Solidworks software. At the same time, the fabrication of the basic structure of the chassis is started. The basic structure of the chassis includes the frame of the chassis and the cockpit of the go-kart. From the static test performed on the structure and fabrication, preliminary results is obtained. After the preliminary results is obtained, the preparation of final year project 1 report is started and followed by the report submission. Lastly, the final year project process ended after the final year project 1 presentation is conducted.

The flow chart of the final year project 2 is shown in Figure 3.3. From the beginning of the final year project 2, the static test is performed to ensure the safety to continue fabrication. Once the simulation of the static test shown acceptable factor of safety, the modification of the basic part of the chassis is started. The structure of the chassis is developed based design from the previous stage. Once the modification of the basic part is completed, the detail drawing of the chassis is prepared as well as the materials and components in completing the complete chassis is determined. The detail drawing of the chassis includes the engine part, suspensions, driveline and the wheels of the go-kart. After the materials needed is acquainted, the fabrication of the whole chassis is started. Then, when the whole chassis is fabricated, the chassis is combined with other parts of the go-kart such as the front wing and the rear wing of the body as well as the installation of the Electrical Power Steering system (EPS). After the combination with other parts is done, the vibration test is conducted on the Go-Kart using sensors and aided with programming codes. Results that obtained from the vibration test is analyzed and the final year project 2 is ended.

3.3 Vibration Test Block Diagram

The vibration test on the chassis designed is done using IMU sensor and Arduino programming codes. The block diagram of the vibration test is as follows:

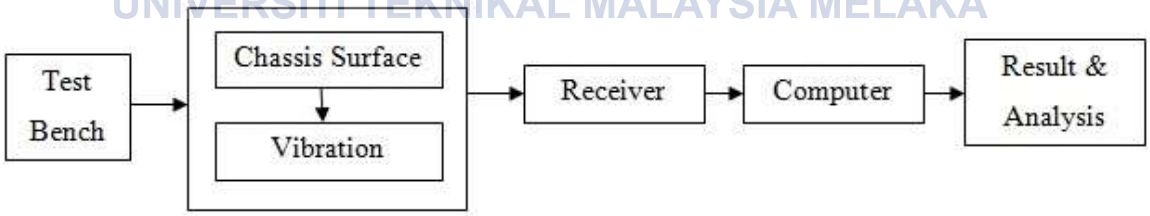

Figure 3.4: Block Diagram Of Vibration Test

The vibration analysis conducted on the structure designed is shown in Figure 3.4. The test bench is the go-kart developed and the second block is sensing setup for the vibration analysis. The test points is set up on the chassis surface while the testing parameter of the test is vibration. During the test, the vibration of the go-kart is detected by IMU sensor which act as the receiver. The data obtained from the receiver is transferred to the personal computer. The result is then recorded and transferred to MATLAB software for graph plotting then analyzed. Based on [8], the vibration analysis is performed on the chassis structure in order to obtain the frequency of the vibration on the chassis structure. The vibration test is done on different points located throughout the whole surface of the chassis designed. This method is similar to the analysis done by [6,7,8]. The points selected on the chassis are located at the front part, middle part and the rear part of the chassis. There are 4 points for each part of the chassis to be tested using IMU sensor. The vibration test on the chassis structure designed can be illustrated in the figure 3.5 below. In figure 3.5, the test points are clearly shown and the points are chosen throughout the chassis in order to determine the parts of the chassis having the largest vibration.

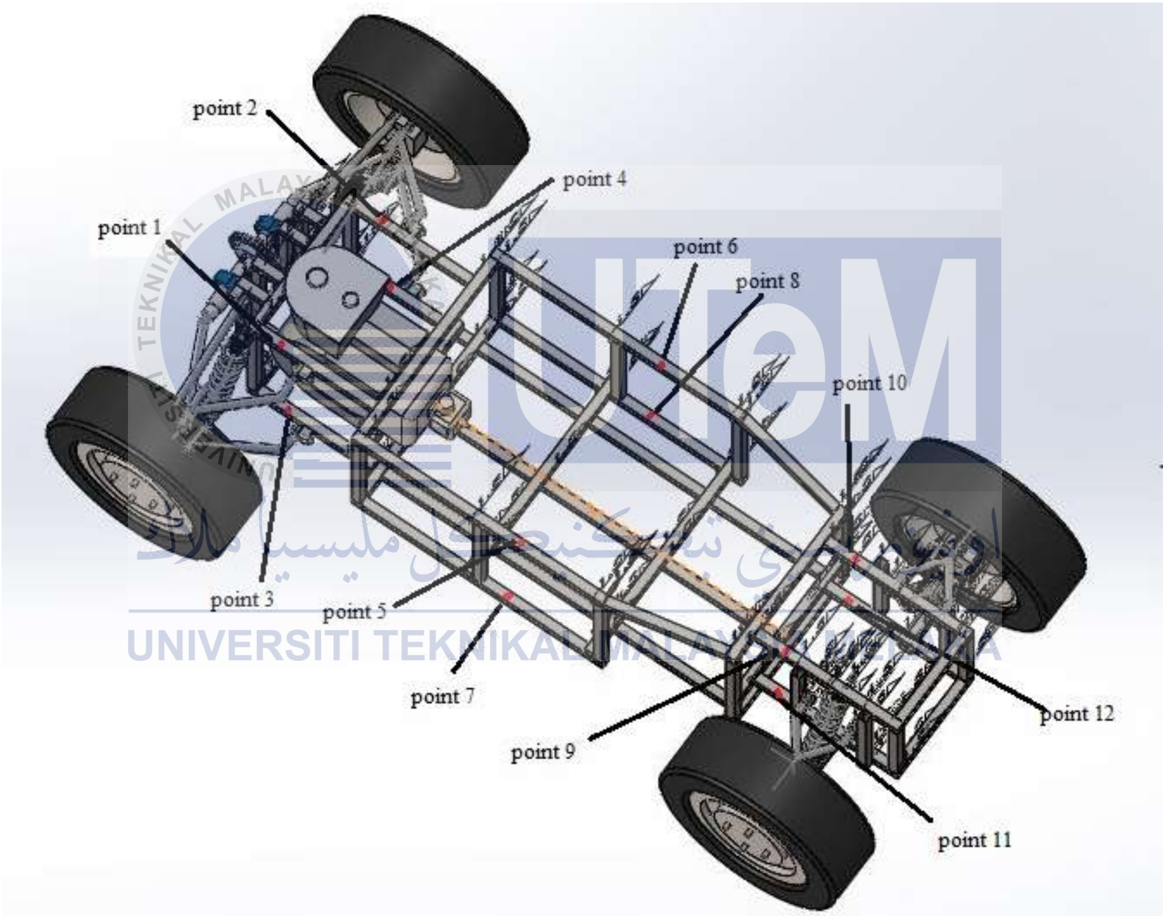

Figure 3.5: Points To Perform Vibration Test

The points selected as testing points and the points are tested separately for 15 seconds during the engine is in free gear and during the engine is in 1st gear. Therefore, the highest frequency of the vibration can be determined and the chassis can further improved in the future to reduce the vibration.

3.4 Process Flow Chart

The process of the project is divided into 2 parts which is the static analysis using simulation in Solidworks software and vibration analysis using sensors and programming codes.

3.4.1 Static Analysis Flow Chart

The static analysis flow chart is as follows:

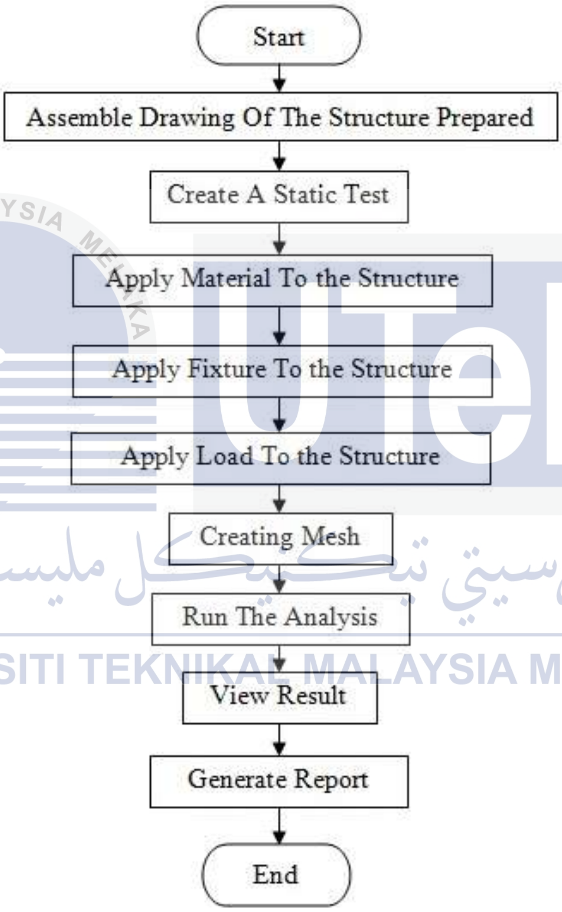

Figure 3.6: Flow Chart Of Static Test Using Solidworks Software

The flow chart shown in Figure 3.6 illustrated the process flow of conducting the static test on the chassis frame design in Solidworks software. The static test is conducted using the simulation function from the Solidworks software. At the beginning, the assemble drawing of the chassis designed is prepared by connecting all the parts included in the chassis design. Then, the static test function is selected in order to start the experiment on the chassis structure. After that, the material of the chassis is chosen from the list provided in the database of the Solidworks software. Some specifications of the materials can be edited and need to be edited if the material used having different specifications. Then, the fixtures for the chassis is applied. Fixtures that available in the software are such as fixed geometry, fixed hinge and roller/slider. Then, the load is applied to the chassis structure. The value of the load is based on the total chassis weight and driver's weight, multiplied by the desired factor of safety. After that, mesh is created. Meshing is a process of splitting the geometry of the design into small and simple shaped called finite elements. The finer the elements will increase the accuracy of the data obtained from the experiment. After the meshing is done, the test is started and the result for the test is obtained. There is a function of creating a report from Solidworks software, therefore a report for the test is generated. The report generated is saved and included in the report as the preliminary result of the report.

3.4.2 Vibration Analysis Flow Chart

The static analysis flow chart is as follows:

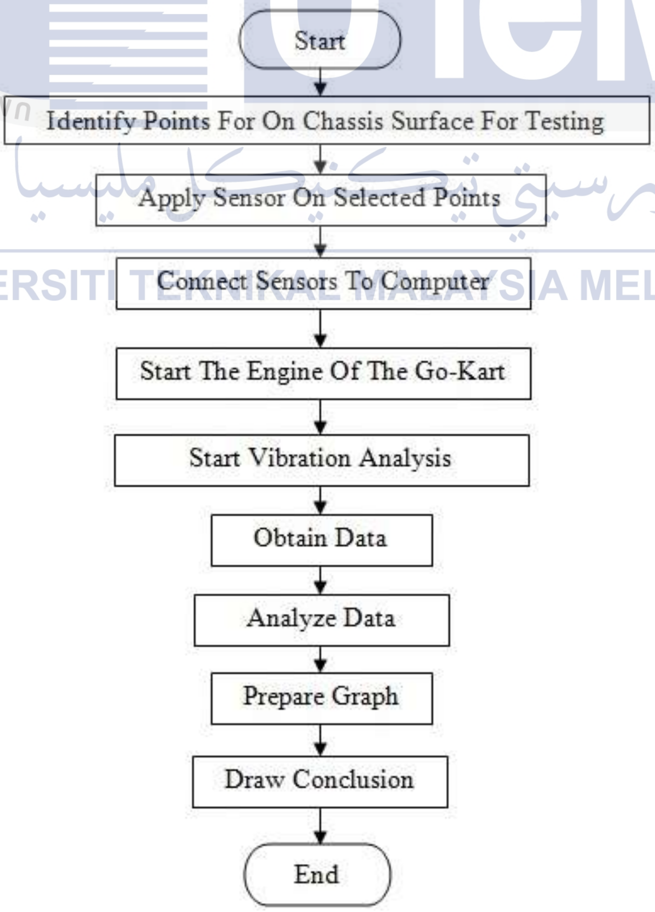

Figure 3.7: Flow Chart Of Vibration Test

The flow chart shown in Figure 3.7 illustrated the process flow of conducting the experiment for vibration test on the developed chassis structure. From the beginning, the testing points are identified on the surface of the chassis structure. The locations of the testing points are distributed around the chassis surface. After the testing points have been identified, the IMU sensor to detect the vibration are applied to the selected testing points. The vibration test is conducted during the engine is in free gear mode and also first gear mode. The IMU sensor is fixed using a tape in order to prevent the IMU sensor from moving as well as obtaining the most accurate data. The Figure 3.8 below shows the connection of IMU on the chassis.

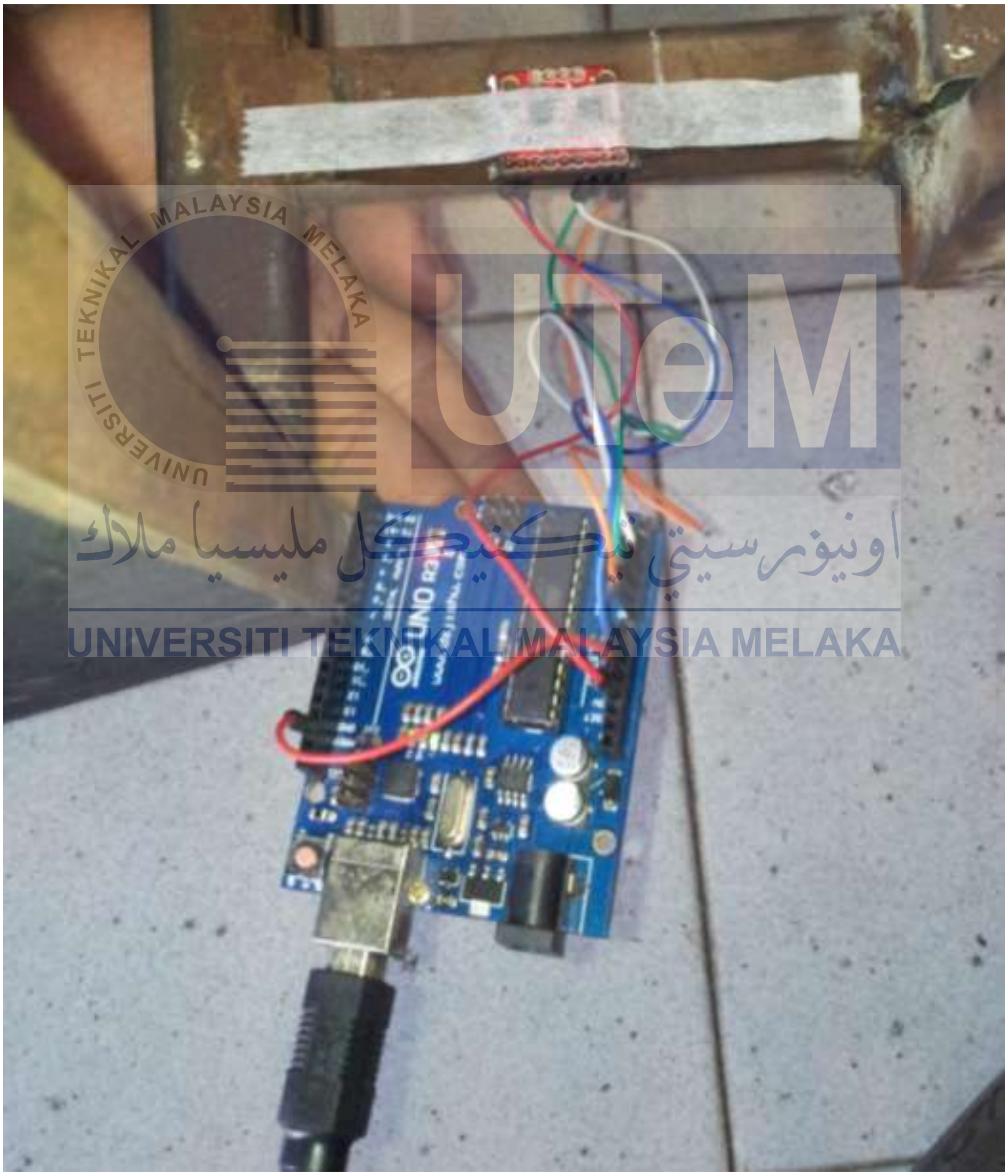

Figure 3.8: Connection Of IMU Onto Chassis

Furthermore, the chassis is set up by jacking up the whole chassis. The Figure 3.9 below shows the experiment test for vibration set up.

Figure 3.9: Experiment Set-up

Then, the IMU sensor with Arduino Uno board are connected to the computer which could obtain the data received by the sensors. The Arduino coding used to obtain the data from IMU is shown in the APPENDIX I. After the preparation work is done, the engine of the go-kart is turned on and the throttle of the go-kart is pressed. While the throttle is pressed, the vibration test is started simultaneously. The data obtained from the accelerometer of IMU is transferred automatically to the computer. The data is recorded and saved into a Notepad file before transferring to MATLAB software for analysis and graph plotting.

After the data is obtained, the data is compared and analyzed. Then, the result obtained is transferred to MATLAB software and the data is illustrated by using plotted graph. A filtered graph that removed the noise frequencies using the MATLAB Butterworth low pass filter is also plotted in order to ease the analyzing process of the data obtained from the IMU. After the analysis of the result is completed, a conclusion for the test is drawn and is recorded textually in the report. The vibration test is ended when the conclusion is drawn.

3.5 House of Quality

The house of quality in the Figure 3.10 illustrated the relationship between the customer requirements and the functional metrics. The level of importance of the customer requirements is also defined in the house of quality. Relationship between each functional metrics is also identified.

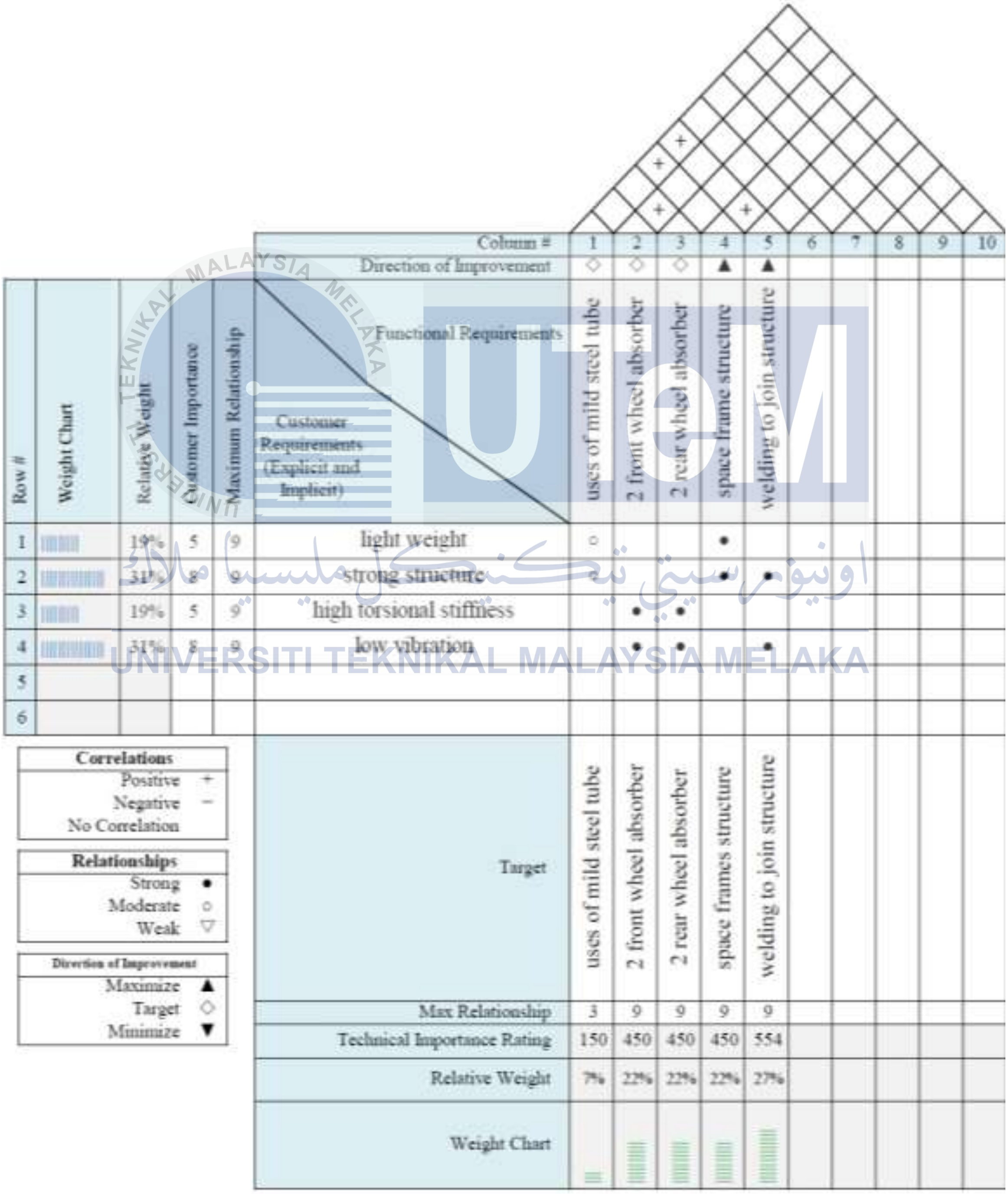

Figure 3.10: House Of Quality

3.6 Component Selection

The components in developing the chassis structure for the go-kart are such as:

3.6.1 Material For Chassis Structure

The material chosen as the material in developing the chassis for the racing can is the 25mm x 25mm mild steel square tube with the thickness of 1.6mm. The reason of choosing this type of material is due to the availability of the material and the low price of the material. The 25mm x 25mm mild steel square tube with the thickness of 1.6mm is preferable compared to aluminium due to the ease of joining using welding method. Mild steel is easier to be welded compared to aluminium although the weight of the aluminium is lighter.

3.6.2 Material For Connecting Joint Of Chassis Structure

Material chosen for connecting the mild steel square tube is the welding rod with the thickness of 2.5mm. The welding rod is chosen because welding method has the strongest connection in connecting mild steel compared to bolt or rivet. Since the chassis of the go-kart has to be very strong, therefore welding rod for welding is chosen.

3.6.3 Material For Joining With Other Parts

In joining the front nose and rear wing of the go-kart, the material chosen to join that particular parts is the mild steel bolt and nut. The bolts that have the standard of M6 is chosen to join the parts onto the chassis body. The reason of choosing bolt and nut because the front nose and rear wing of the go-kart need to be removed when not in use. Besides that, the bolt and nut are capable in withstand the weight of the parts.

For fixing the engine and motor in place at the chassis, mild steel bolts and nuts of M10 are used. The M10 bolt and nut have the higher strength compared to M6 due to the thickness of the structure. The M10 bolt and nut are chosen due to the ease of dismantling from the chassis structure during maintenance work as well as having strong connection.

3.7 Gantt Chart

The Gantt chart of the project is divided into 2 parts which is Final Project 1 (FYP1) and Final Year Project 2 (FYP2) shown in Figure 3.11 as follows:

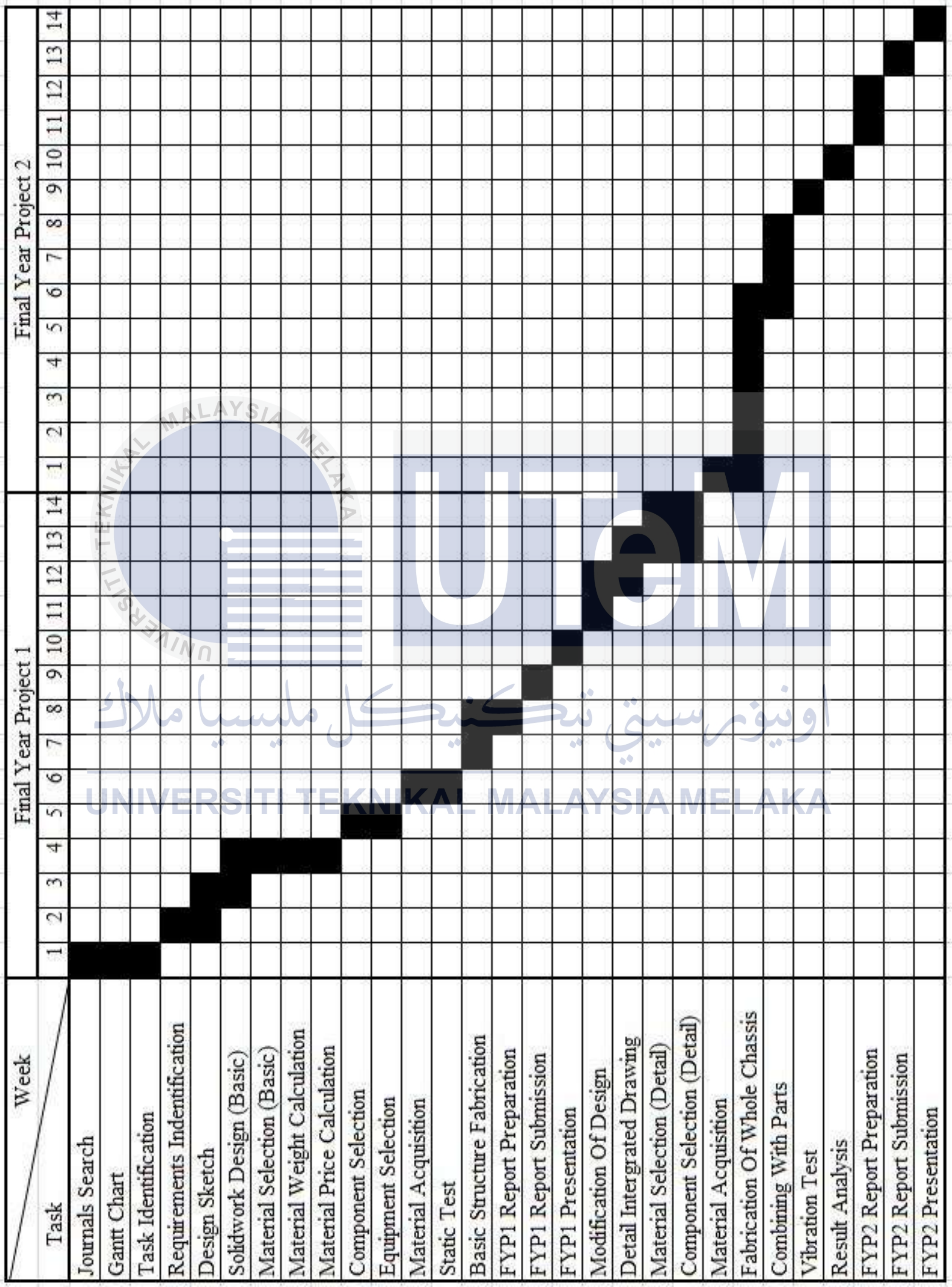

Figure 3.11: Gantt Chart

3.8 Summary

In this chapter, the method of conducting experiments and technique are explained. The flow charts of all the processes involved and block diagram for vibration test are also shown in this chapter. Besides that, the materials used in developing the chassis are also discussed in this chapter 3. Furthermore, the time management tool which is the Gantt chart is also shown in this chapter, illustrating the time allocated for each task involved.

CHAPTER 4

RESULT AND DISCUSSION

4.1 Introduction

The previous chapter explained about the experiments and techniques used in completing the project. In this chapter, the results and outcomes obtained from the experiments done is visualized textually. Diagrams, graphs, charts or tables are included to illustrate the outcomes of the experiments. Furthermore, the discussions and explanations for every result are also included in this chapter.

4.2 Summary Of Chassis Dimension

Based on both Formula UniMAP 2013 and Shell Eco-Marathon technical specification for the chassis design, the dimension and specification of this project is shown in Table 4.1 below:

Table 4.1: Summary Of Chassis Specifications

No. of seat	1
Track Width	min 500mm (midpoint of tyre)
Overall Height	max 900mm from ground
Overall Width	max 1300mm
Wheelbase	min 1000mm
Overall Length	max 3500mm
Ground Clearance	min 50mm with driver onboard
Bodywork Width	less than overall width
Weight	max 140kg without driver
Cockpit	at least 50mm in front of steering wheel
Wheel	300mm - 325mm
Wheel Width	min 100mm, max 163mm
Fuel	Shell unleaded petrol 95/97
No. of Wheels	4

4.3 3D Drawing Of The Basic Chassis Structure

The three dimensional drawing of the basic structure of the designed chassis structure is shown in Figure 4.1. The structure is drawn using Solidworks software.

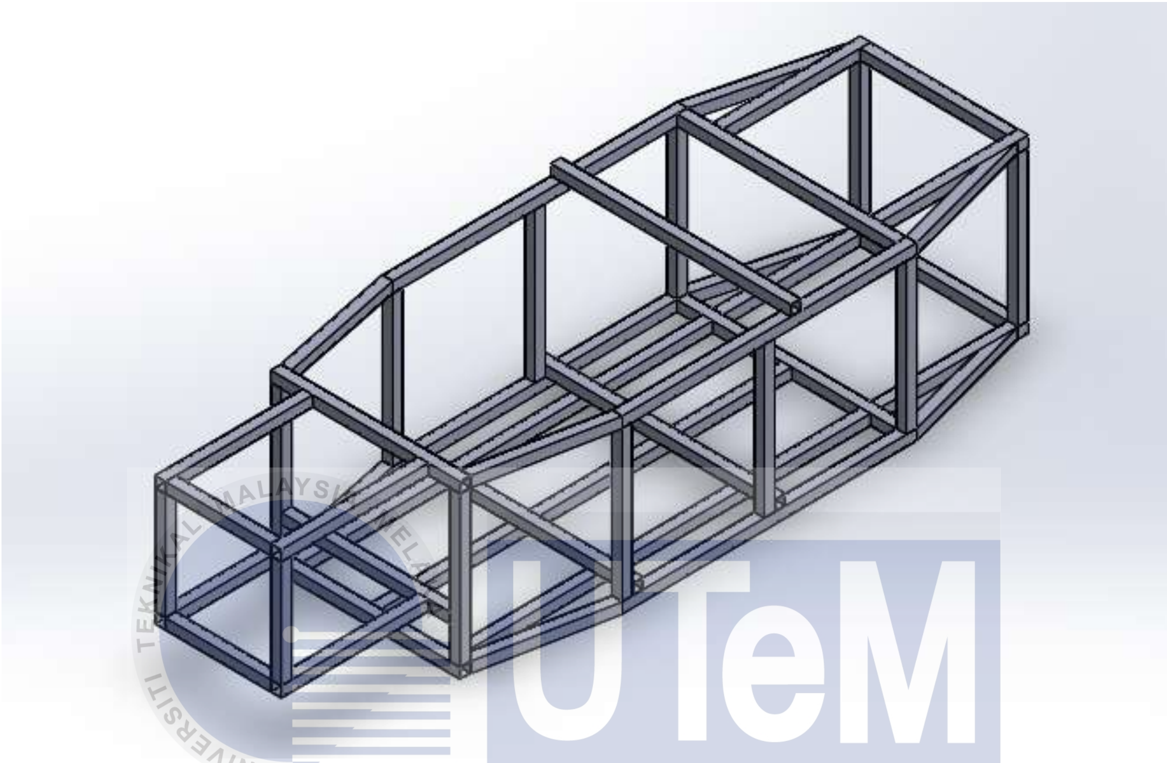

Figure 4.1: Three Dimensional Drawing Of Basic Chassis Structure

4.4 Detail Of The Basic Chassis Structure

The detail of the basic chassis drawing includes the dimension of the joining part for the front nose, the cockpit dimension, the dimension of the joining part of the rear wing and also the overall chassis structure dimension. The dimension of the joining part of the front nose and the cockpit dimension are shown in the Figure 4.2 while the dimension of the joining part for the rear wing is shown in the Figure 4.3. Lastly, the overall chassis structure dimension is shown in figure 4.4 which consists of the top view, front view, back view and the front view of the chassis structure. The dimension shown in the figure is in millimeter (mm).

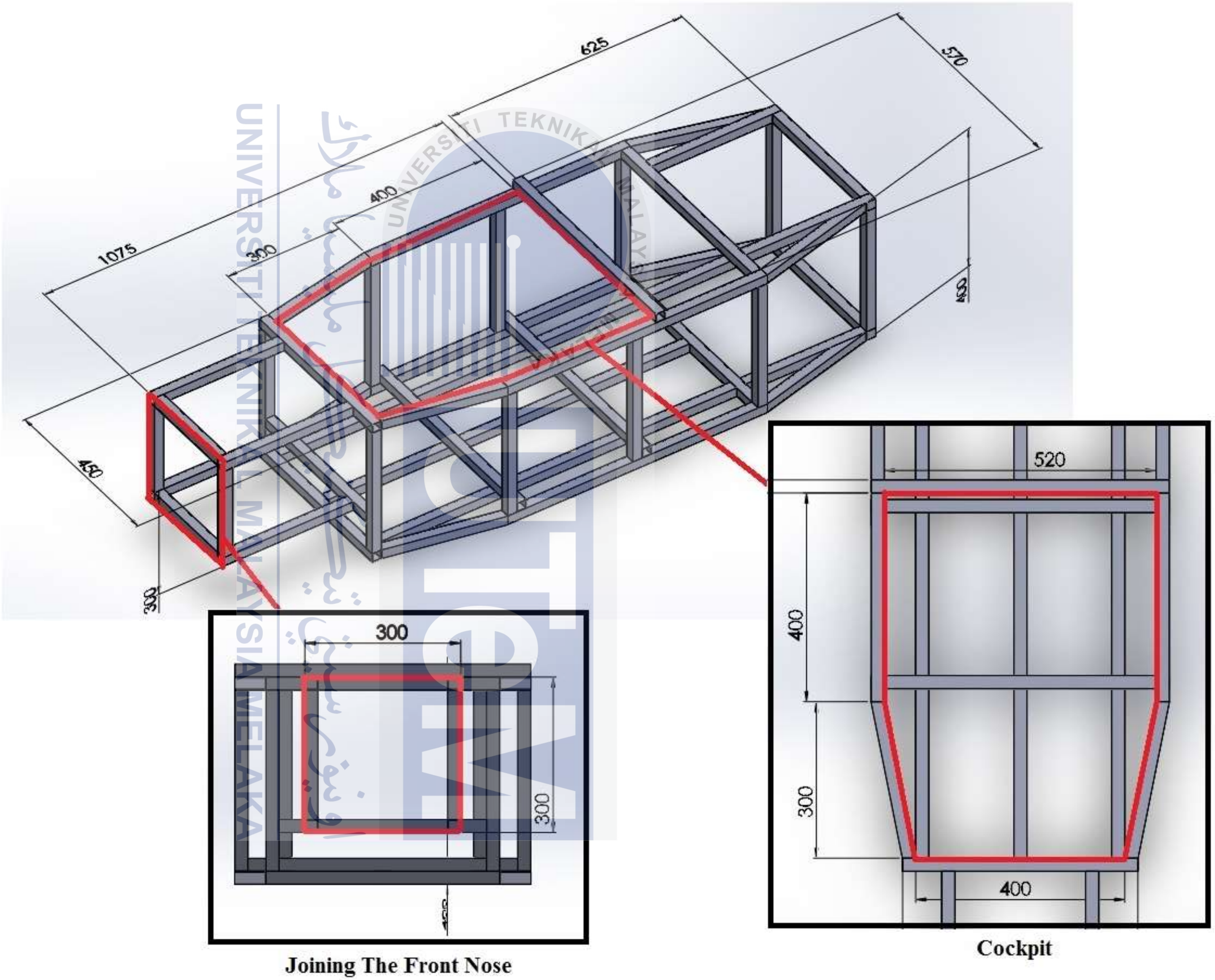

Figure 4.2: Dimension Of The Joining Part Of The Front Nose And Cockpit

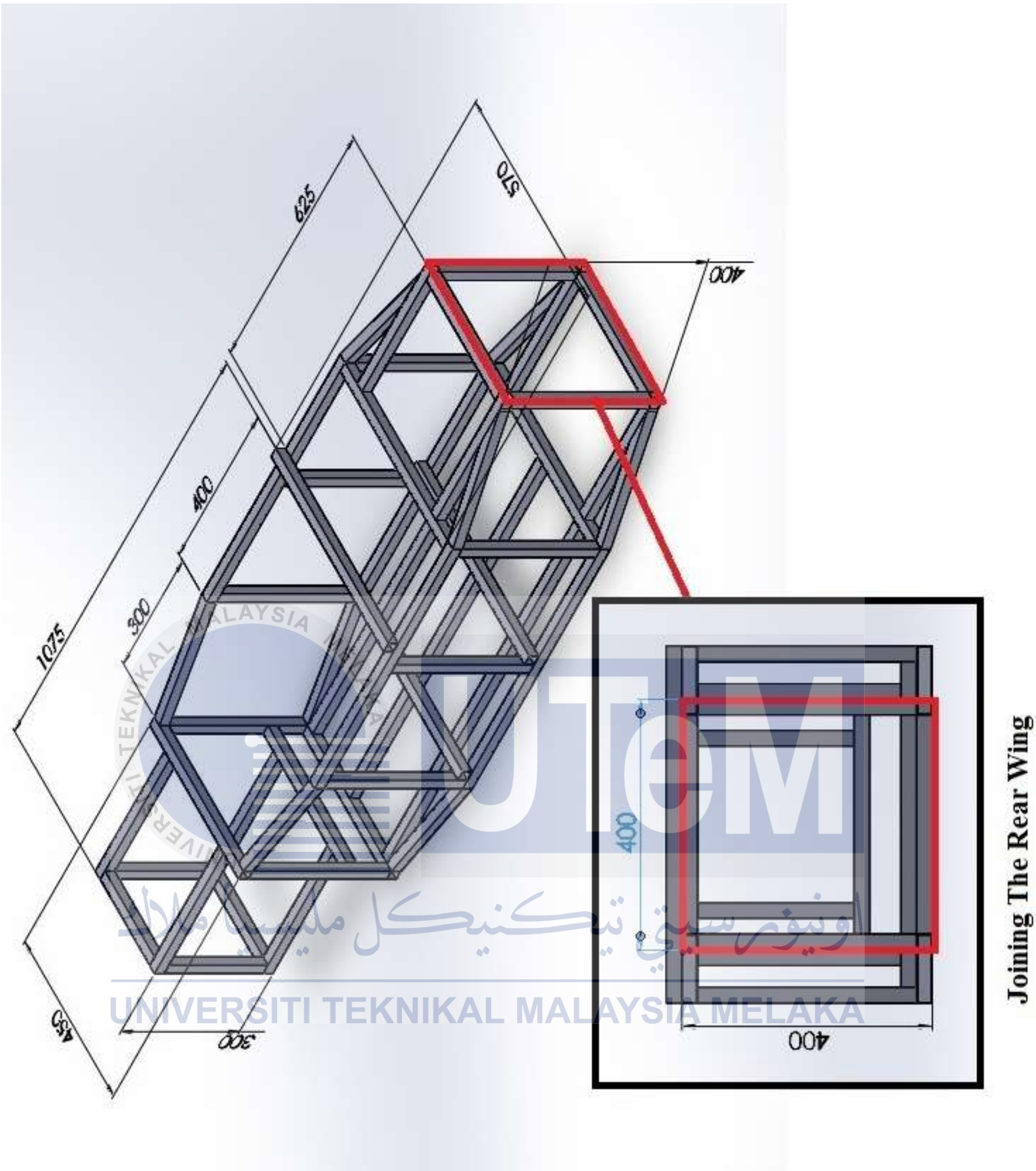

Figure 4.3: Dimension Of The Joining Part Of The Rear Wing

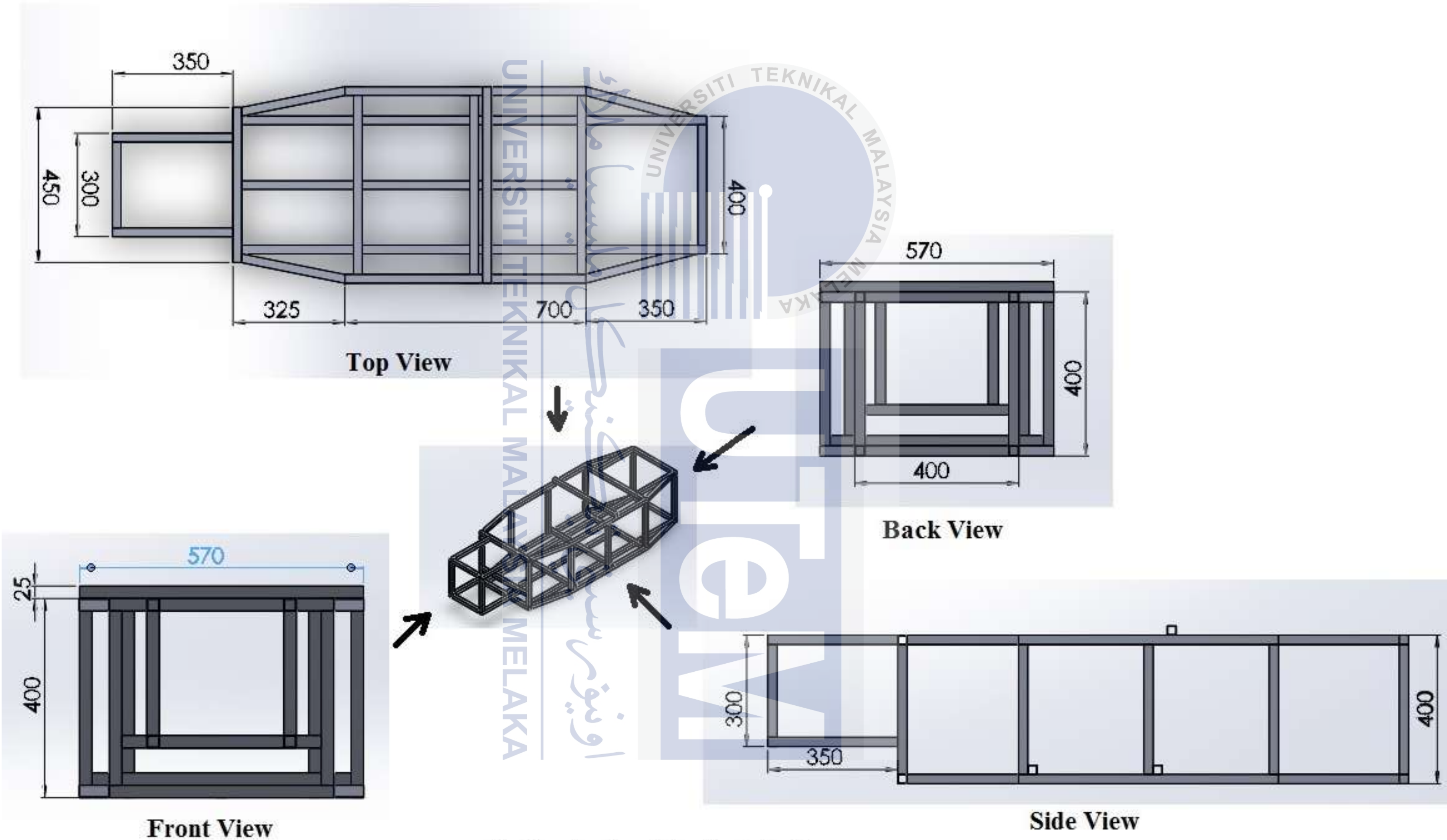

The dimension shown is in milimetre (mm)

Figure 4.4: Overall Chassis Structure Dimension

4.5 3D Drawing Of The Chassis With Combining Parts

The three dimensional drawing of the chassis with all the combining parts such as engine, absorber, drivetrain, wheels, front wing and rear wing is shown in Figure 4.5 below.

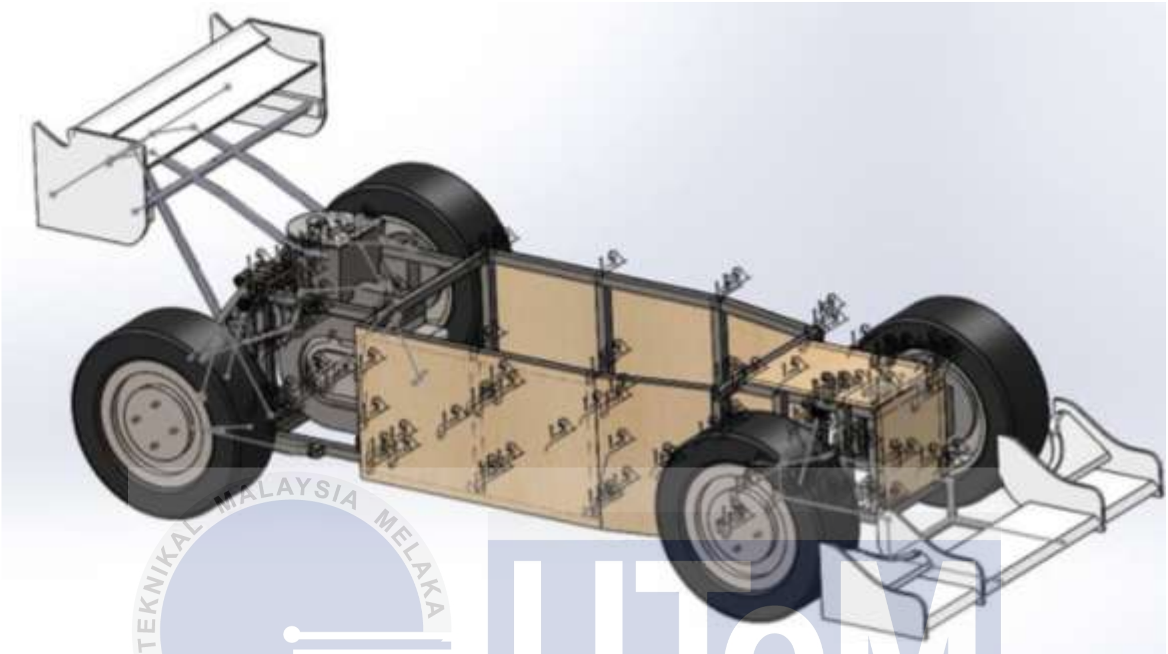

Figure 4.5: 3D Drawing Of The Chassis With Combining Parts

Figure 4.6 (a) below shows the top views of the chassis. Besides that, Figure 4.6 (b) shows the side view while Figure 4.6 (c) and Figure 4.6 (d) show the front view and back view respectively.

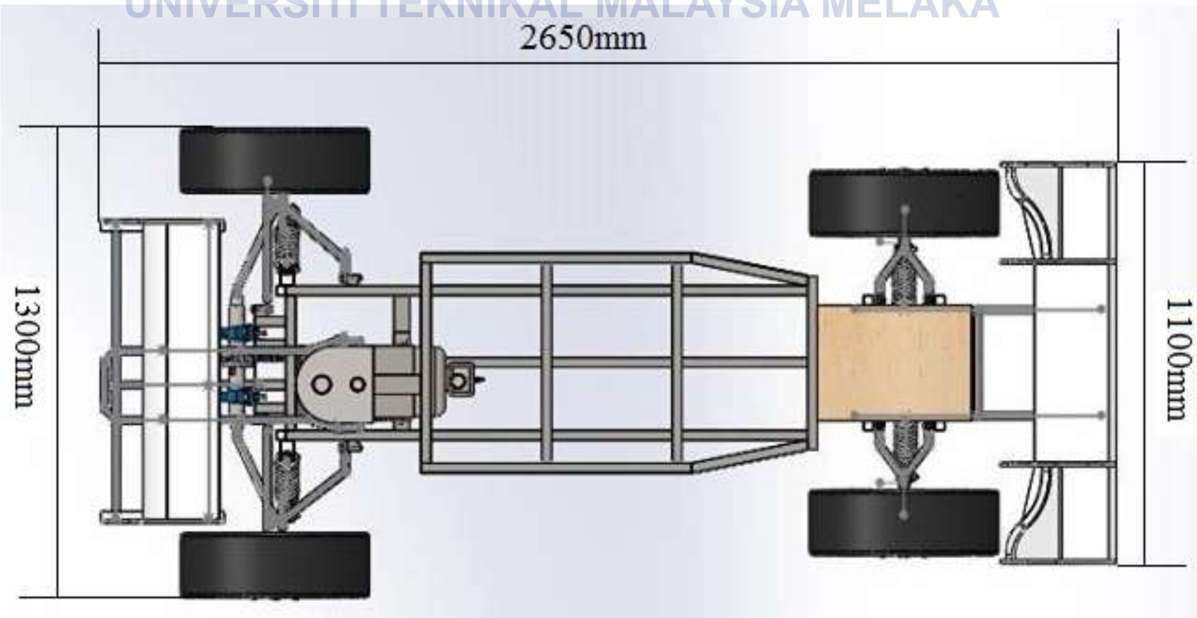

Figure 4.6 (a): Top View Of The Chassis

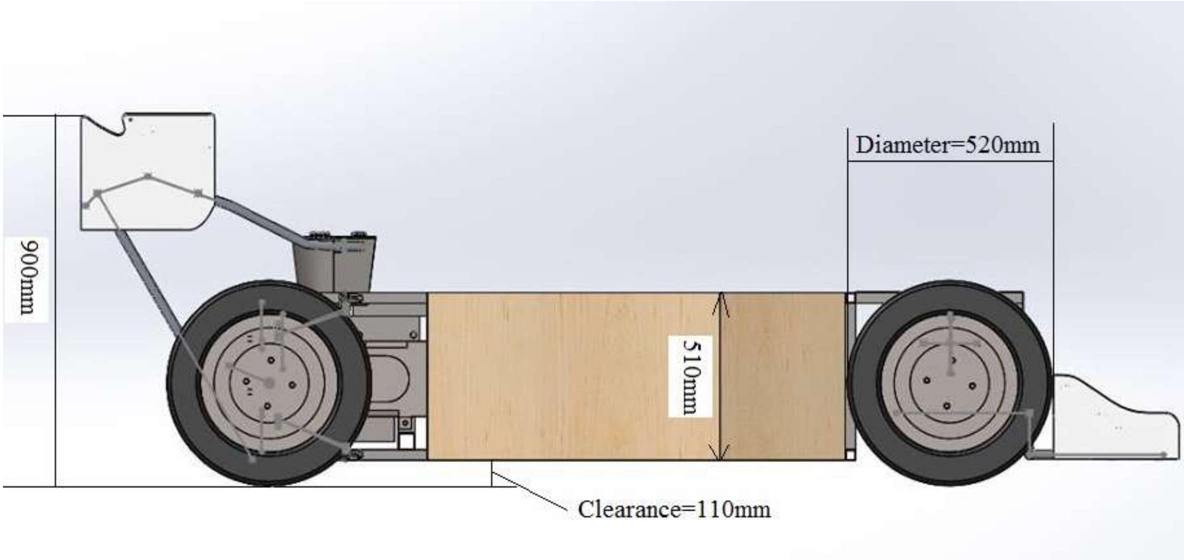

Figure 4.6 (b): Side View Of The Chassis

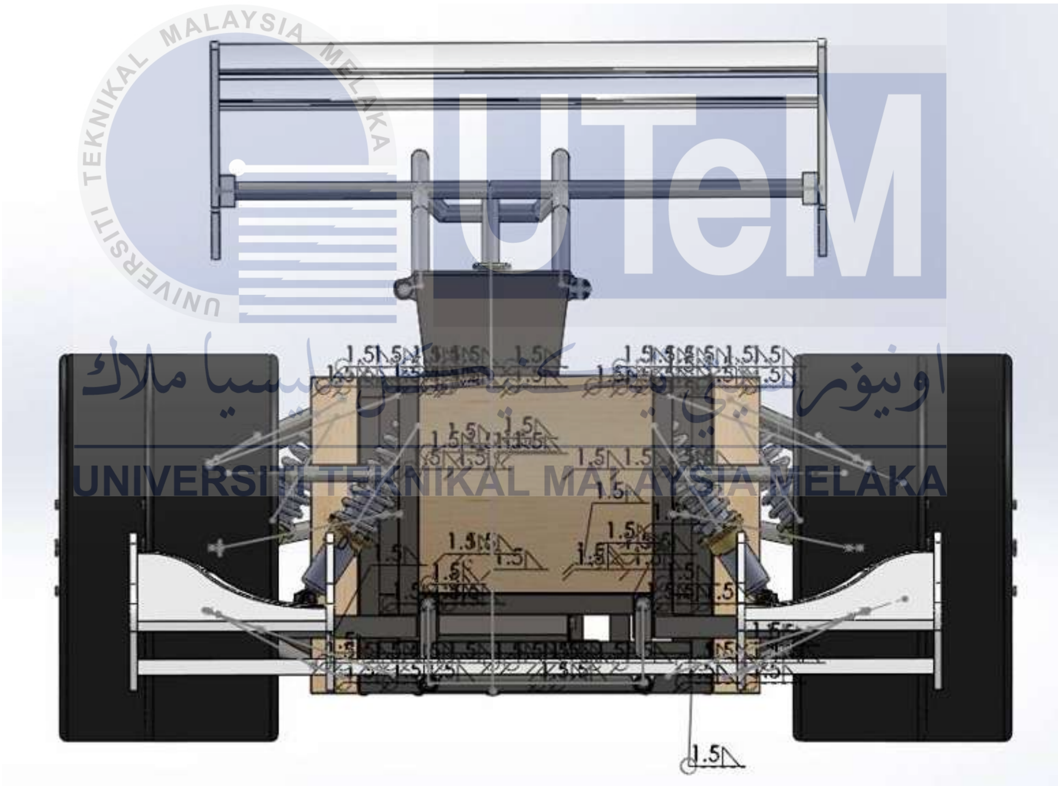

Figure 4.6 (c): Front View Of The Chassis

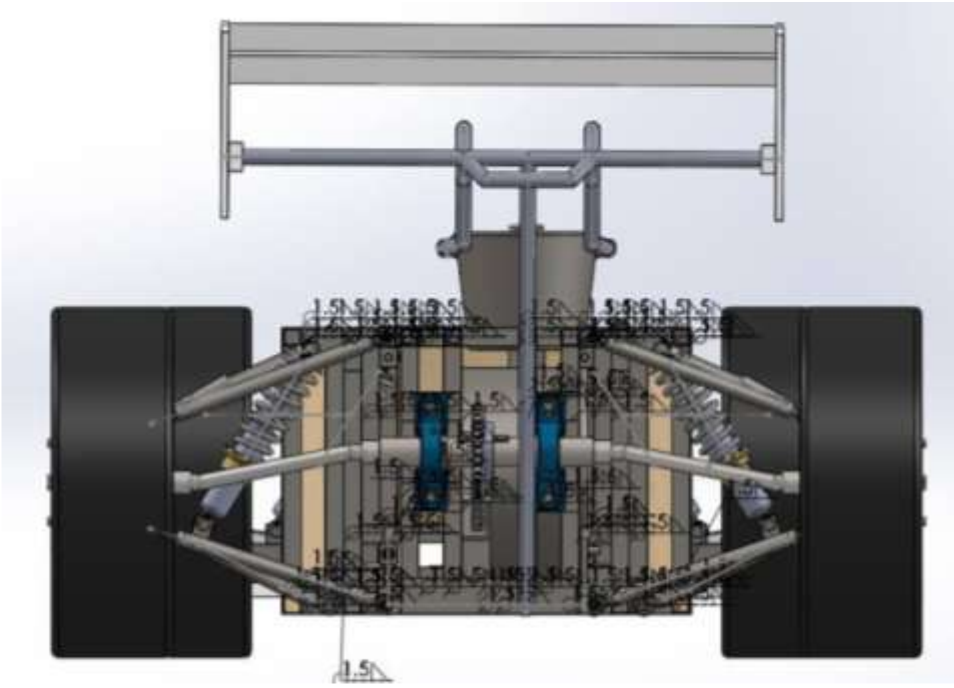

Figure 4.6 (d): Back View Of The Chassis

The details about the 3D chassis is shown in the Figure 4.7 below.

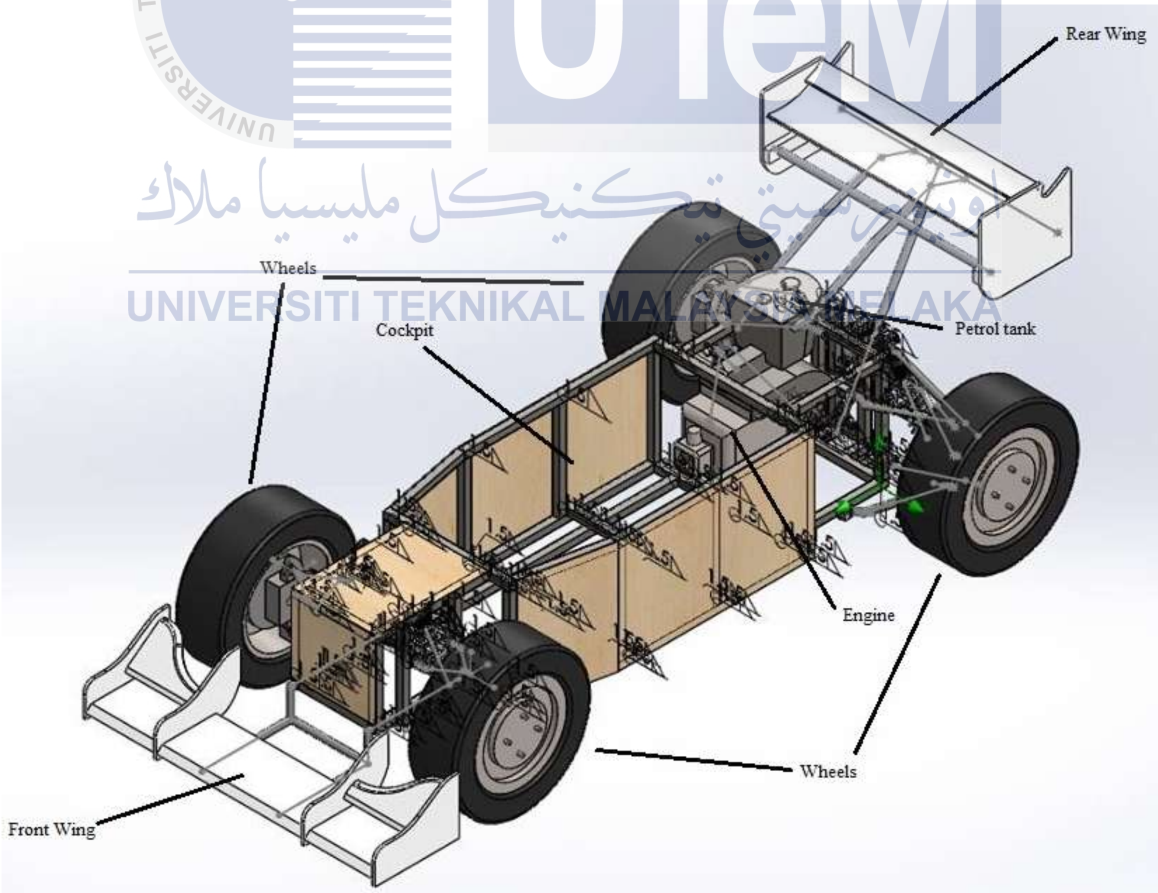

Figure 4.7: Details Of 3D Chassis

4.6 Fabricated Detailed Chassis With Combining Parts

The chassis is developed in the laboratory of Faculty of Electrical Engineering and the Figure 4.8 below shown the fabricated detailed chassis structure with combining parts.

Figure 4.8: Fabricated Chassis

Figure 4.9 (a) shown below is the side view of the fabricated chassis. Furthermore, Figure 4.9 (b) and Figure 4.9 (c) are the front view and back view of the fabricated chassis.

Figure 4.9 (a): Side View Of Fabricated Chassis

Figure 4.9 (b): Front View Of Fabricated Chassis

Figure 4.9 (c): Back View Of Fabricated Chassis

4.6.1 Fabricated Drivetrain

The Figure 4.10 below shown is the drivetrain fabricated using 2 block bearing UCF 208, steel shaft, Perodua Kancil drive shaft and 40 teeth sprocket as drive.

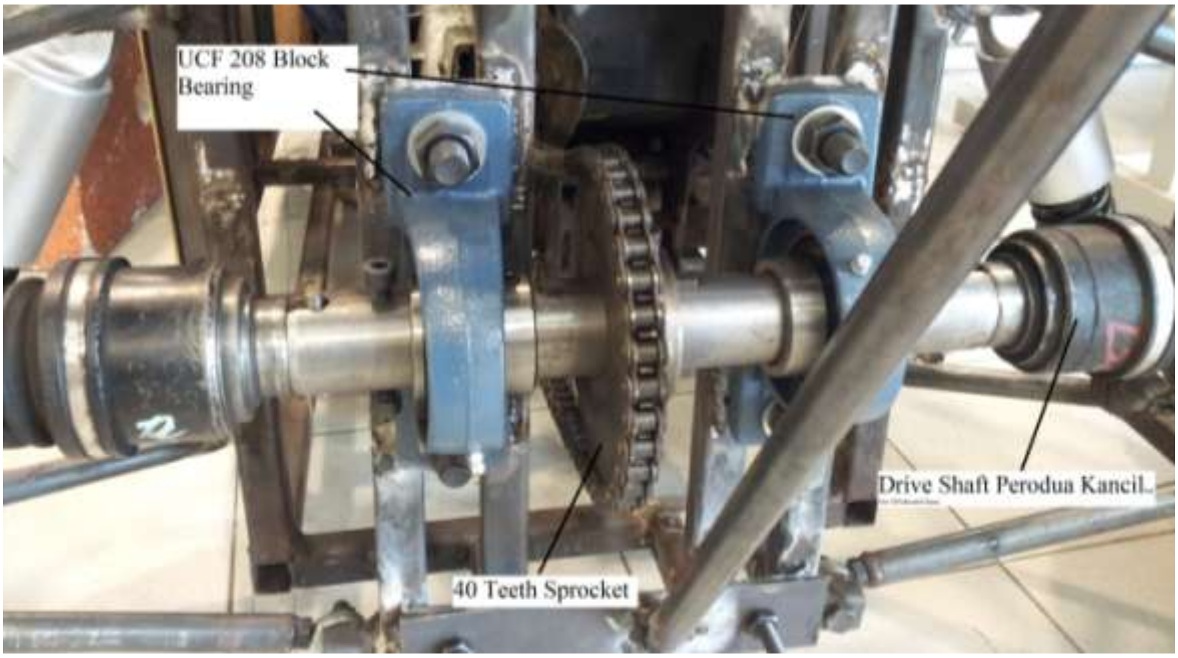

Figure 4.10: Drivetrain

4.6.2 Fabricated Arm

The Figure 4.11 (a) shown below is the upper front arm of the chassis made by mild steel tube and rod end bearing while Figure 4.11 (b) shown below is the upper and lower rear arm of the chassis.

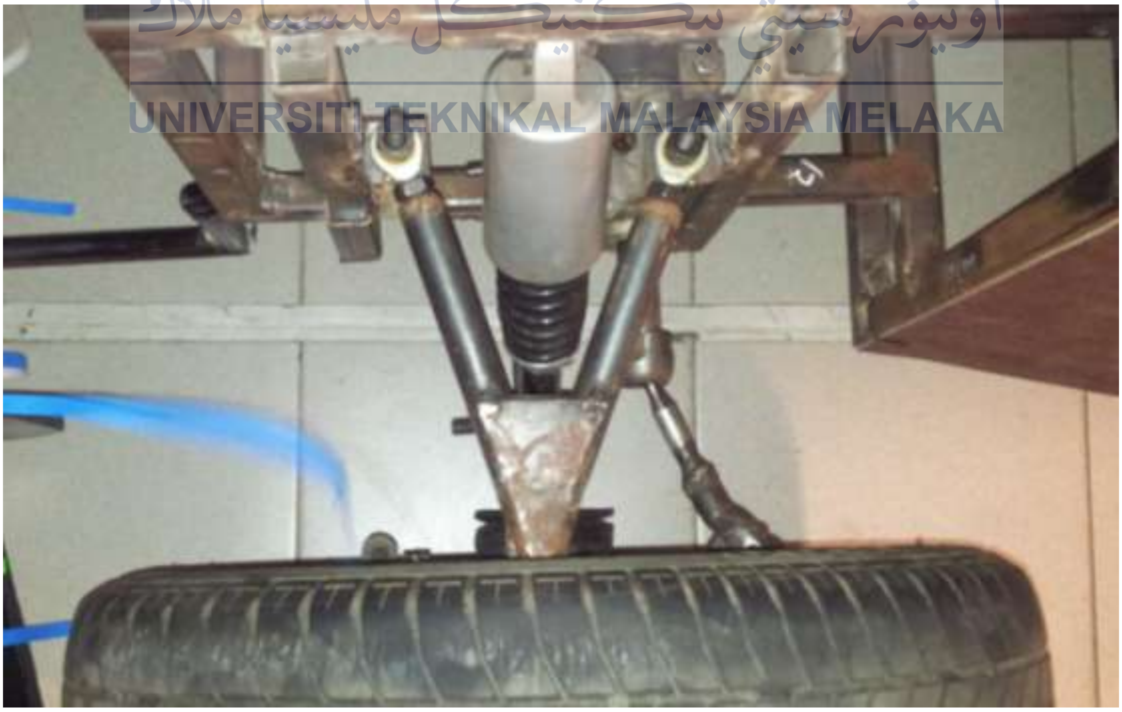

Figure 4.11 (a): Upper Front Arm

Figure 4.11 (b): Upper And Lower Rear Arm

4.7 Static Test Simulation

The static test on the chassis is done using the Solidworks software. The result obtained is saved using Microsoft Office Words. The static test is mainly focused on obtaining the static stress and static strain experienced by the chassis as well as obtaining the displacement of the chassis after a desired force is exerted on the chassis.

4.7.1 Study Properties Of The Chassis In Solidworks Software

The properties of the static test is shown in Table 4.2.

Table 4.2: Study Properties Of Static Test

Study name	Study 1
Analysis type	Static
Mesh type	Solid Mesh
Thermal Effect:	On
Thermal option	Include temperature loads
Zero strain temperature	298 Kelvin
Include fluid pressure effects from Solidworks Flow Simulation	Off
Solver type	FFEPlus
In plane Effect:	Off
Soft Spring:	Off
Inertial Relief:	Off
Incompatible bonding options	Automatic
Large displacement	Off
Compute free body forces	On
Friction	Off
Use Adaptive Method:	Off
Result folder	Solidworks document (C:\Users\sclimDaviD\Desktop\Chassis\SOLIDWORKS Drawing\B drawing)

4.7.2 Unit Used In The Static Test

The unit system of the static test is shown in the Table 4.3.

Table 4.3: Unit System Of The Static Test

Unit system:	SI (MKS)
Length/Displacement	mm
Temperature	Kelvin
Angular velocity	rad/sec
Pressure/Stress	N/m^2

4.7.3 Load And Fixture Of The Static Test

In order to perform static test on the chassis structure, the fixtures have to be defined to determine how the structure is supported while the load applied to the structure is at 5000 N which is about 2.5 times the maximum weight of 140kg chassis and the assumption weight of 60kg of the driver. The load and fixture of the static test is shown in the Table 4.4.

Table 4.4: Load And Fixture

Fixture name	Fixture Image	Fixture Details
Fixed-1	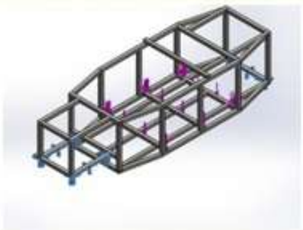	Entities: 3 face(s) Type: Fixed Geometry

Load name	Load Image	Load Details
Force-1	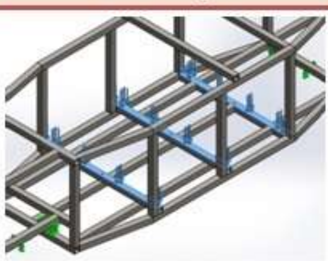	Entities: 3 face(s) Type: Apply normal force Value: 5000 N

The fixture is fixed at the front and the rear part of the structure. The type of fixture chosen is the fixed geometry while the applied load of 5000 N which equal to a 5000 N normal force acting on the place where the driver is seated and the engine is located. The fixture image is shown in the Figure 4.12 below and the load image is shown in the Figure 4.13 below. The fixture of the chassis is indicated by using the blue colour arrows shown in Figure 4.12. The load applied to the structure is illustrated by using the blue colour arrows in Figure 4.13.

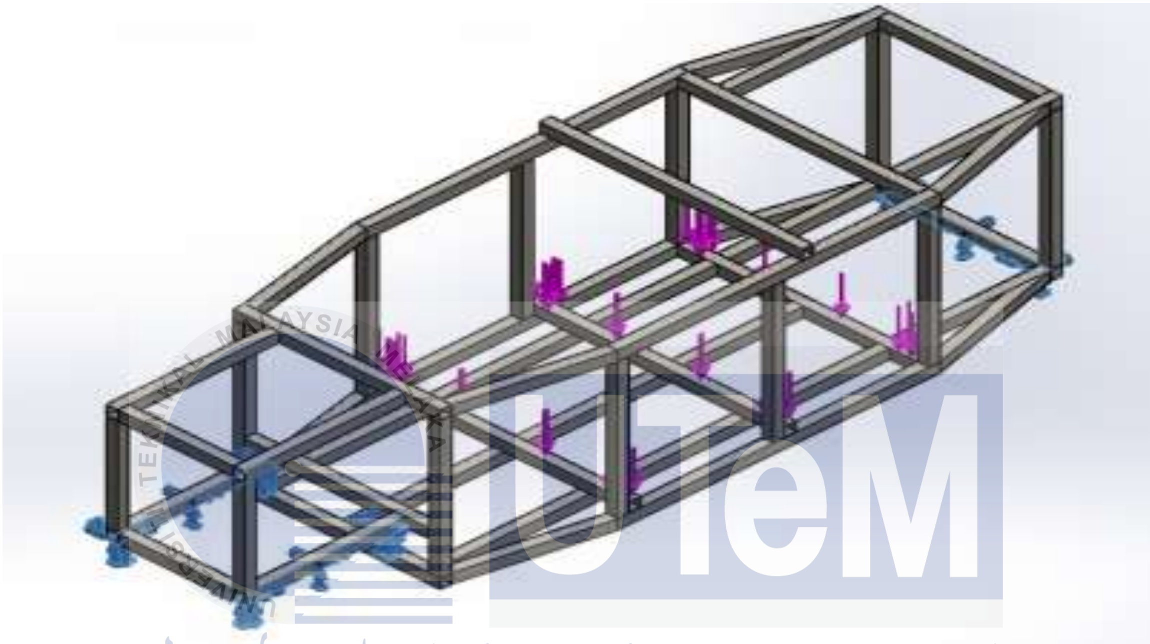

Figure 4.12: Fixture Image

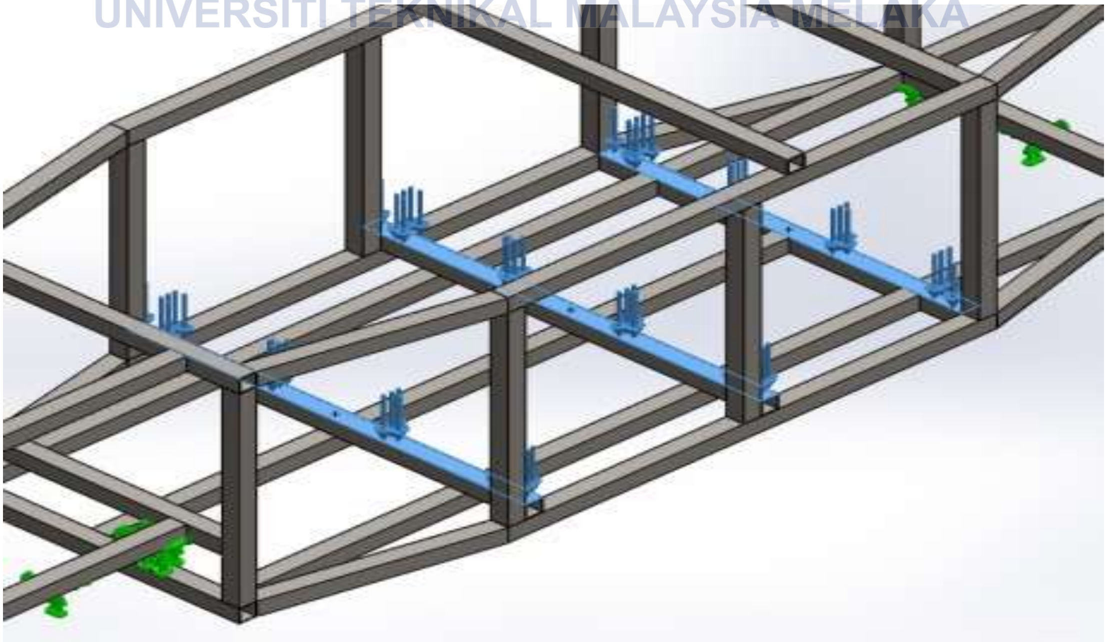

Figure 4.13: Applied Load Image

4.7.4 Mesh Information Of The Static Test

The mesh properties used in performing the static test is the finest mesh available for the test. The meshing information of the chassis structure is shown in Table 4.5 while the details of the mesh information is shown in Table 4.6.

Table 4.5: Mesh Information

Mesh type	Solid Mesh
Mesher Used:	Standard mesh
Automatic Transition:	Off
Include Mesh Auto Loops:	Off
Jacobian points	4 Points
Element Size	19.458 mm
Tolerance	0.972902 mm
Mesh Quality	High
Remesh failed parts with incompatible mesh	Off

Table 4.6: Detailed Mesh Information

Total Nodes	66710
Total Elements	36014
Maximum Aspect Ratio	138.67
% of elements with Aspect Ratio < 3	0.475
% of elements with Aspect Ratio > 10	89.3
% of distorted elements(Jacobian)	0
Time to complete mesh(hh;mm;ss):	00:00:23
Computer name:	SCLIMDAVID-PC

4.7.5 Diagram Of Meshed Structure

After meshing is done on the chassis design, the structure of the chassis is shown in the Figure 4.14. The mesh detailed diagram is shown in Figure 4.15.

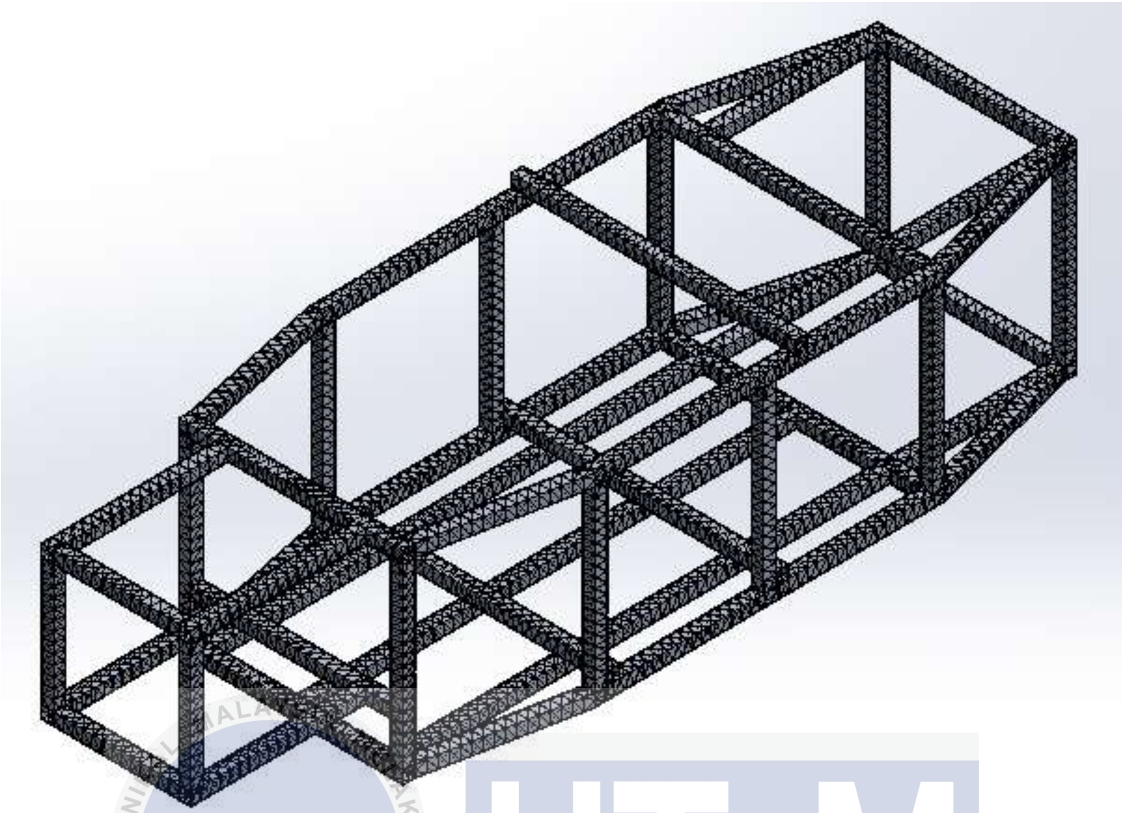

Figure 4.14: Meshed Structure Of The Chassis

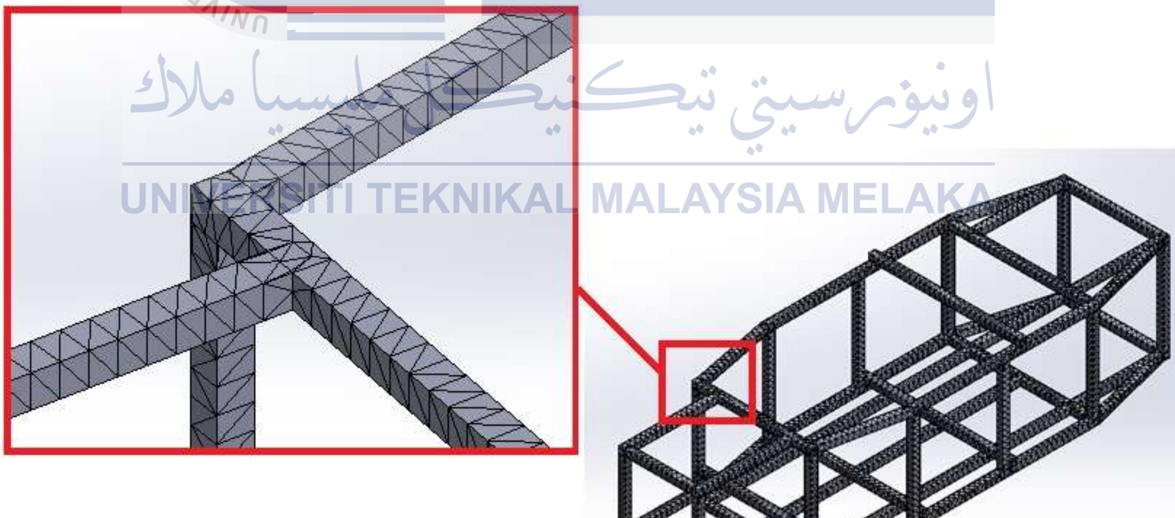

Figure 4.15: Detail Mesh Structure Image

4.7.6 Static Test Result (Von Mises Stress)

The static test is done after all the pre-requisite steps is completed. The result of the Von Mises Stress test is shown in Figure 4.16.

Name	Type	Min	Max
Stress1	VON: von Mises Stress	1387.38 N/m^2 Node: 25769	1.7893e+008 N/m^2 Node: 20979

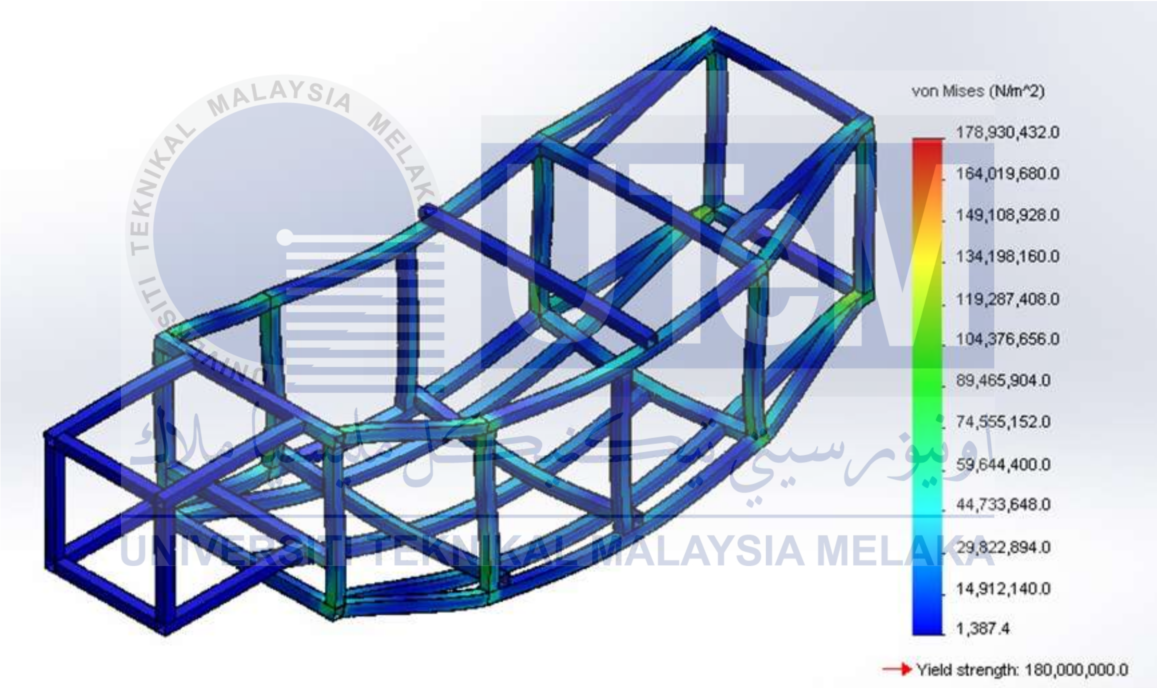

Figure 4.16: Von Mises Stress Result

4.7.7 Static Test Result (Resultant Displacement)

The resultant displacement is shown in Figure 4.17.

Name	**Type**	**Min**	**Max**
Displacement1	URES: Resultant Displacement	0 mm Node: 16510	2.32277 mm Node: 9568

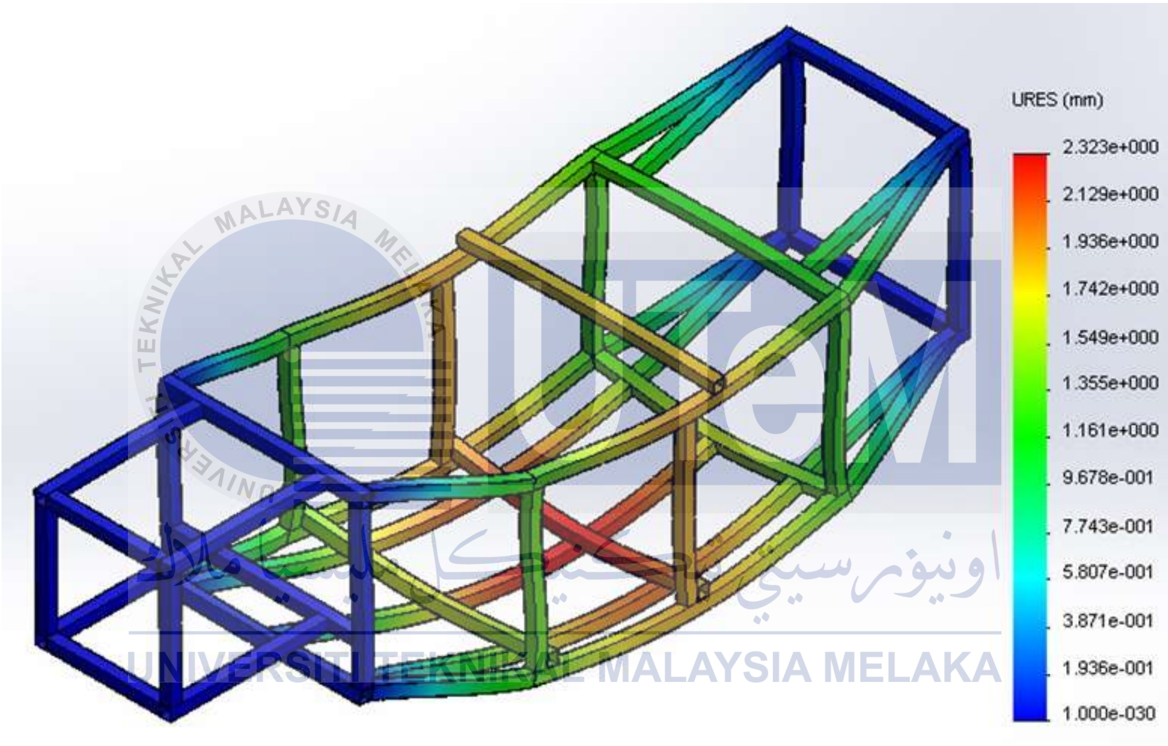

Figure 4.17: Resultant Displacement Result

4.7.8 Static Test Result (Equivalent Strain)

The result of equivalent strain is shown in the Figure 4.18.

Name	Type	Min	Max
Strain1	ESTRN: Equivalent Strain	7.67918e-009 Element: 13271	0.000703849 Element: 18371

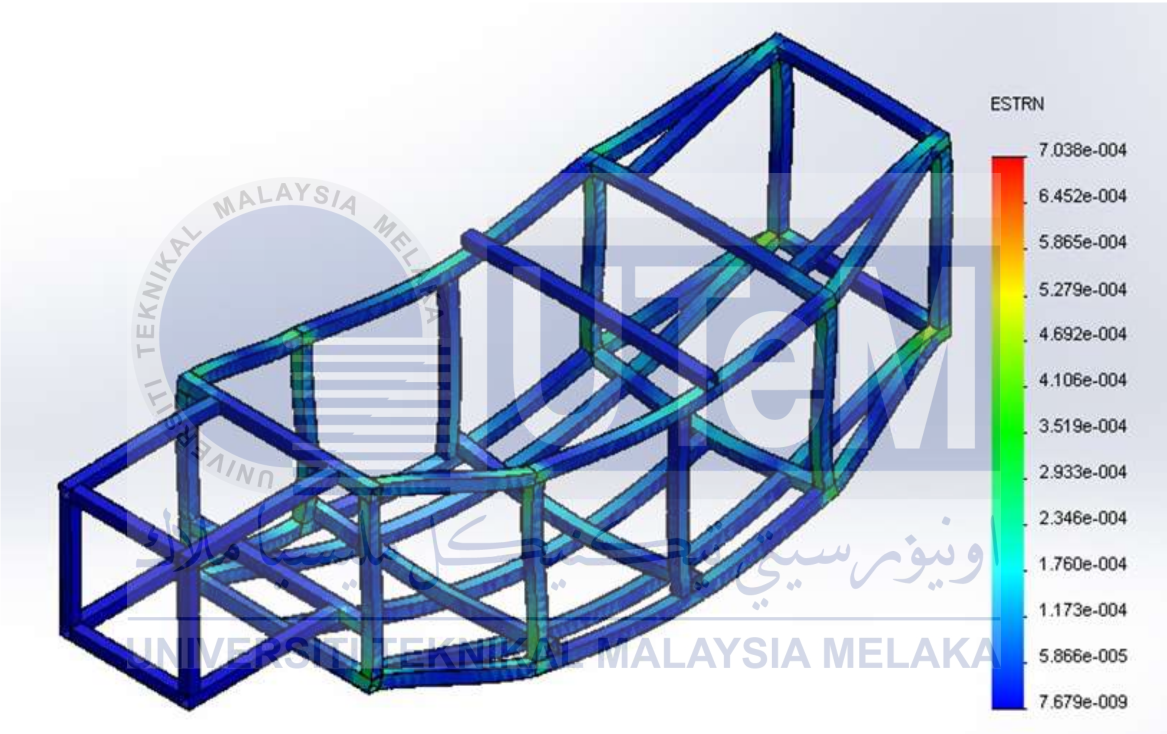

Figure 4.18: Strain Equivalent Result

4.7.9 Static Test Result (Deformed Shape)

The deformed shape after the static test is shown in the Figure 4.19.

Name	Type
Displacement1{1}	Deformed Shape

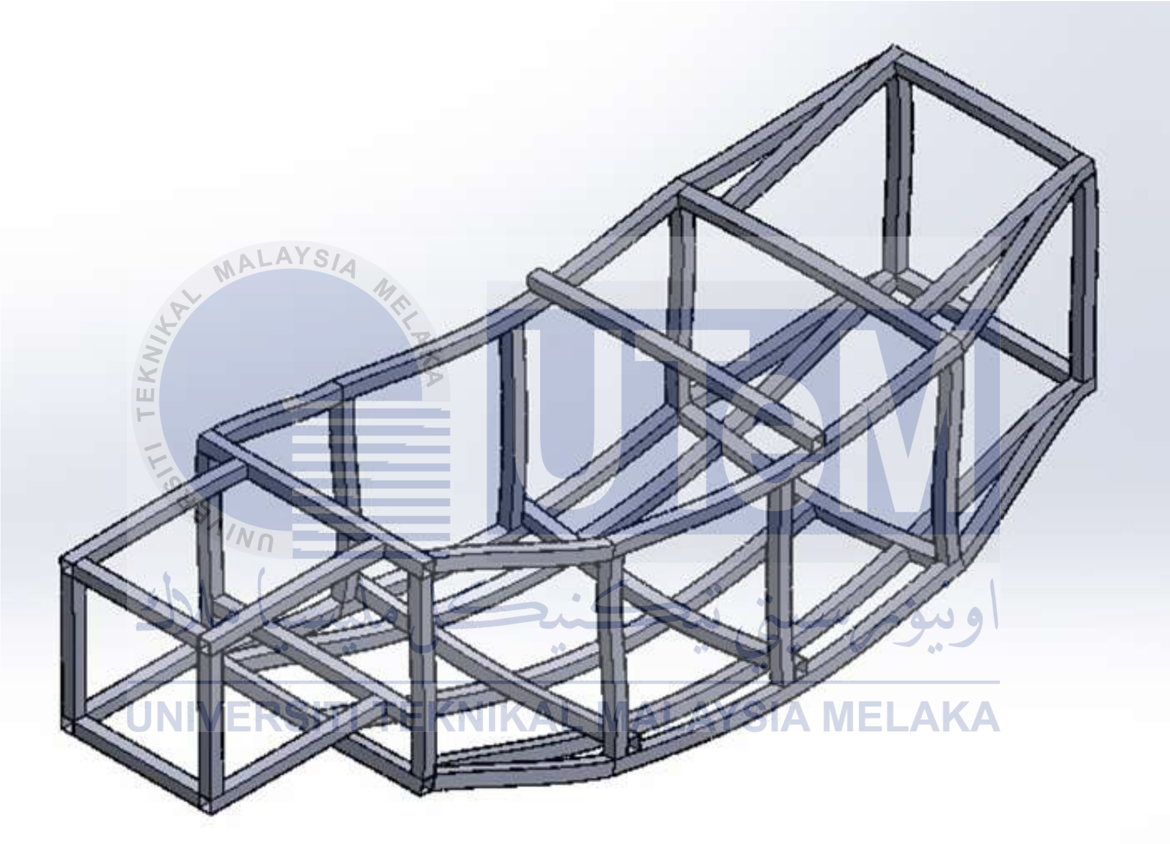

Figure 4.19: Deformed Shape

4.8 Vibration Test

The vibration test on the chassis is done using the IMU. The result obtained is saved using Notepad and 600 lines of data transferred to MATLAB software for graph plotting. 600 lines which are equivalent to approximately 15 seconds of data obtained. The vibration test is conducted on the twelve points stated in Chapter 3, Methodology. In each point on the chassis, 2 experiments are conducted which are during the engine is on free gear and during the engine is in first gear. Each experiment is conducted twice and the average of the data is calculated in Microsoft Excel software. The vibration test is mainly focusing on obtaining the vibration experienced by the chassis body. The graph obtained from MATLAB software is filtered using Butterworth low pass filter in order to eliminate the noise frequency and smooth the output graph. Both graphs before filtered and after filtered are shown accordingly. In the graph, the blue color line indicates the data from X-axis accelerometer and the green color line indicates the data from Y-axis accelerometer. Last and not least, the red color line indicates the data from Z-axis accelerometer.

4.8.1 Point 1

The Figure 4.20 (a) below is the graph plotted using MATLAB software without applying filter showing the vibration experienced by the chassis body during free gear at point 1 while the Figure 4.20 (b) below is the graph plotted using MATLAB software with applied Butterworth low pass filter as smoothing agent.

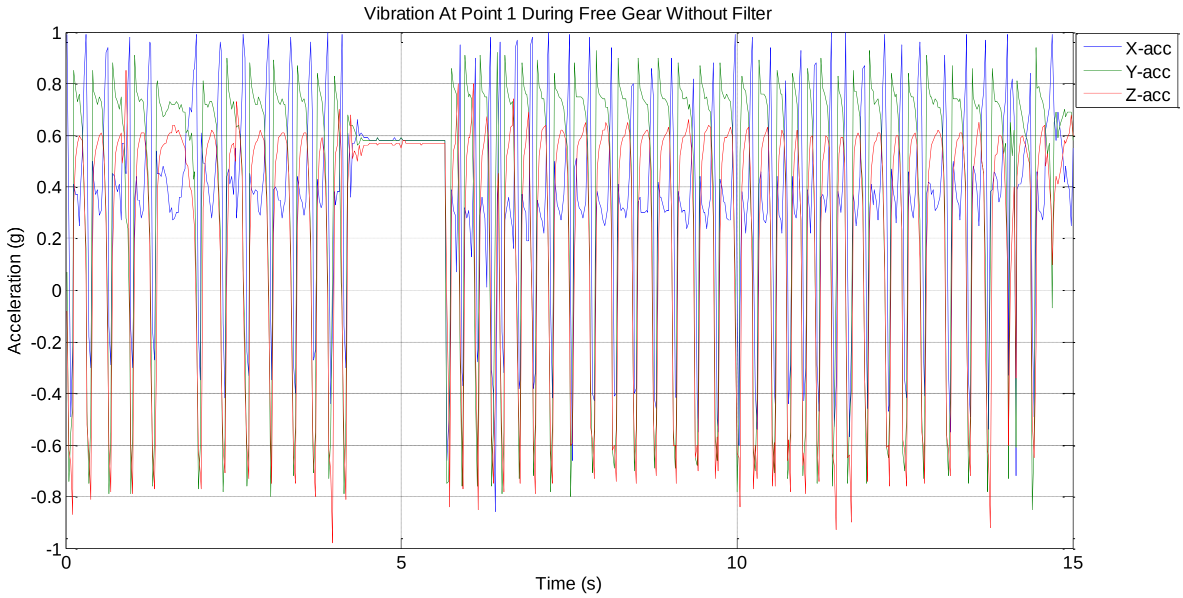

Figure 4.20 (a): Vibration At Point 1 During Free Gear Without Filter

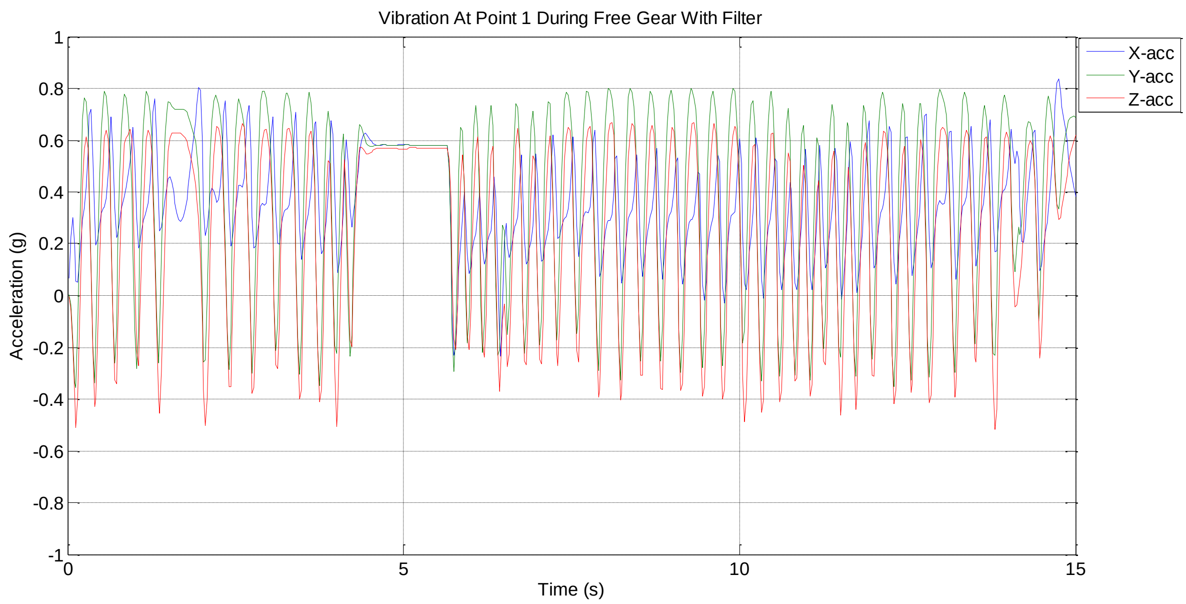

Figure 4.20 (b): Vibration At Point 1 During Free Gear With Filter

The Figure 4.20 (c) below is the graph plotted using MATLAB software without applying filter showing the vibration experienced by the chassis body during first gear at point 1 while the Figure 4.20 (d) below is the graph plotted using MATLAB software with applied Butterworth low pass filter as smoothing agent.

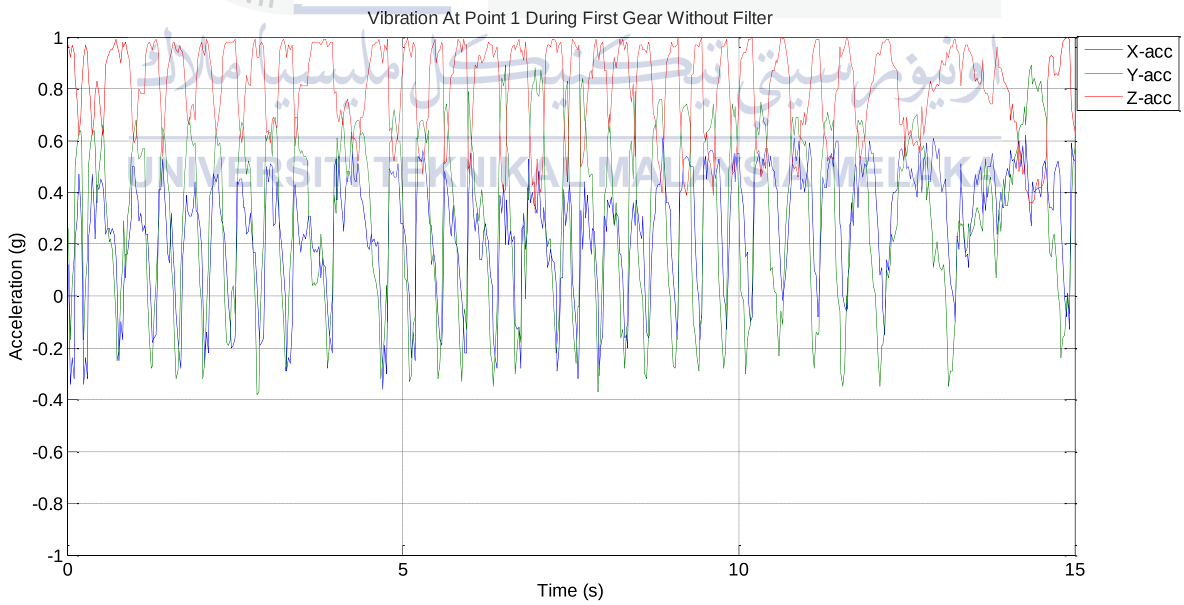

Figure 4.20 (c): Vibration At Point 1 During First Gear Without Filter

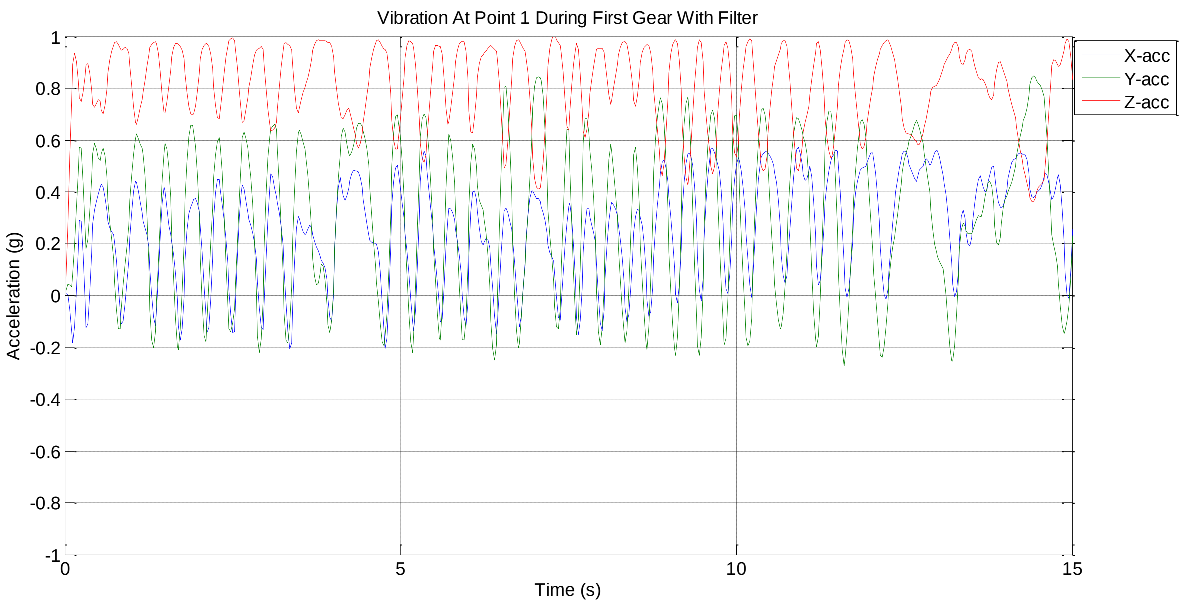

Figure 4.20 (d): Vibration At Point 1 During First Gear With Filter

4.8.2 Point 2

The Figure 4.21 (a) below is the graph plotted using MATLAB software without applying filter showing the vibration experienced by the chassis body during free gear at point 2 while the Figure 4.21 (b) below is the graph plotted using MATLAB software with applied Butterworth low pass filter as smoothing agent.

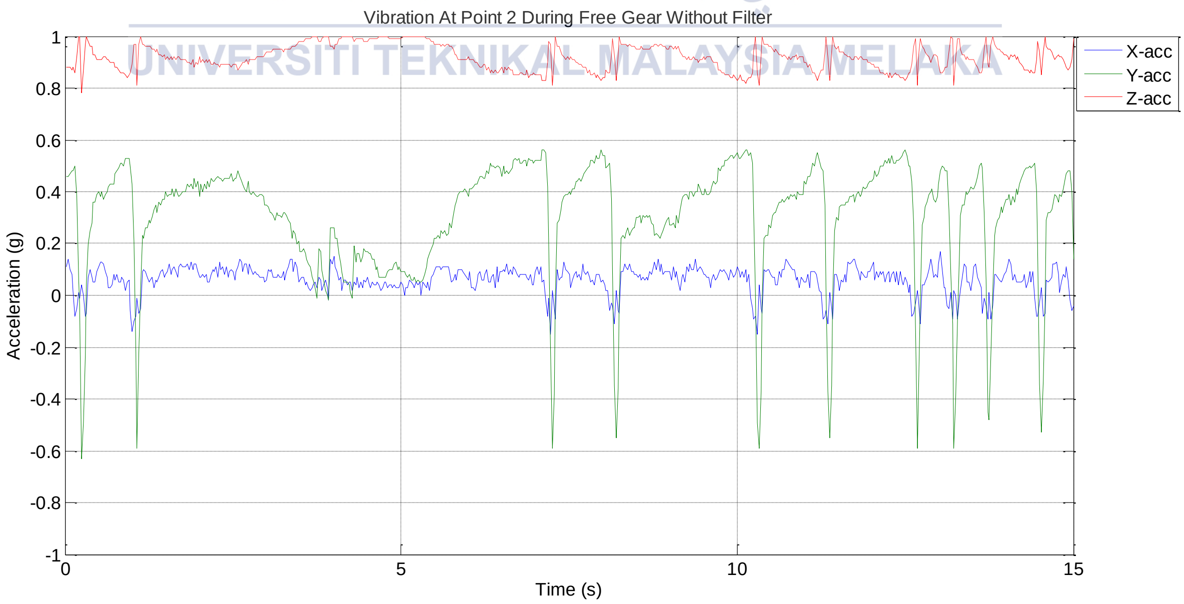

Figure 4.21 (a): Vibration At Point 2 During Free Gear Without Filter

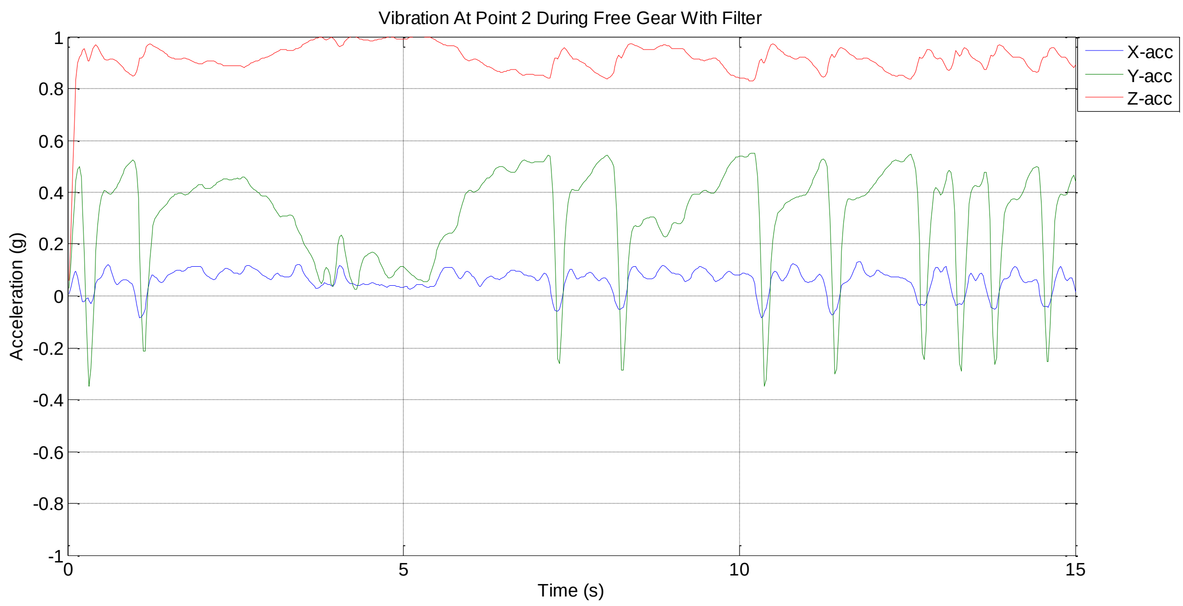

Figure 4.21 (b): Vibration At Point 2 During Free Gear With Filter

The Figure 4.21 (c) below is the graph plotted using MATLAB software without applying filter showing the vibration experienced by the chassis body during first gear at point 2 while the Figure 4.21 (d) below is the graph plotted using MATLAB software with applied Butterworth low pass filter as smoothing agent.

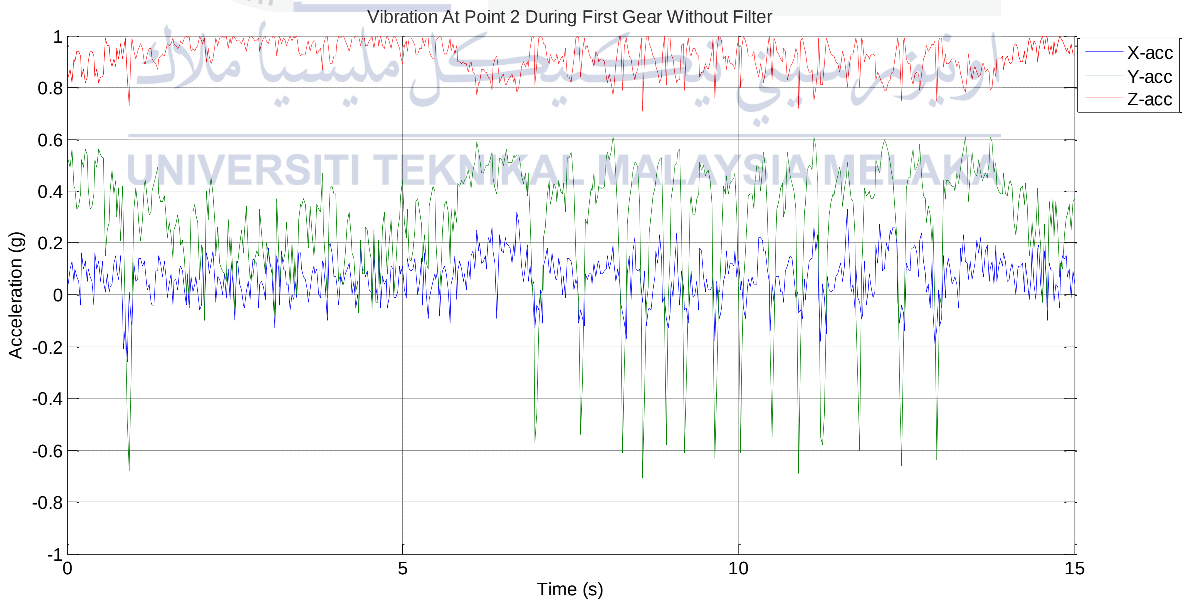

Figure 4.21 (c): Vibration At Point 2 During First Gear Without Filter

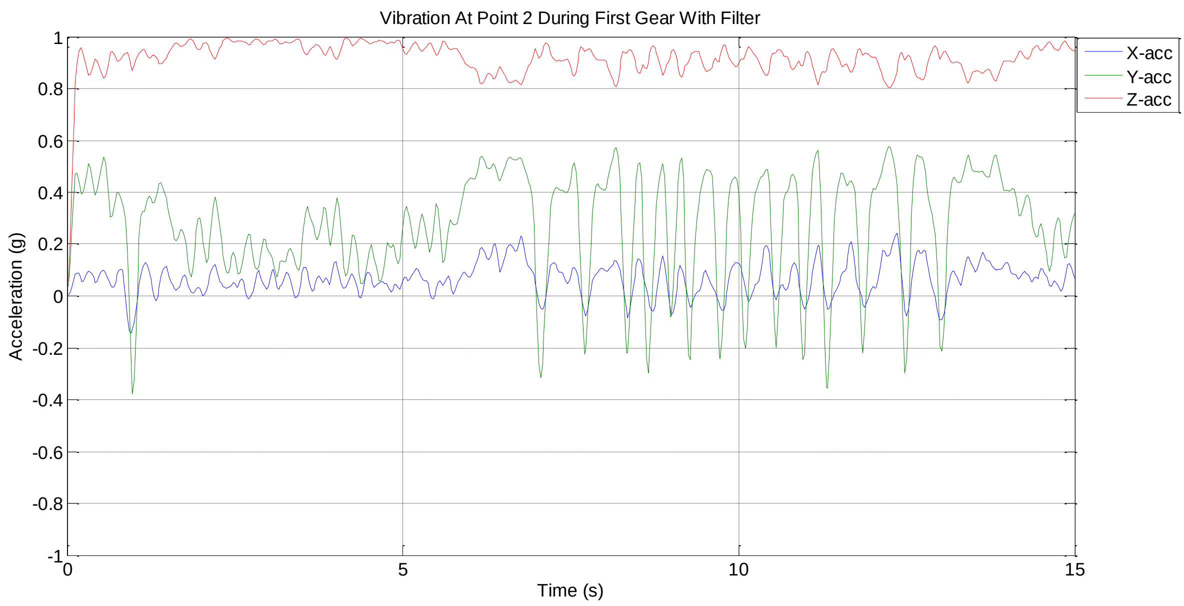

Figure 4.21 (d): Vibration At Point 2 During First Gear With Filter

4.8.3 Point 3

The Figure 4.22 (a) below is the graph plotted using MATLAB software without applying filter showing the vibration experienced by the chassis body during free gear at point 3 while the Figure 4.22 (b) below is the graph plotted using MATLAB software with applied Butterworth low pass filter as smoothing agent.

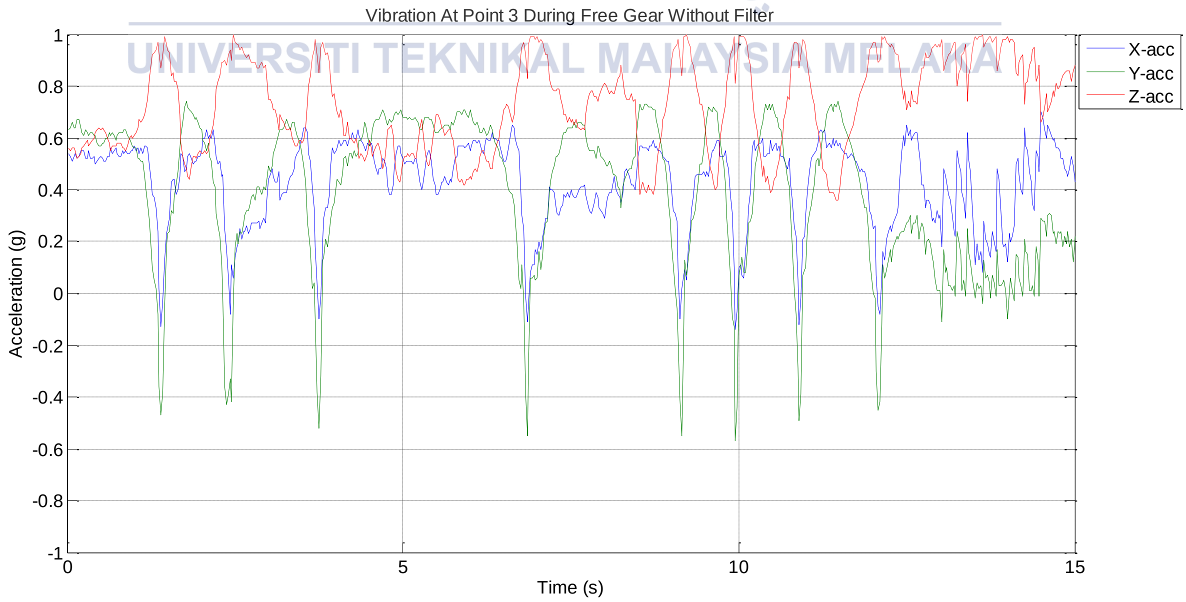

Figure 4.22 (a): Vibration At Point 3 During Free Gear Without Filter

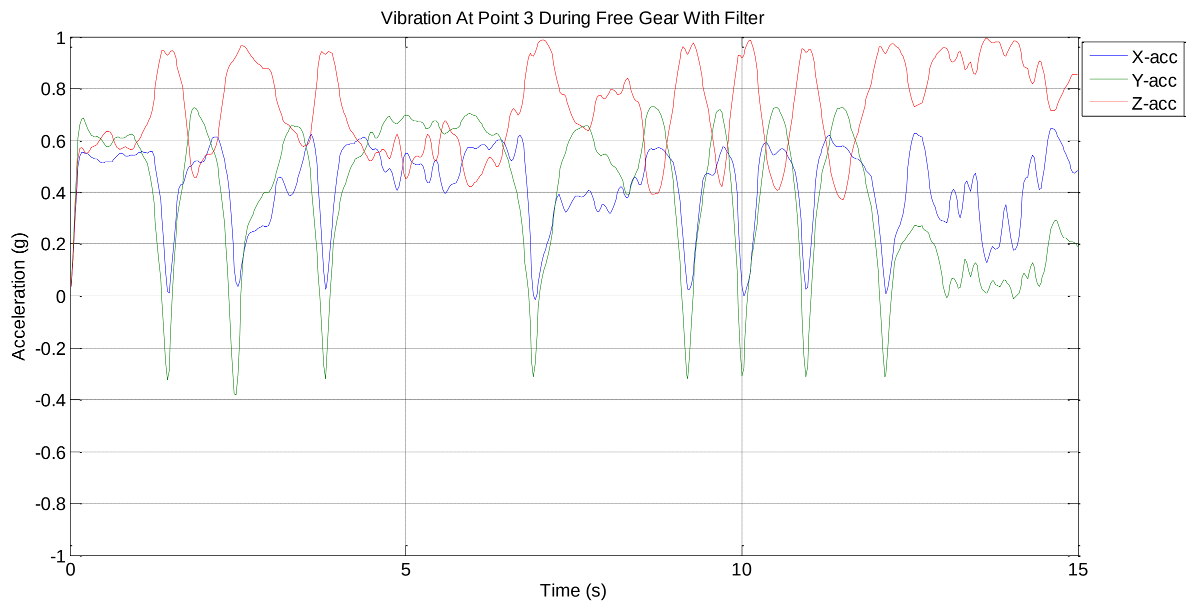

Figure 4.22 (b): Vibration At Point 3 During Free Gear With Filter

The Figure 4.22 (c) below is the graph plotted using MATLAB software without applying filter showing the vibration experienced by the chassis body during first gear at point 3 while the Figure 4.22 (d) below is the graph plotted using MATLAB software with applied Butterworth low pass filter as smoothing agent.

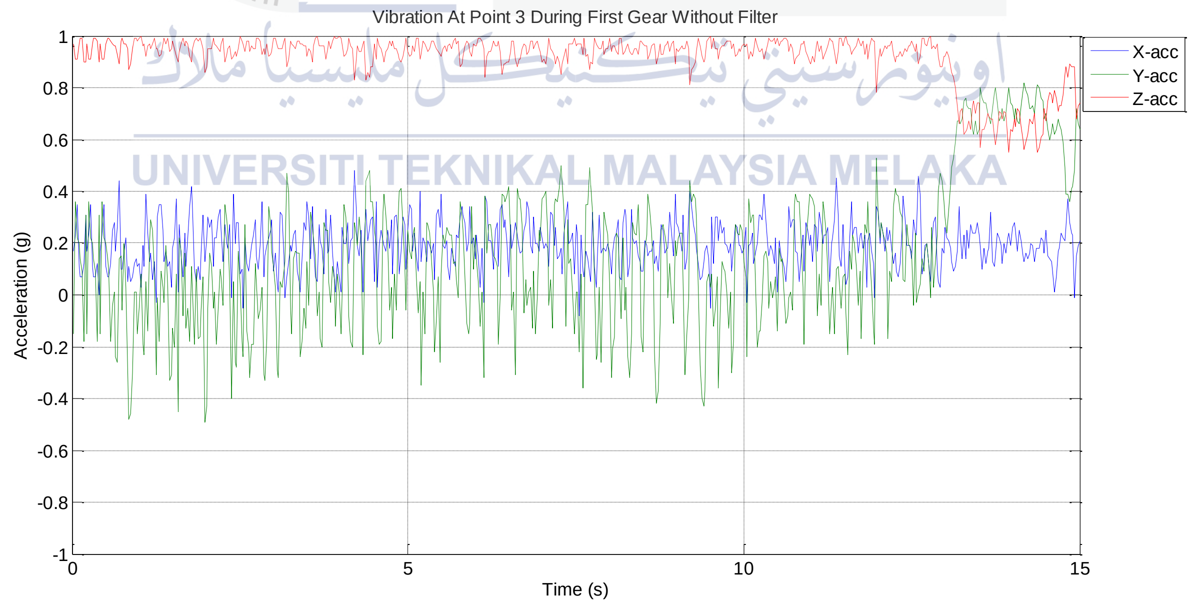

Figure 4.22 (c): Vibration At Point 3 During First Gear Without Filter

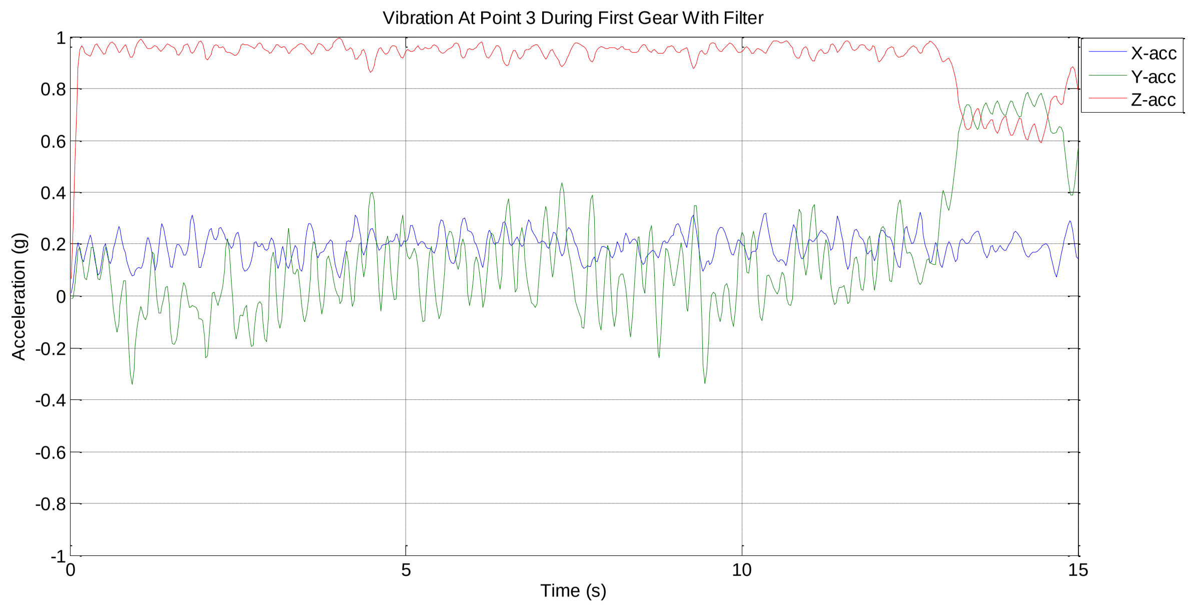

Figure 4.22 (d): Vibration At Point 3 During First Gear With Filter

4.8.4 Point 4

The Figure 4.23 (a) below is the graph plotted using MATLAB software without applying filter showing the vibration experienced by the chassis body during free gear at point 4 while the Figure 4.23 (b) below is the graph plotted using MATLAB software with applied Butterworth low pass filter as smoothing agent.

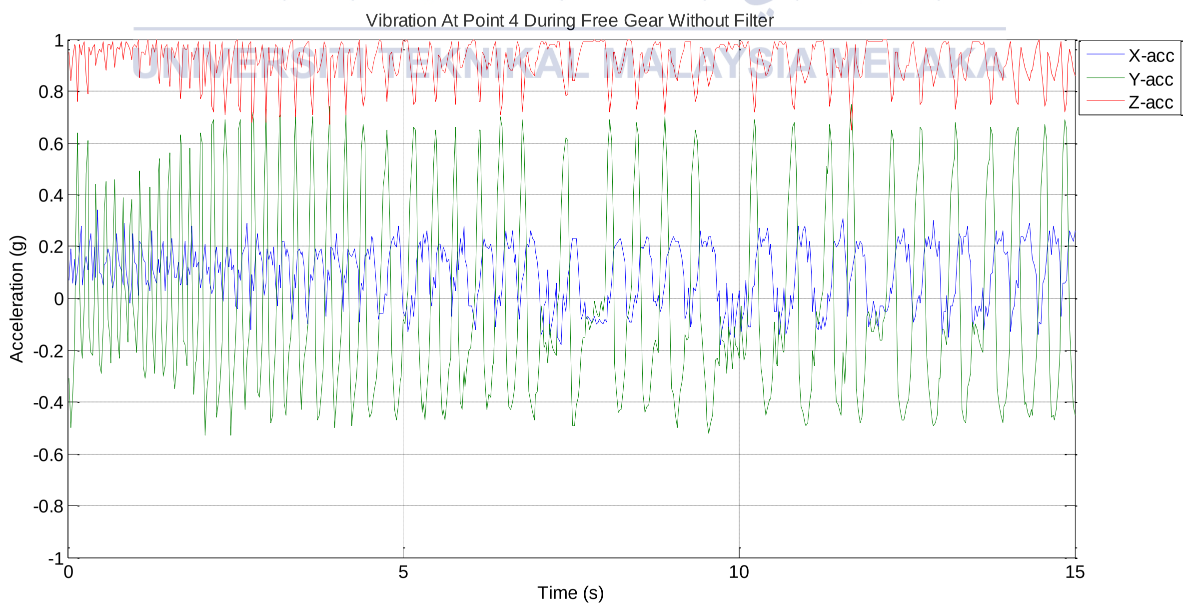

Figure 4.23 (a): Vibration At Point 4 During Free Gear Without Filter

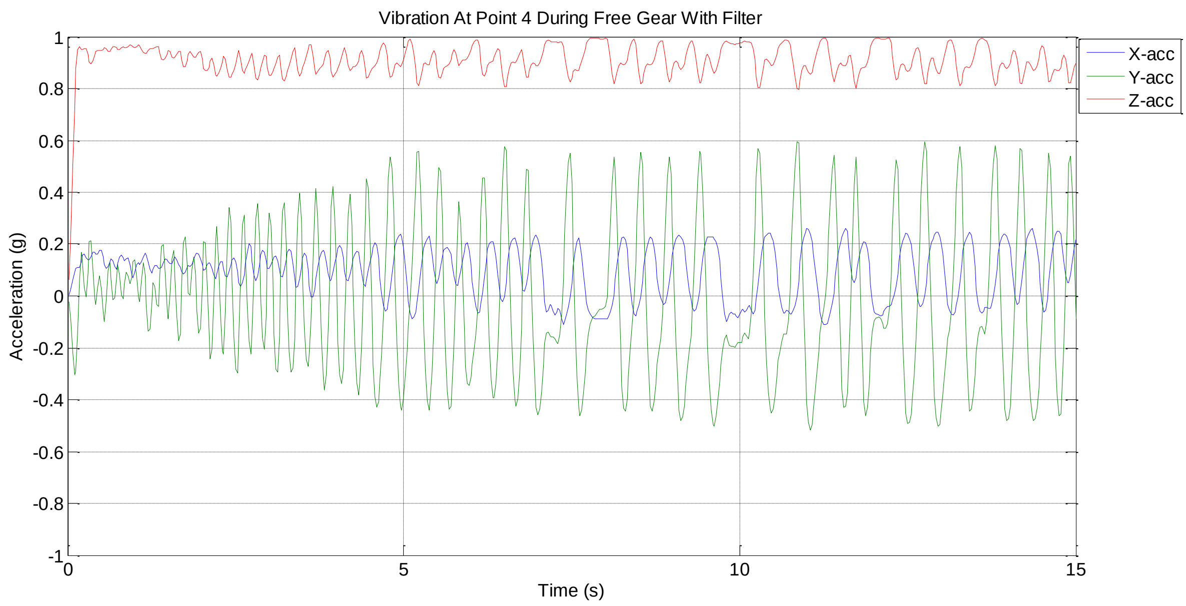

Figure 4.23 (b): Vibration At Point 4 During Free Gear With Filter

The Figure 4.23 (c) below is the graph plotted using MATLAB software without applying filter showing the vibration experienced by the chassis body during first gear at point 4 while the Figure 4.23 (d) below is the graph plotted using MATLAB software with applied Butterworth low pass filter as smoothing agent.

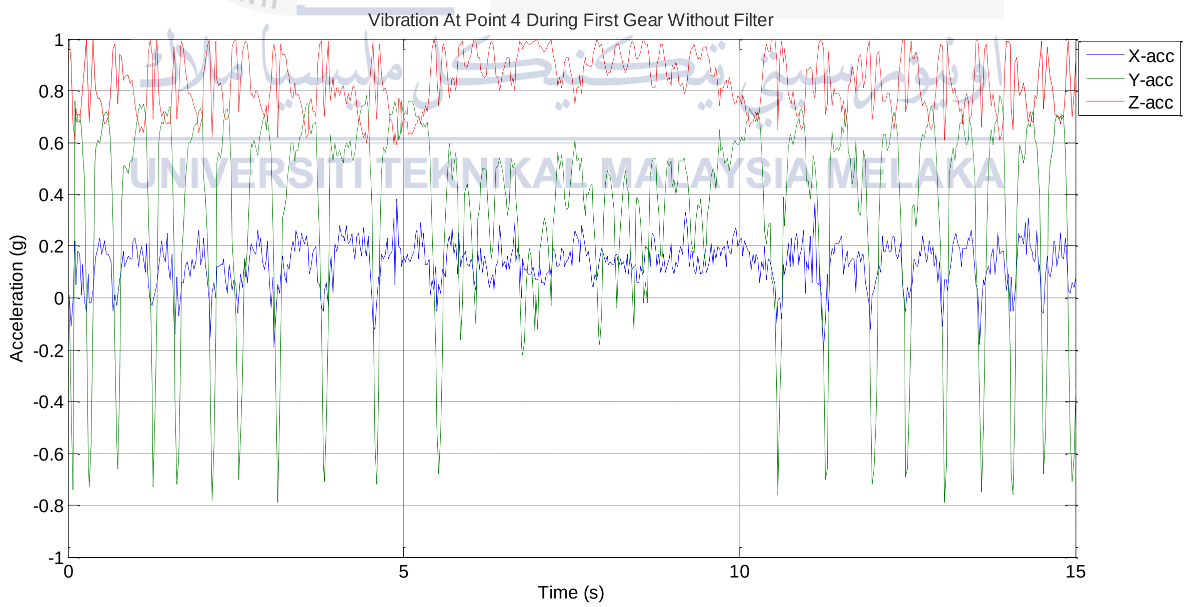

Figure 4.23 (c): Vibration At Point 4 During First Gear Without Filter

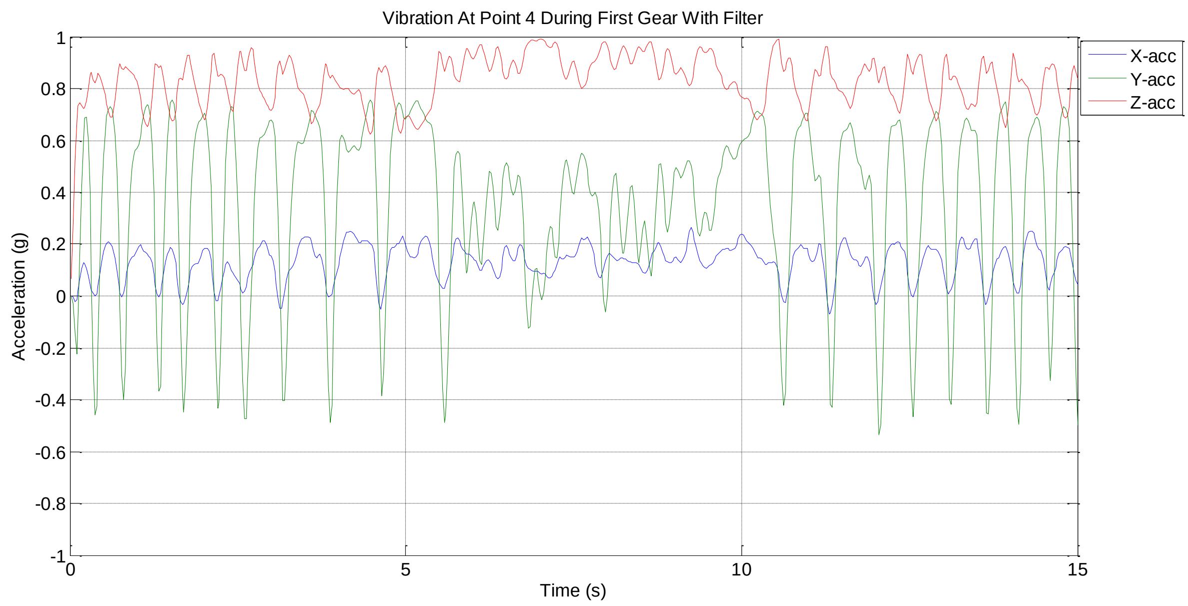

Figure 4.23 (d): Vibration At Point 4 During First Gear With Filter

4.8.5 Point 5

The Figure 4.24 (a) below is the graph plotted using MATLAB software without applying filter showing the vibration experienced by the chassis body during free gear at point 5 while the Figure 4.24 (b) below is the graph plotted using MATLAB software with applied Butterworth low pass filter as smoothing agent.

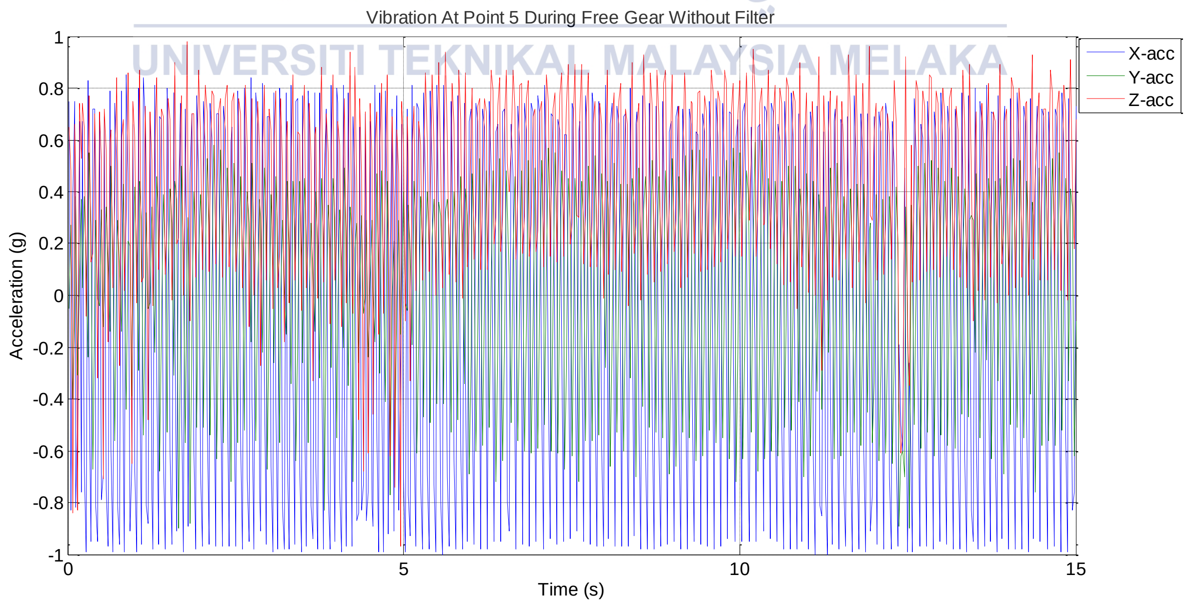

Figure 4.24 (a): Vibration At Point 5 During Free Gear Without Filter

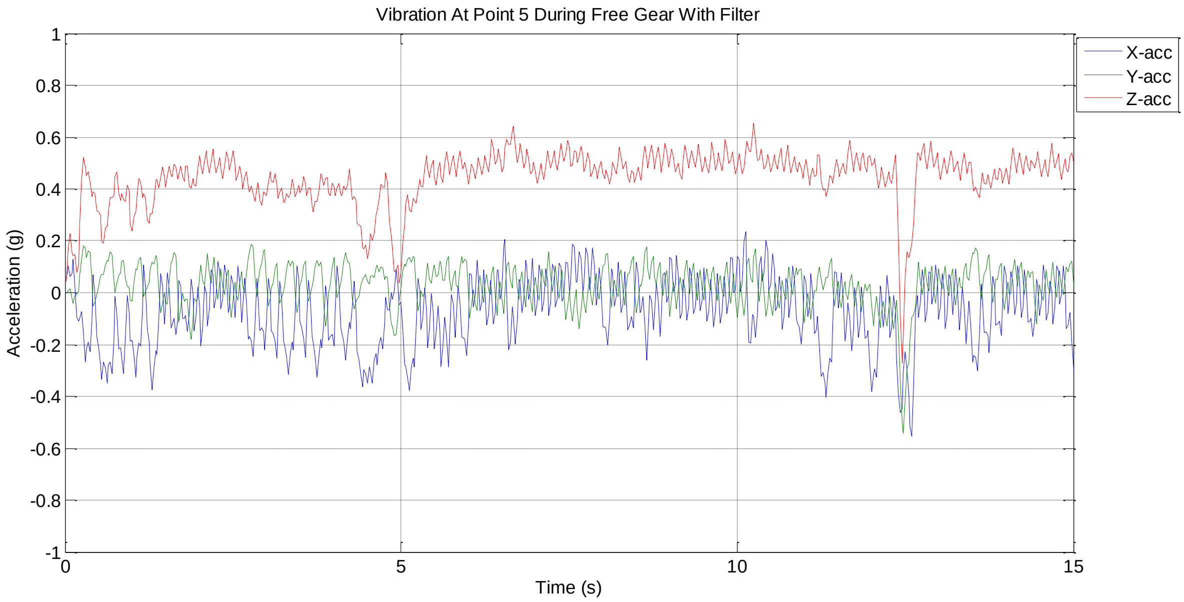

Figure 4.24 (b): Vibration At Point 5 During Free Gear With Filter

The Figure 4.24 (c) below is the graph plotted using MATLAB software without applying filter showing the vibration experienced by the chassis body during first gear at point 5 while the Figure 4.24 (d) below is the graph plotted using MATLAB software with applied Butterworth low pass filter as smoothing agent.

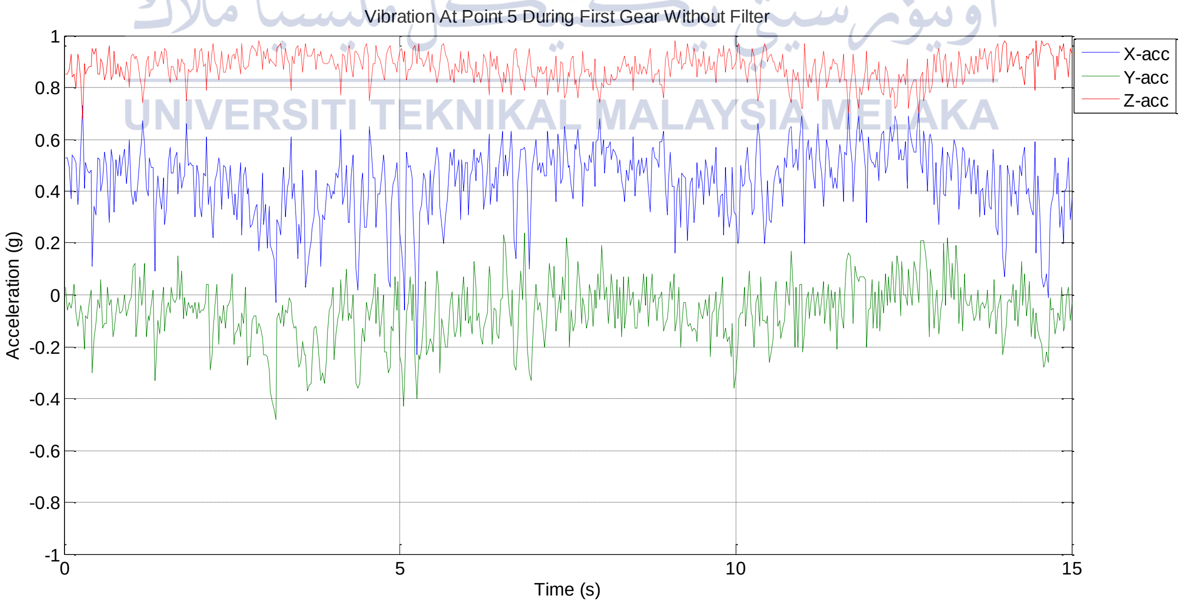

Figure 4.24 (c): Vibration At Point 5 During First Gear Without Filter

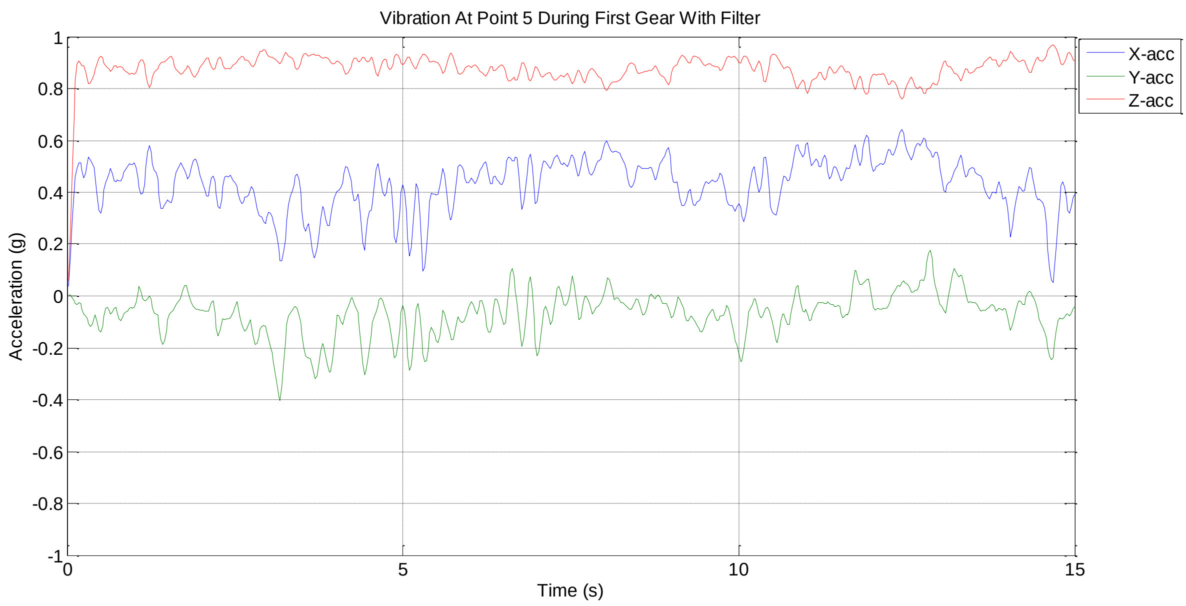

Figure 4.24 (d): Vibration At Point 5 During First Gear With Filter

4.8.6 Point 6

The Figure 4.25 (a) below is the graph plotted using MATLAB software without applying filter showing the vibration experienced by the chassis body during free gear at point 6 while the Figure 4.25 (b) below is the graph plotted using MATLAB software with applied Butterworth low pass filter as smoothing agent.

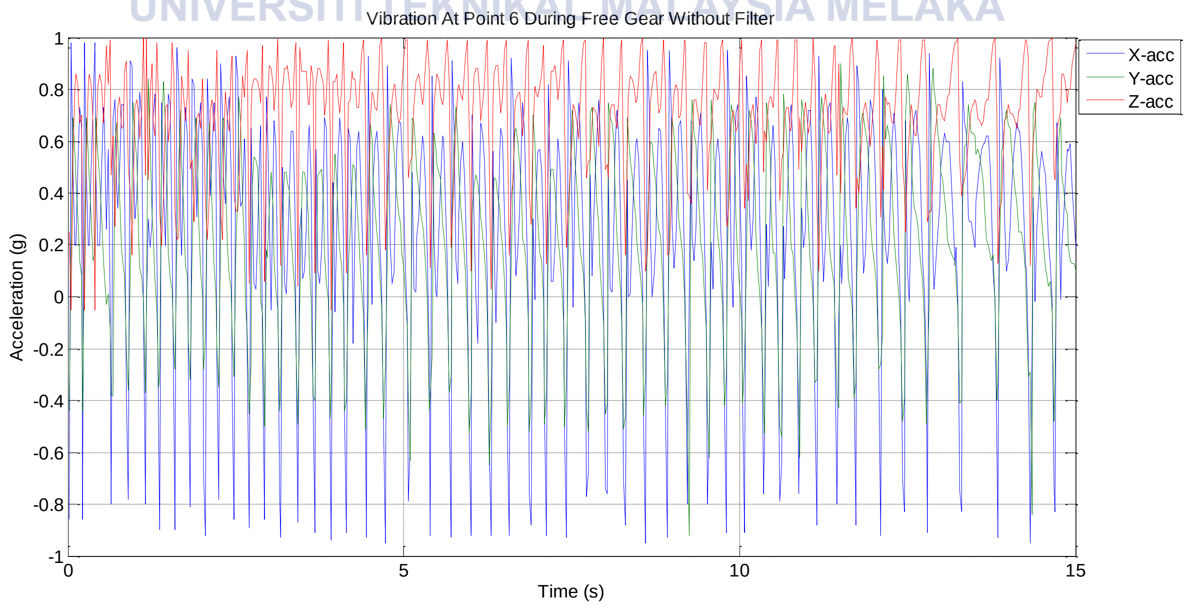

Figure 4.25 (a): Vibration At Point 6 During Free Gear Without Filter

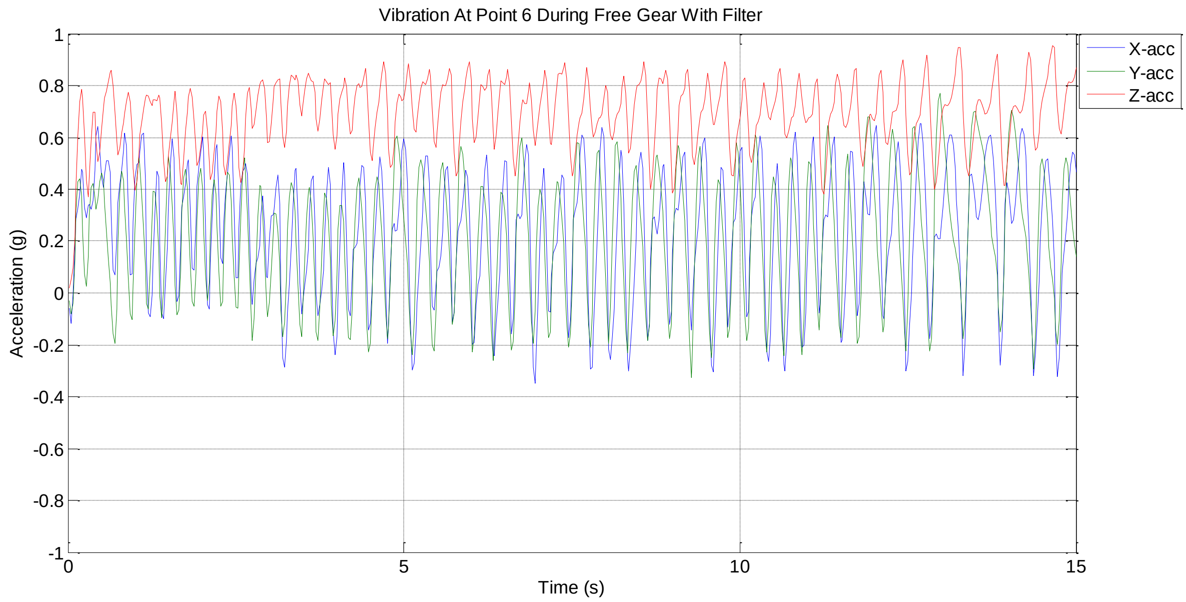

Figure 4.25 (b): Vibration At Point 6 During Free Gear With Filter

The Figure 4.25 (c) below is the graph plotted using MATLAB software without applying filter showing the vibration experienced by the chassis body during first gear at point 1 while the Figure 4.25 (d) below is the graph plotted using MATLAB software with applied Butterworth low pass filter as smoothing agent.

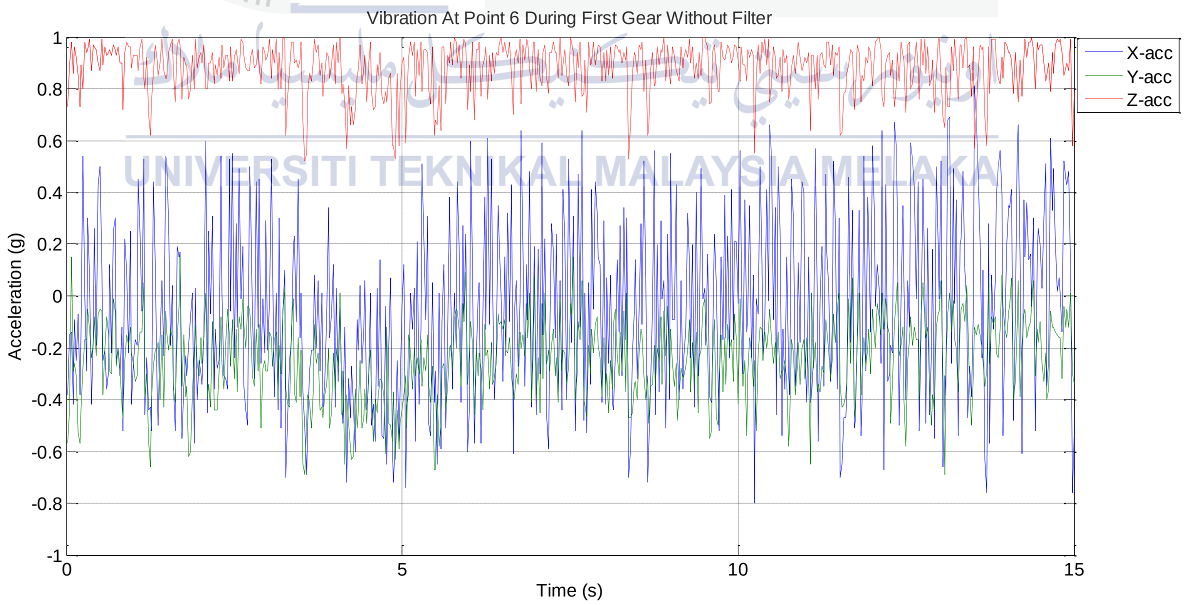

Figure 4.25 (c): Vibration At Point 6 During First Gear Without Filter

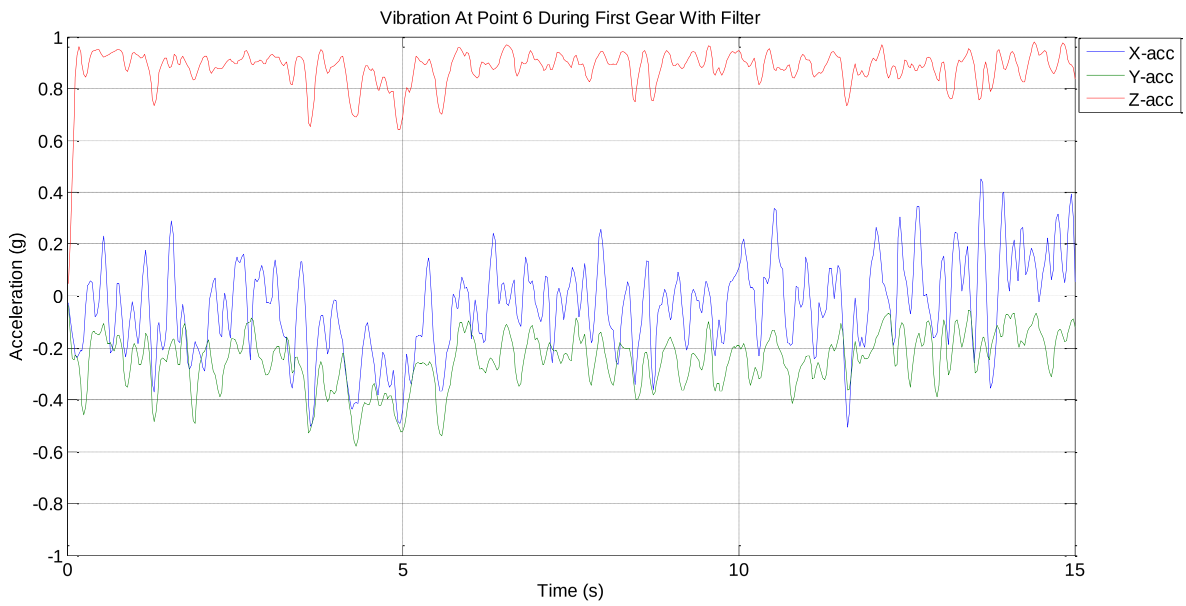

Figure 4.25 (d): Vibration At Point 6 During First Gear With Filter

4.8.7 Point 7

The Figure 4.26 (a) below is the graph plotted using MATLAB software without applying filter showing the vibration experienced by the chassis body during free gear at point 7 while the Figure 4.26 (b) below is the graph plotted using MATLAB software with applied Butterworth low pass filter as smoothing agent.

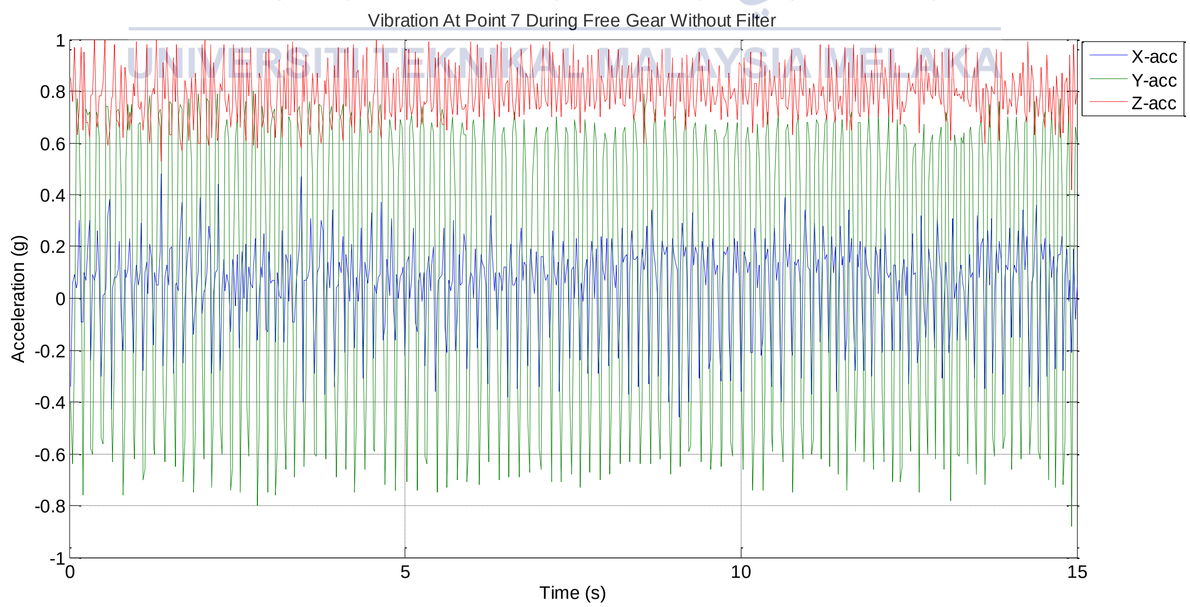

Figure 4.26 (a): Vibration At Point 7 During Free Gear Without Filter

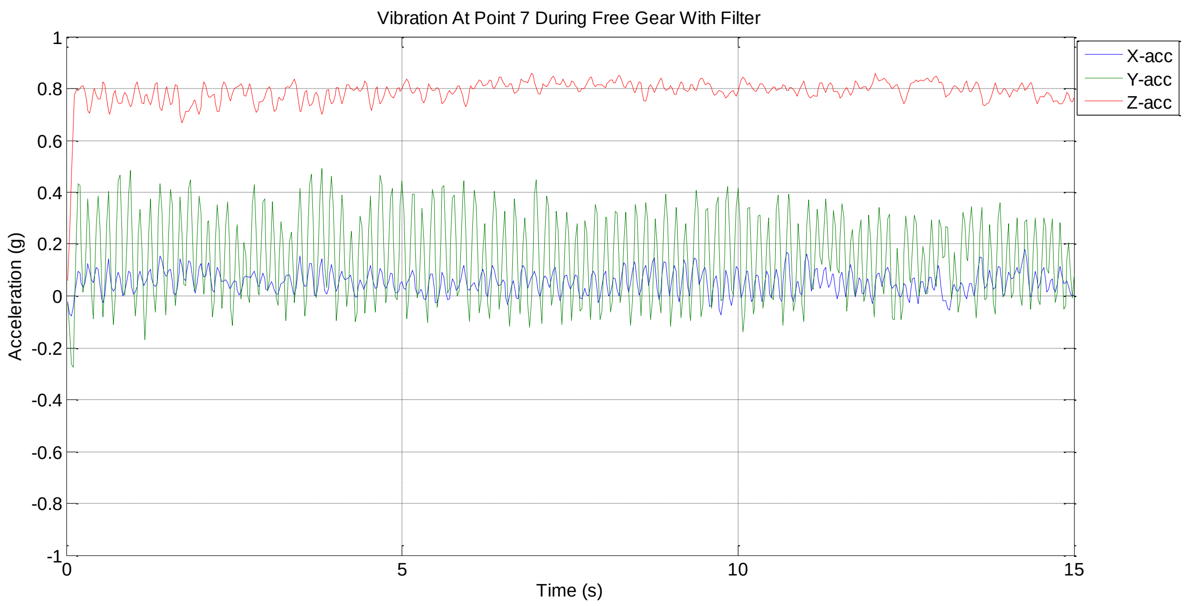

Figure 4.26 (b): Vibration At Point 7 During Free Gear With Filter

The Figure 4.26 (c) below is the graph plotted using MATLAB software without applying filter showing the vibration experienced by the chassis body during first gear at point 7 while the Figure 4.26 (d) below is the graph plotted using MATLAB software with applied Butterworth low pass filter as smoothing agent.

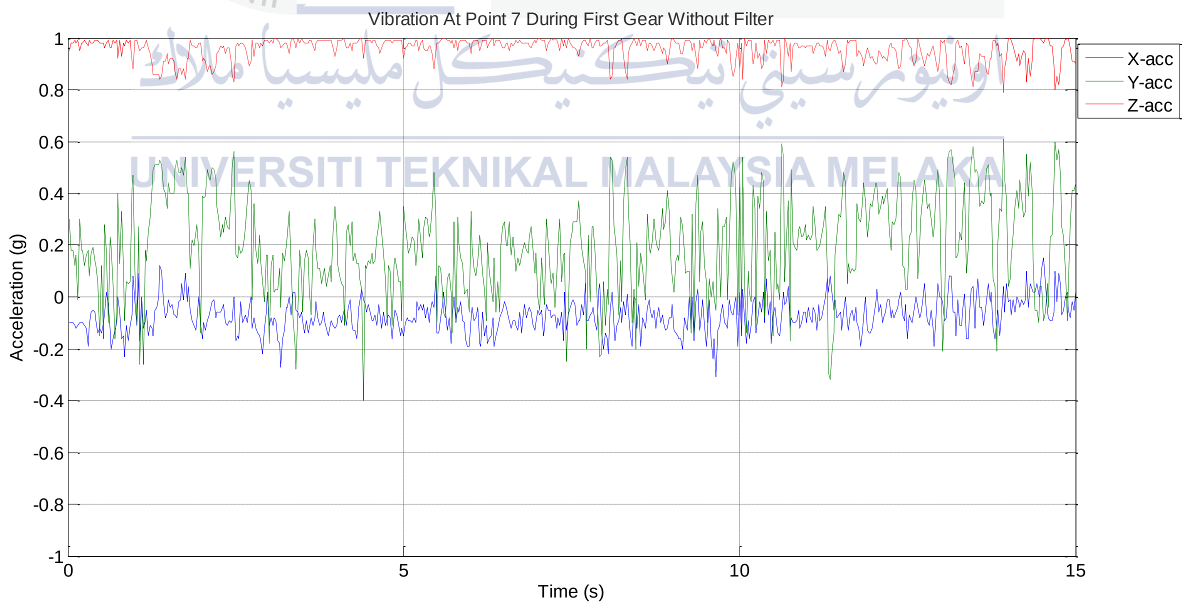

Figure 4.26 (c): Vibration At Point 7 During First Gear Without Filter

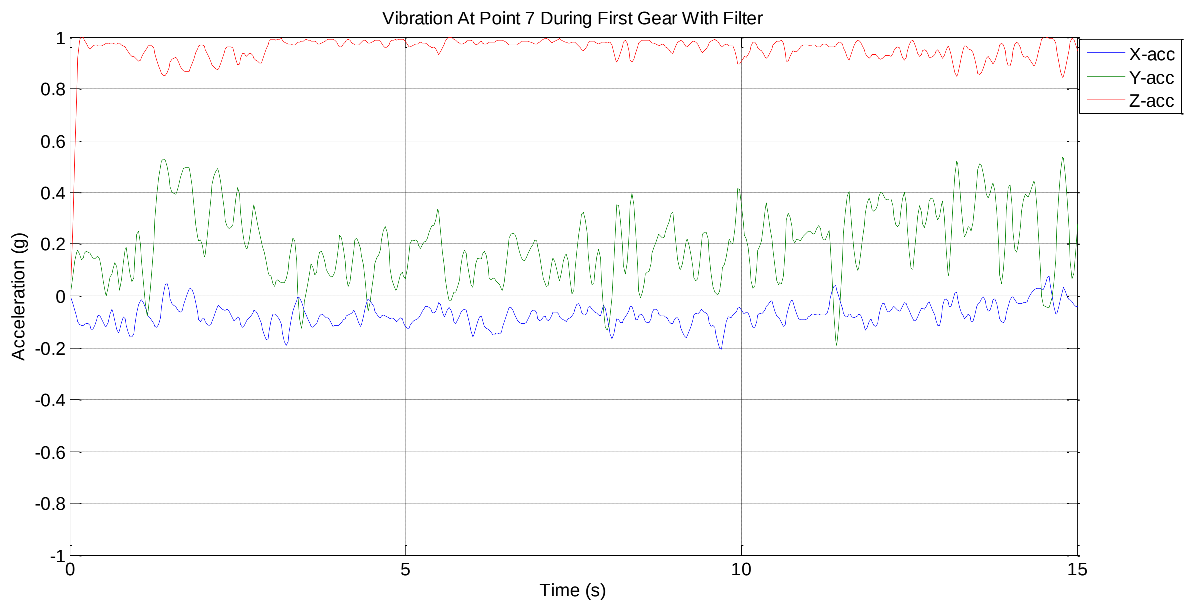

Figure 4.26 (d): Vibration At Point 7 During First Gear With Filter

4.8.8 Point 8

The Figure 4.27 (a) below is the graph plotted using MATLAB software without applying filter showing the vibration experienced by the chassis body during free gear at point 8 while the Figure 4.27 (b) below is the graph plotted using MATLAB software with applied Butterworth low pass filter as smoothing agent.

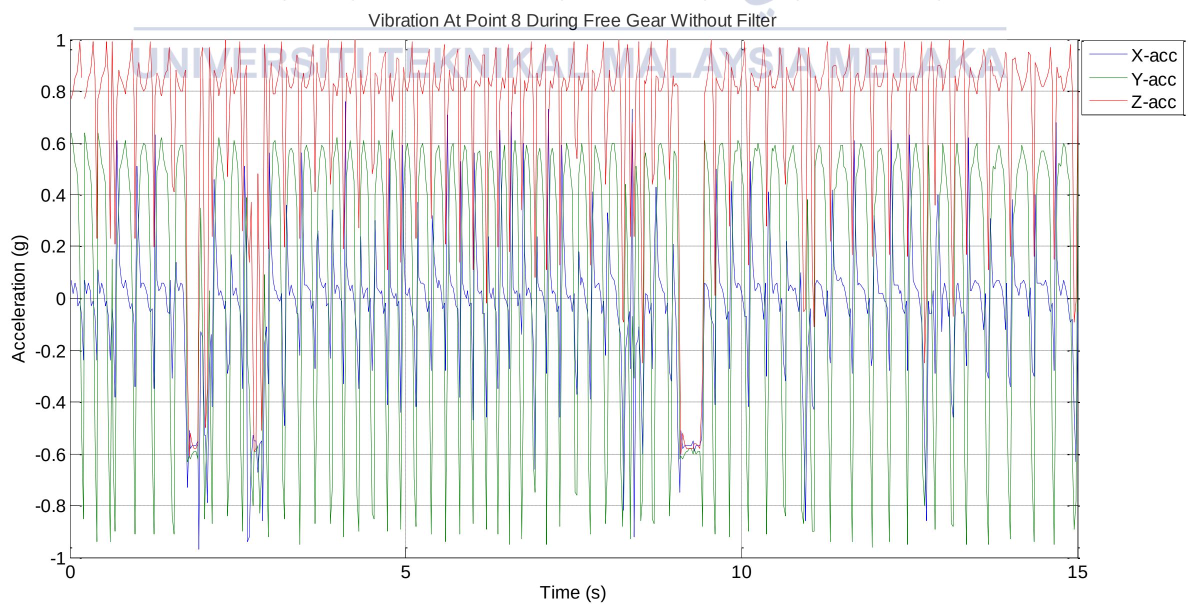

Figure 4.27 (a): Vibration At Point 8 During Free Gear Without Filter

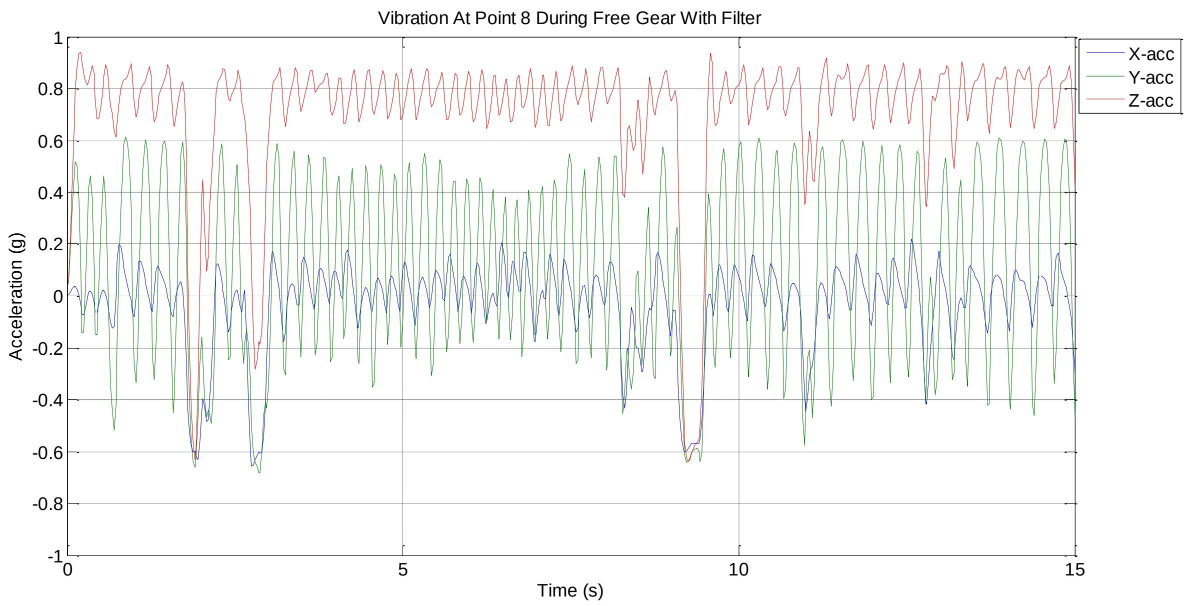

Figure 4.27 (b): Vibration At Point 8 During Free Gear With Filter

The Figure 4.27 (c) below is the graph plotted using MATLAB software without applying filter showing the vibration experienced by the chassis body during first gear at point 8 while the Figure 4.27 (d) below is the graph plotted using MATLAB software with applied Butterworth low pass filter as smoothing agent.

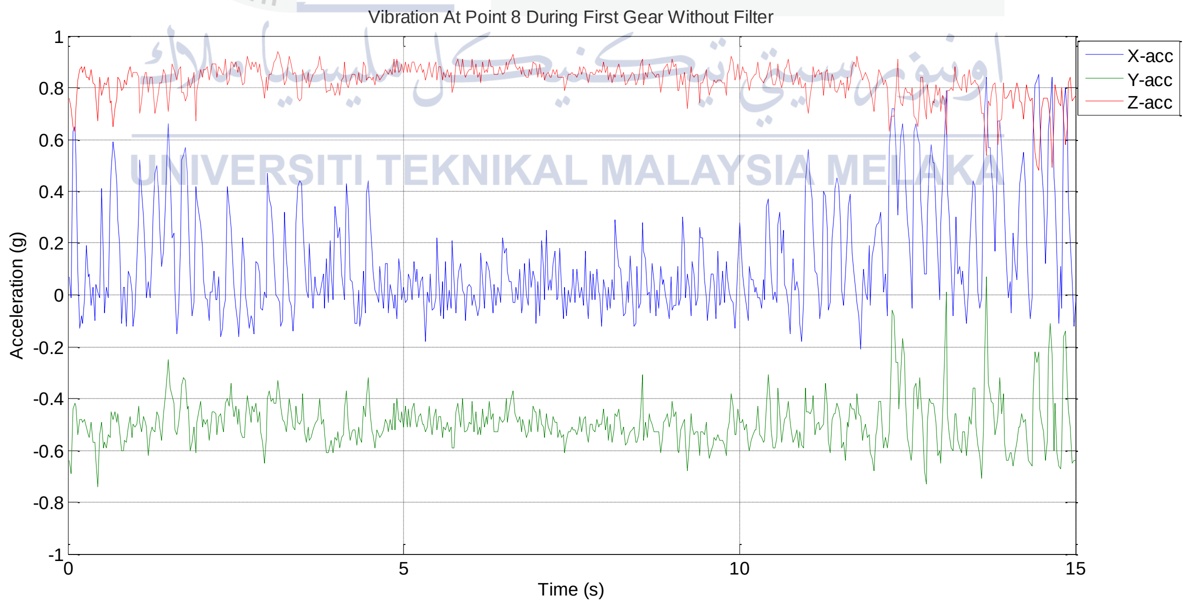

Figure 4.27 (c): Vibration At Point 8 During First Gear Without Filter

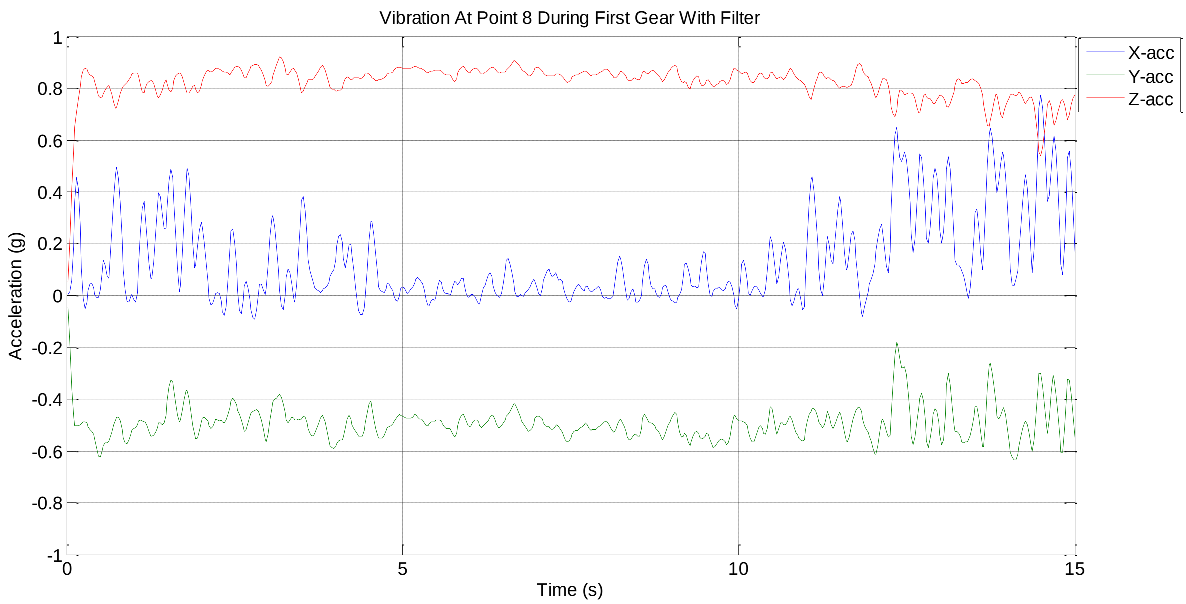

Figure 4.27 (d): Vibration At Point 8 During First Gear With Filter

4.8.9 Point 9

The Figure 4.28 (a) below is the graph plotted using MATLAB software without applying filter showing the vibration experienced by the chassis body during free gear at point 9 while the Figure 4.28 (b) below is the graph plotted using MATLAB software with applied Butterworth low pass filter as smoothing agent.

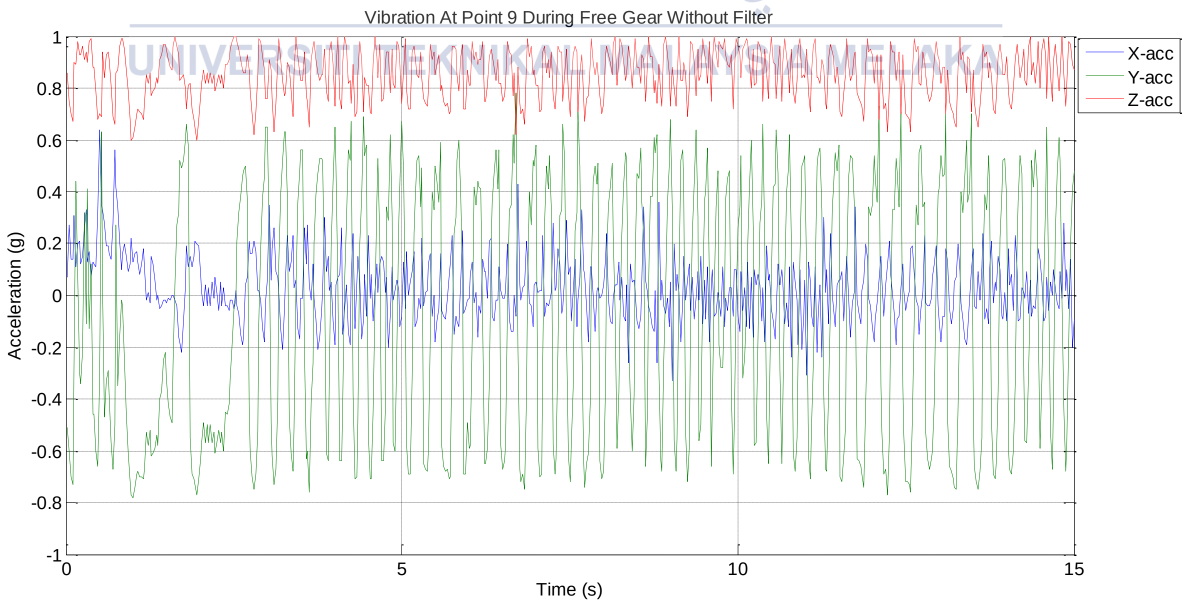

Figure 4.28 (a): Vibration At Point 9 During Free Gear Without Filter

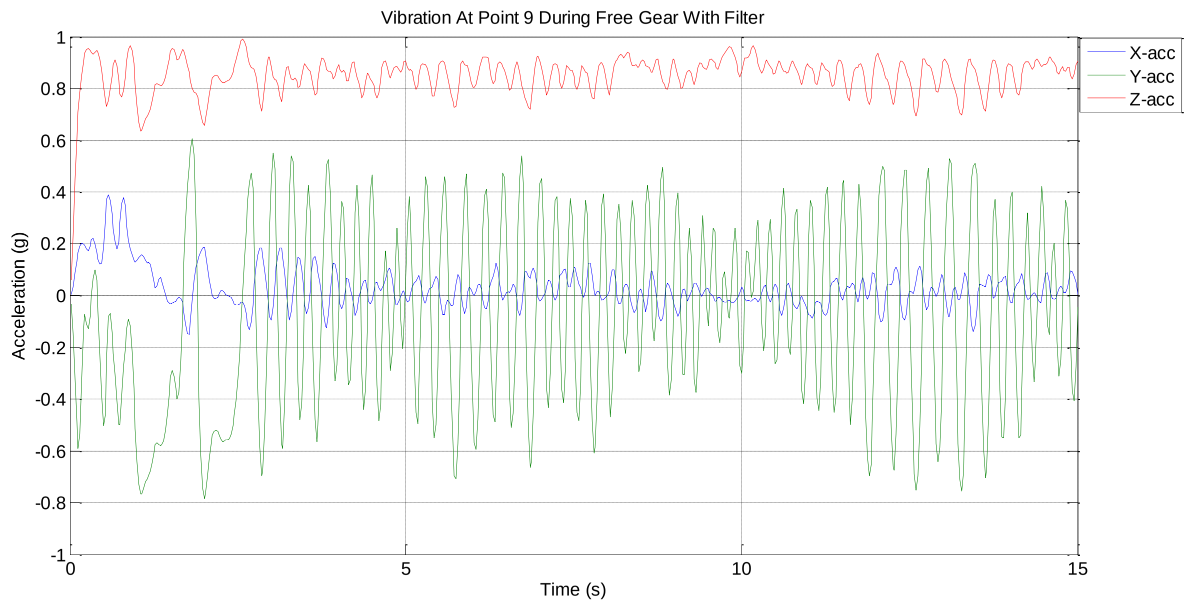

Figure 4.28 (b): Vibration At Point 9 During Free Gear With Filter

The Figure 4.28 (c) below is the graph plotted using MATLAB software without applying filter showing the vibration experienced by the chassis body during first gear at point 9 while the Figure 4.28 (d) below is the graph plotted using MATLAB software with applied Butterworth low pass filter as smoothing agent.

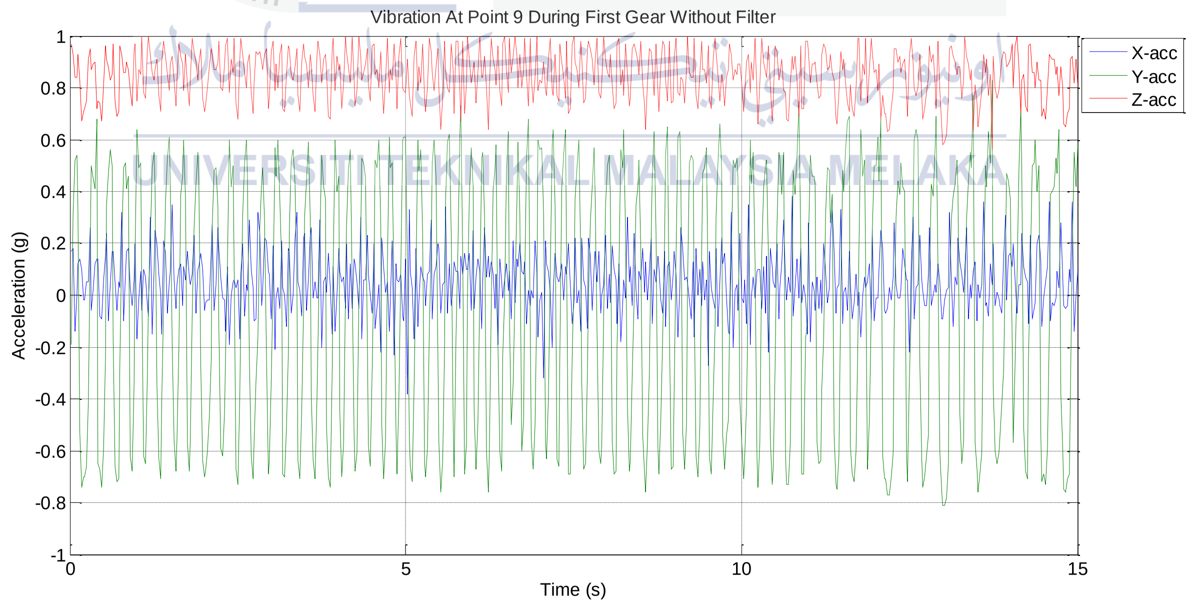

Figure 4.28 (c): Vibration At Point 9 During First Gear Without Filter

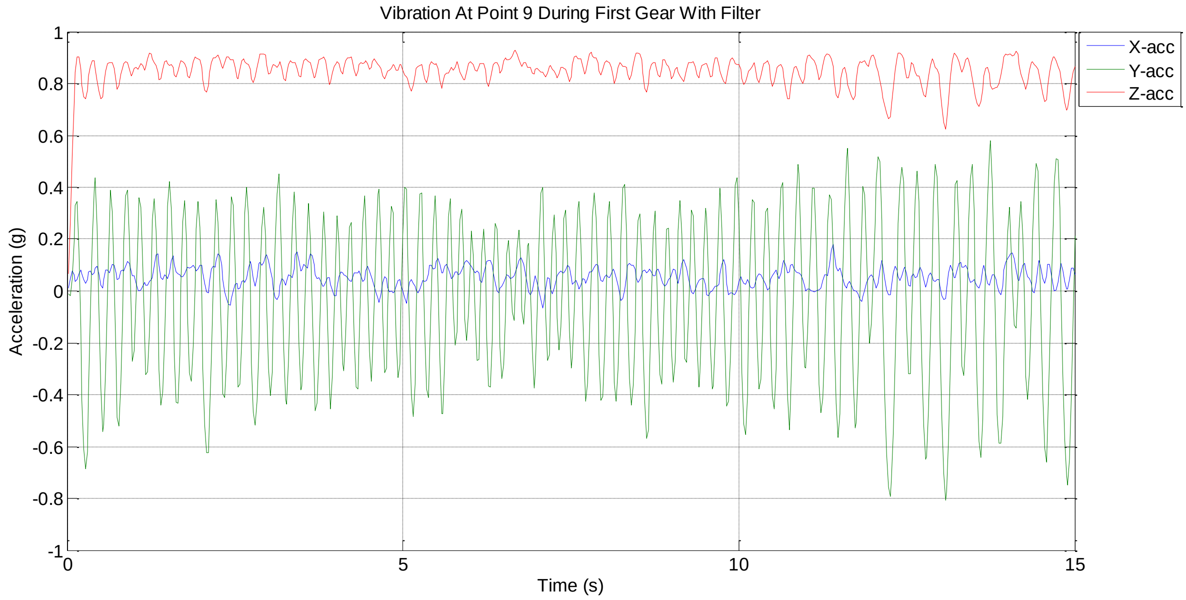

Figure 4.28 (d): Vibration At Point 9 During First Gear With Filter

4.8.10 Point 10

The Figure 4.29 (a) below is the graph plotted using MATLAB software without applying filter showing the vibration experienced by the chassis body during free gear at point 10 while the Figure 4.29 (b) below is the graph plotted using MATLAB software with applied Butterworth low pass filter as smoothing agent.

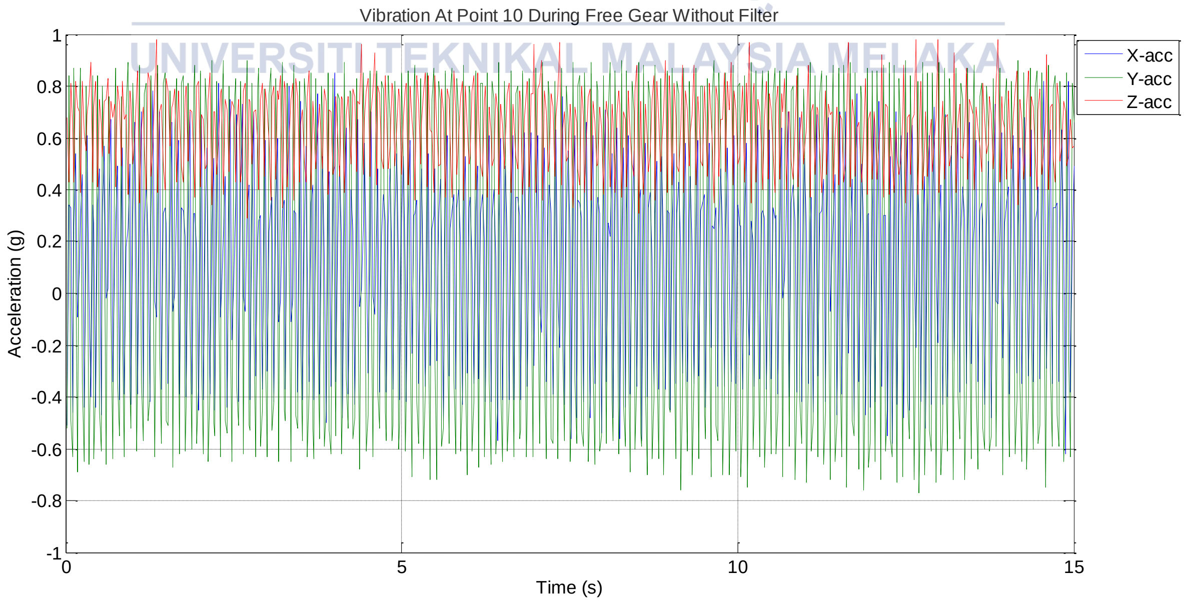

Figure 4.29 (a): Vibration At Point 10 During Free Gear Without Filter

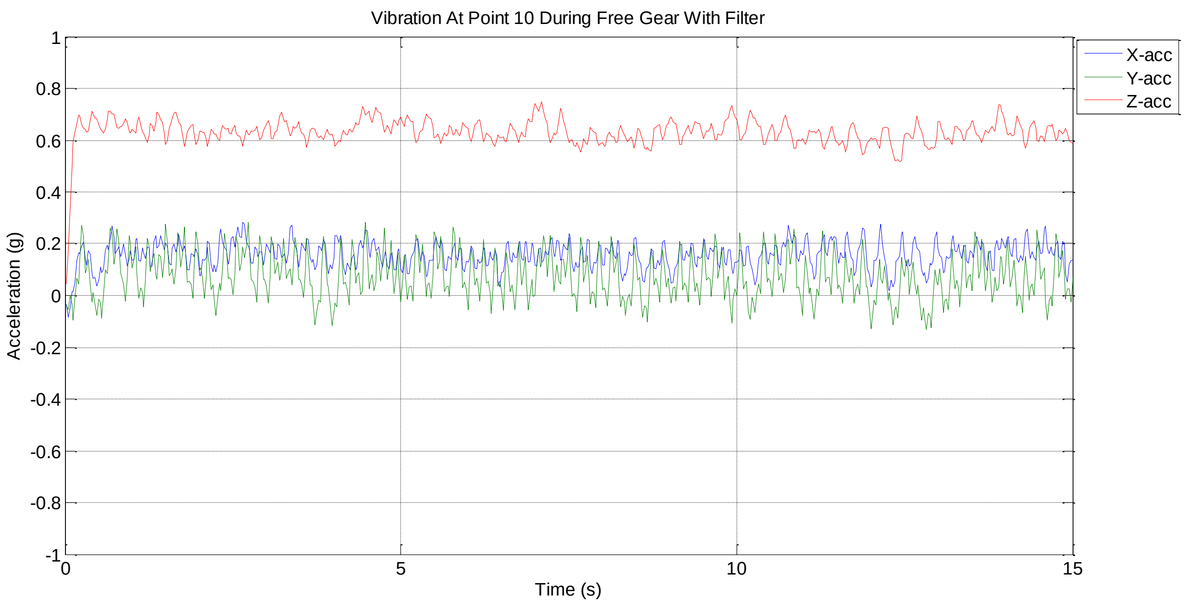

Figure 4.29 (b): Vibration At Point 10 During Free Gear With Filter

The Figure 4.29 (c) below is the graph plotted using MATLAB software without applying filter showing the vibration experienced by the chassis body during first gear at point 10 while the Figure 4.29 (d) below is the graph plotted using MATLAB software with applied Butterworth low pass filter as smoothing agent.

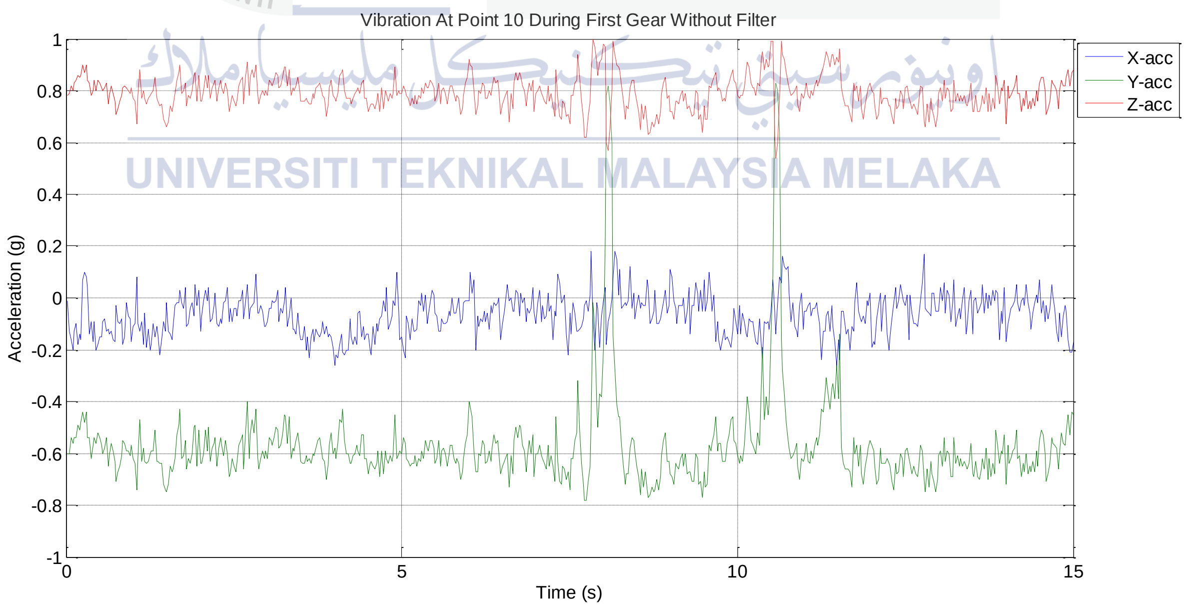

Figure 4.29 (c): Vibration At Point 10 During First Gear Without Filter

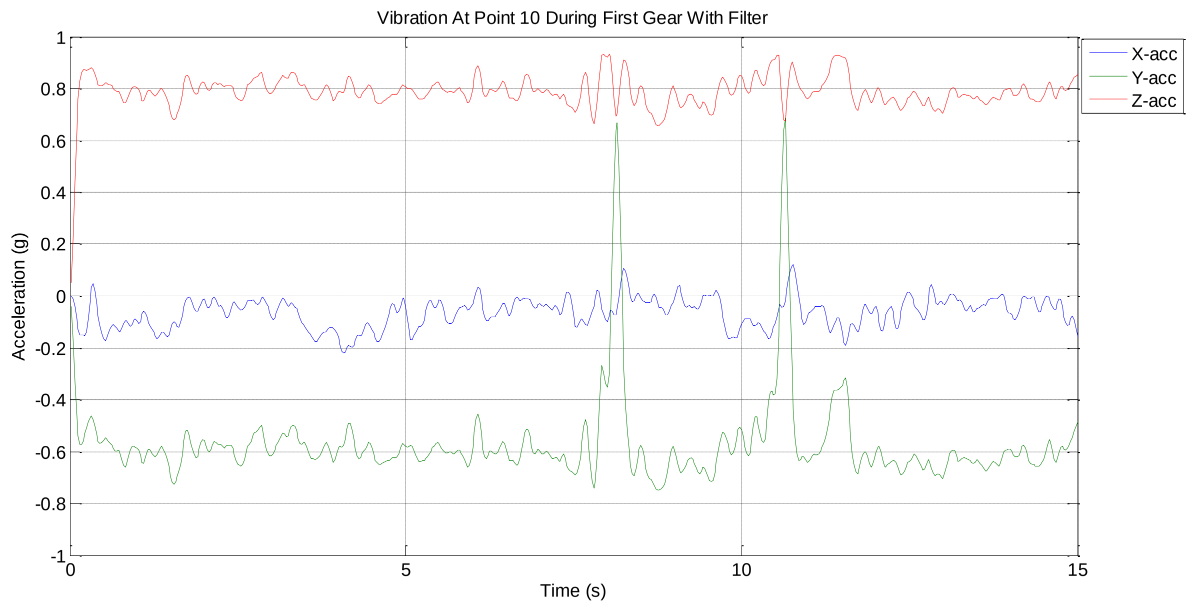

Figure 4.29 (d): Vibration At Point 10 During First Gear With Filter

4.8.11 Point 11

The Figure 4.30 (a) below is the graph plotted using MATLAB software without applying filter showing the vibration experienced by the chassis body during free gear at point 11 while the Figure 4.30 (b) below is the graph plotted using MATLAB software with applied Butterworth low pass filter as smoothing agent.

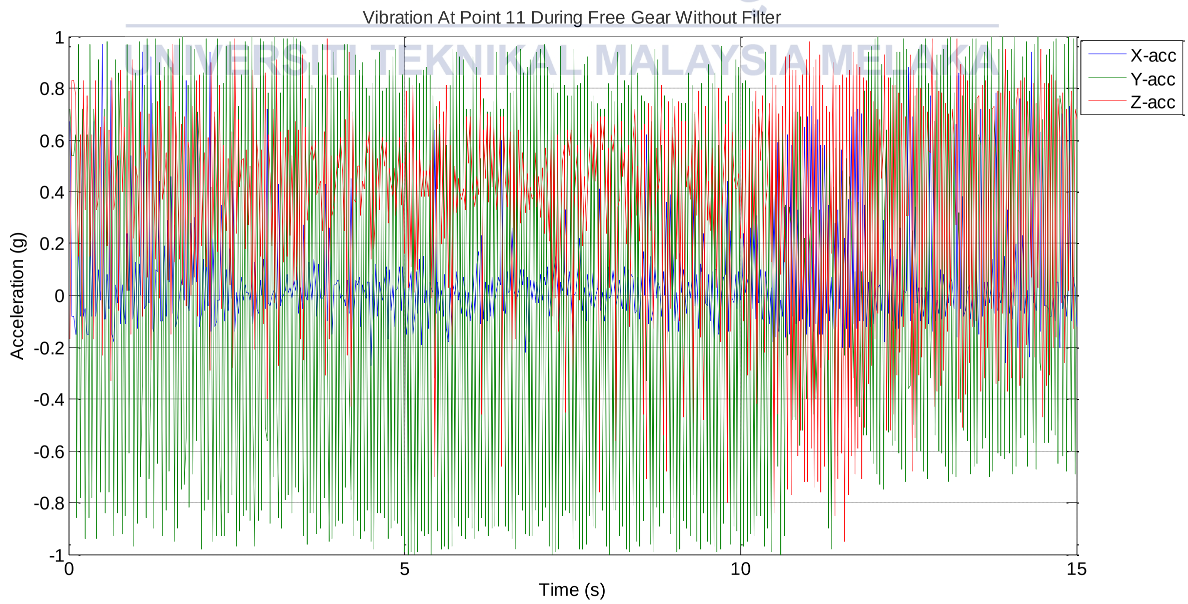

Figure 4.30 (a): Vibration At Point 11 During Free Gear Without Filter

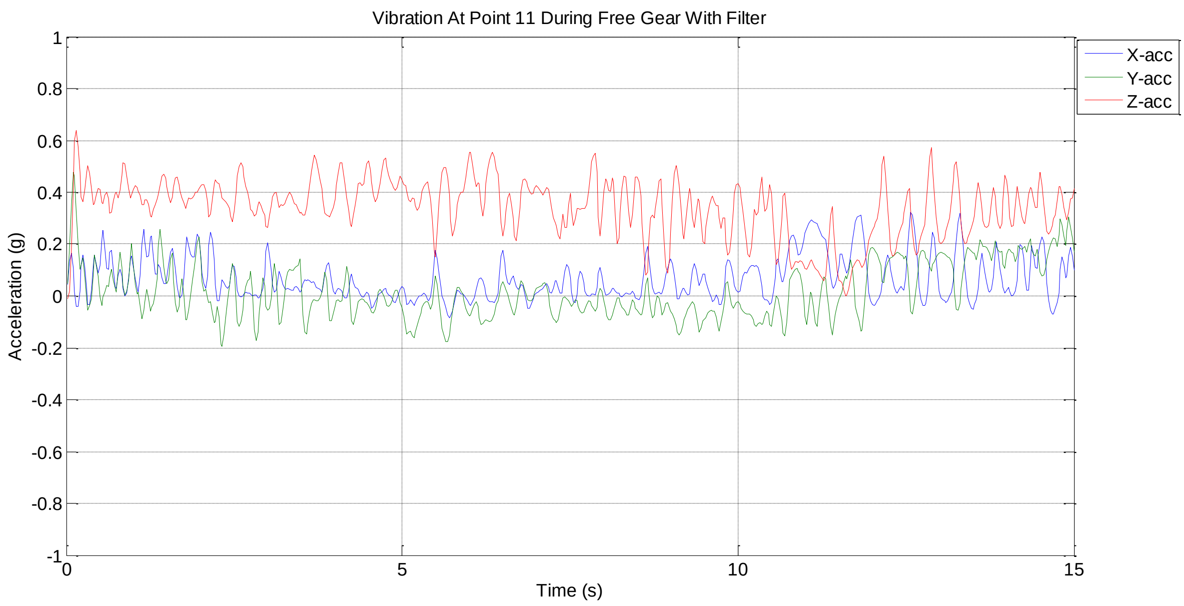

Figure 4.30 (b): Vibration At Point 11 During Free Gear With Filter

The Figure 4.30 (c) below is the graph plotted using MATLAB software without applying filter showing the vibration experienced by the chassis body during first gear at point 11 while the Figure 4.30 (d) below is the graph plotted using MATLAB software with applied Butterworth low pass filter as smoothing agent.

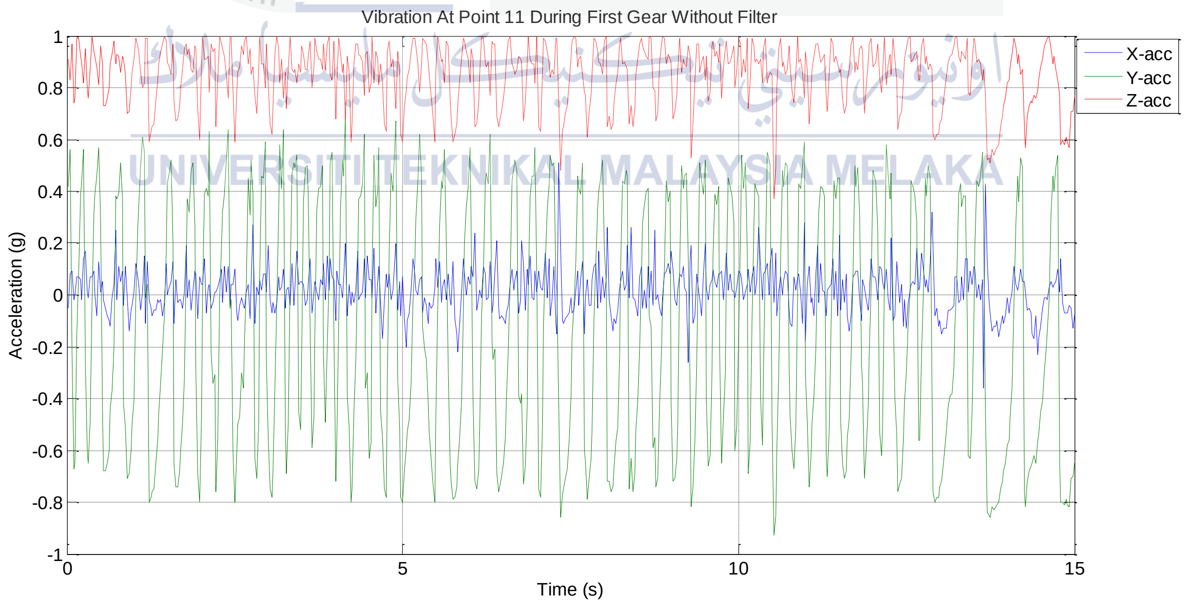

Figure 4.30 (c): Vibration At Point 11 During First Gear Without Filter

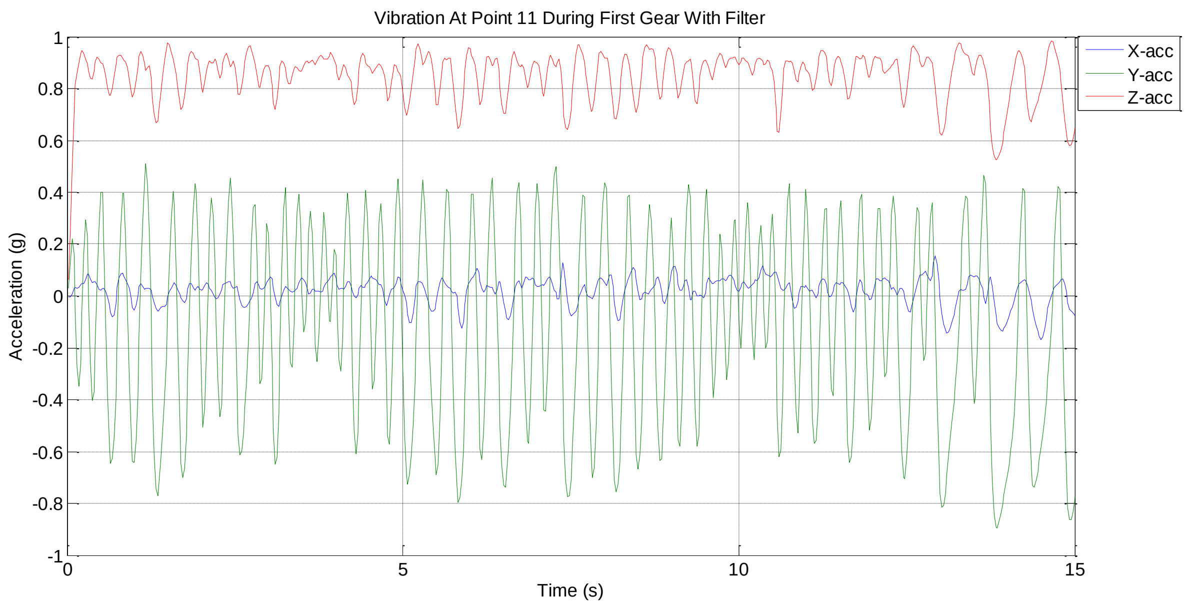

Figure 4.30 (d): Vibration At Point 11 During First Gear With Filter

4.8.12 Point 12

The Figure 4.31 (a) below is the graph plotted using MATLAB software without applying filter showing the vibration experienced by the chassis body during free gear at point 12 while the Figure 4.31 (b) below is the graph plotted using MATLAB software with applied Butterworth low pass filter as smoothing agent.

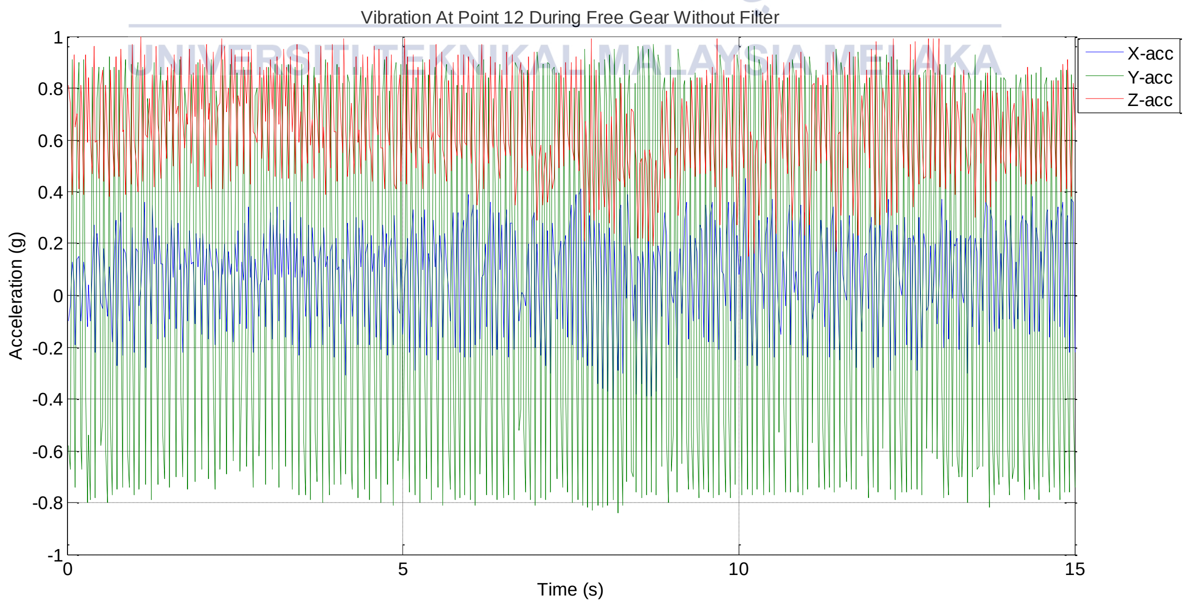

Figure 4.31 (a): Vibration At Point 12 During Free Gear Without Filter

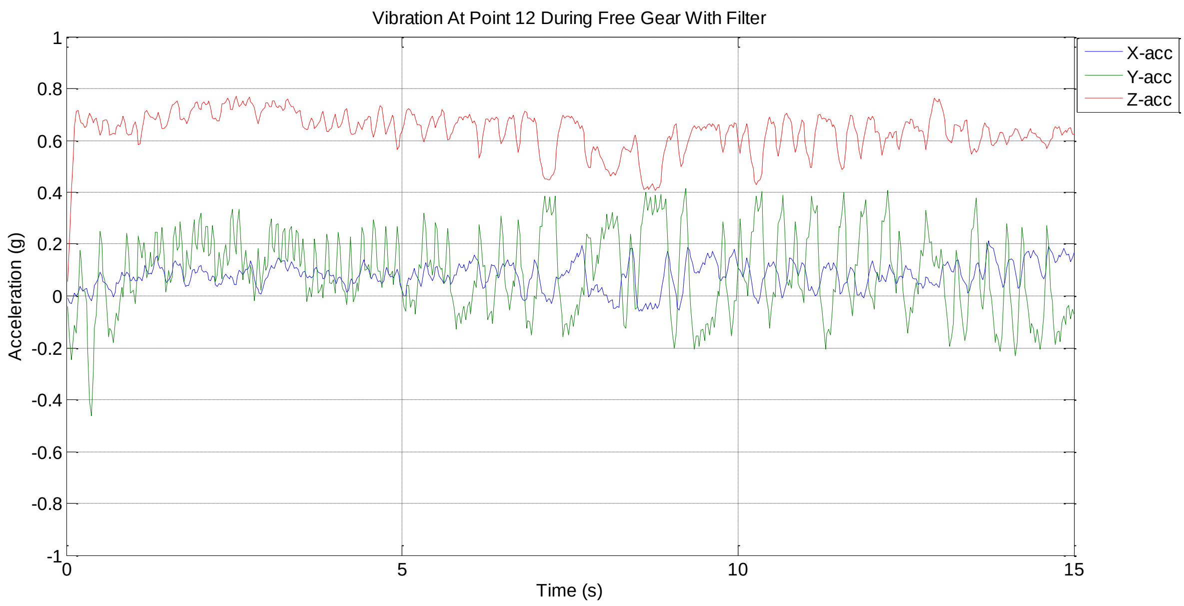

Figure 4.31 (b): Vibration At Point 12 During Free Gear With Filter

The Figure 4.31 (c) below is the graph plotted using MATLAB software without applying filter showing the vibration experienced by the chassis body during first gear at point 12 while the Figure 4.31 (d) below is the graph plotted using MATLAB software with applied Butterworth low pass filter as smoothing agent.

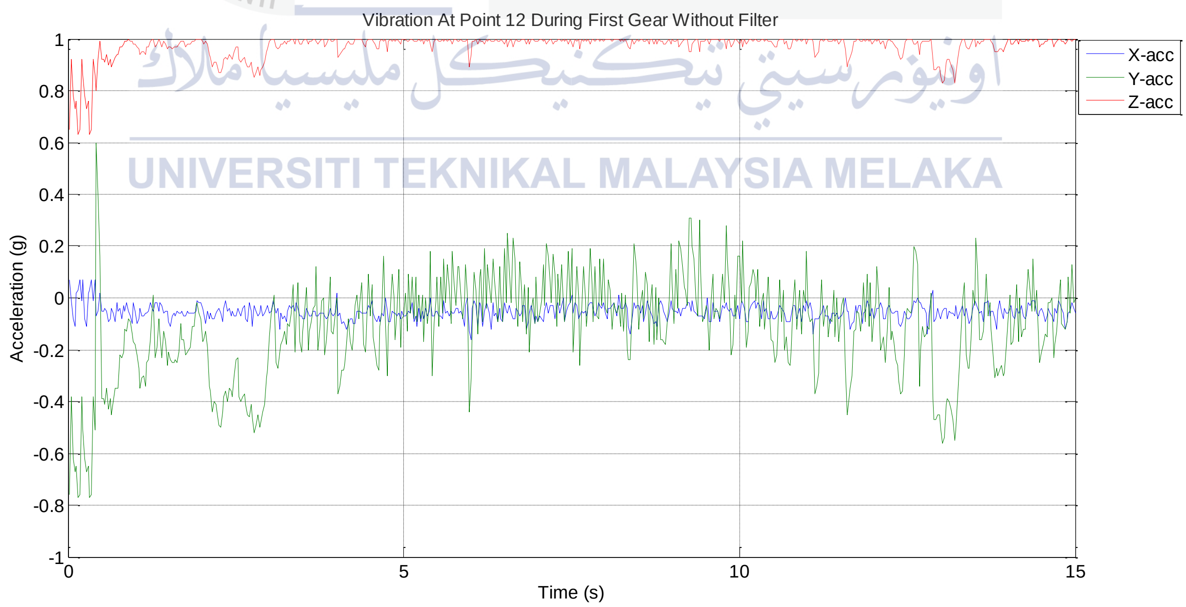

Figure 4.31 (c): Vibration At Point 12 During First Gear Without Filter

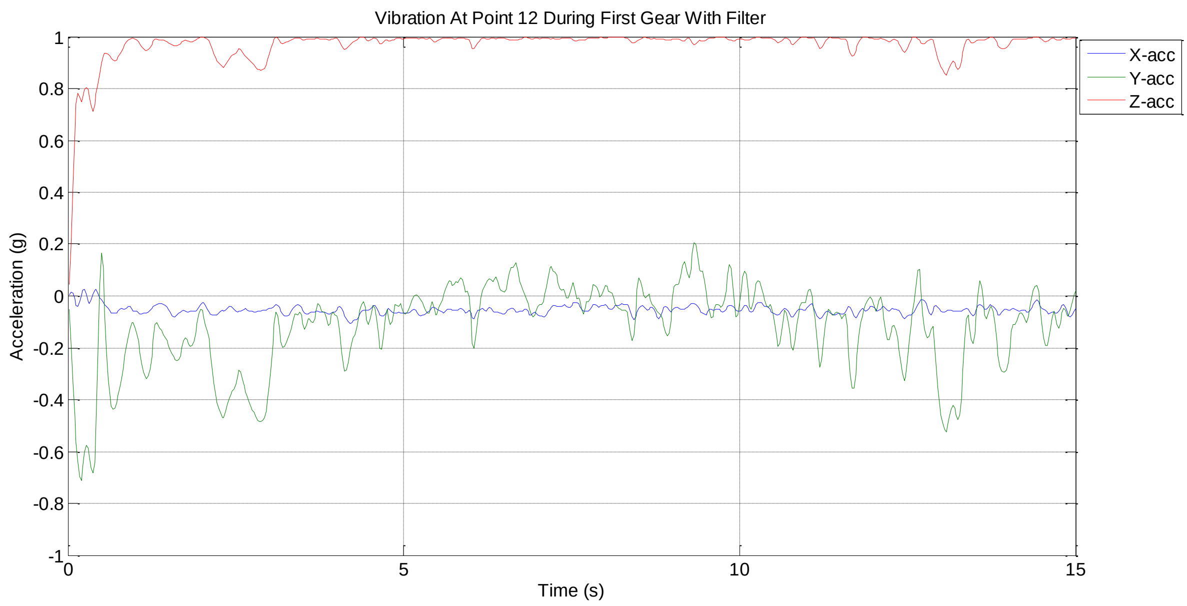

Figure 4.31 (d): Vibration At Point 12 During First Gear With Filter

4.9 Analysis And Discussion (Static Test)

The analysis and discussion of the of the results obtained from the static test are divided into parts which are Von Mises Stress result analysis and discussion, resultant displacement result analysis and discussion and strain equivalent result analysis and discussion.

4.9.1 Von Mises Stress Result Analysis And Discussion

Based on the result shown in Figure 4.10, the Von Mises stress is distributed across the body of the chassis and the yield strength of the structure is at 1.8 x 10^8 Nm^{-2}. The maximum value of Von Mises stress experienced by the body is 1.7893x10^8 Nm^{-2} while the minimum value of Von Mises stress is 1387.39 Nm^{-2}. From the contour that resemble the magnitude of stress, it is clearly seen that most of the part of the structure having the Von Mises stress from the range 1387.39 Nm^{-2} until 5.9644 x 10^7 Nm^{-2}. This has shown that the factor of safety of most part of the chassis structure have the minimum value of 3. This has shown that the chassis structure about to withstand the applied load that we assigned during the test which has the magnitude of 5000N.

However, the Von Mises stress at the joint of the chassis experience higher stress compared to other part. The joint part of the chassis is the part where we applied the method of welding to form the shape of the structure. The Von Mises stress experienced at the joint part is from the range of $5.9644 \text{ x } 10^{7}\ \text{Nm}^{-2}$ until $1.1929 \text{ x } 10^{8}\ \text{Nm}^{-2}$. At the joint part, the factor of safety has the magnitude of 1.5 which need to be improved. Although the factor of safety is at 1.5, but it could be more safety to improve the safety factor until it reaches at least 2 to ensure the safety of the users.

The Von Mises stress is highly concentrated at the joint part due to the area of connection between parts. In order to decrease the stress concentration, the area of connection can be increased by using a mounting brackets. By using the mounting brackets in joint connection, not only the stress concentration can be reduced, it can also increase the strength of the structure due to the increasing of connection with the surface of the chassis.

4.9.2 Resultant Displacement Result Analysis And Discussion

Based on Figure 4.11, the maximum resultant displacement experienced by the chassis structure has the magnitude of 2.323mm while the minimum resultant displacement has the magnitude of $1.0 \text{ x } 10^{-30}$. From the contour diagram shown in Figure 4.11, the front and the rear part near to the fixture experienced the least displacement while the middle part of the chassis where the applied load is located experienced the most resultant displacement.

The resultant displacement of the structure could be significant due to the pressure from the applied load is acting on the supporting square tube is high. Based on the bending of the figure, the structure of the chassis has to be modified to increase the support at the middle part of the chassis to ensure minimum displacement. The uses of rubber mounting or increases the number of supporting tube could be the solution in reducing the resultant displacement. The usage of mounting could absorb some of the pressure exerted during the load applied to the structure. The increases of supporting tube on the chassis structure could allow the applied load to be distributed or divided to other portion of the chassis and reduces the resultant displacement.

The higher the resultant displacement could causes the structure of the chassis become unstable or even breaks. Furthermore, the higher the displacement could also cause the centre of mass of the structure to deviate and cause the structure to be imbalance. Imbalance in a chassis structure could cause the efficiency and the performance of the whole vehicle to drop indirectly.

4.9.3 Strain Equivalent Result Analysis And Discussion

Strain experienced by the chassis structure can be seen from the Figure 4.12. The figure shown the strain distribution on the chassis structure, having the highest strain of 7.038 x 10^{-4} and the lowest strain of 7.679 x 10^{-9}. Similar to the Von Mises stress distribution, the strain distribution has the highest concentration at the joint of the chassis structure based on the contour. At the joint of the structure, the strain concentration is at the range from 3.519 x 10^{-4} till 7.038 x 10^{-4} which the magnitude need to be taken considerably. The magnitude of strain concentration at that particular location has to be reduced. Besides that, the minimum strain concentration at the range of 7.679 x 10^{-9} until 1.173 x 10^{-5} on most location of the chassis structure can be considered as low strain concentration.

The higher the strain experienced by the chassis structure determines the easier the structure of the chassis to displace or experience elongation. Strain can be reduced by reducing the stress experienced by the chassis structure since stress and strain are having direct correlation relationship. Therefore, the method of reducing stress can also been applied to reduce the strain experienced by the structure.

4.10 Analysis And Discussion (Vibration Test)

The analysis and discussion of the of the results obtained from the vibration test are divided into 4 parts which are vibration analysis which are vibration analysis in rear part of the chassis for free gear and first gear, vibration analysis in middle part of the chassis for free gear and first gear, vibration analysis in front part of the chassis for free gear and first gear and discussion. The analysis of the vibration is based on the unfiltered and filtered graphs plotted using MATLAB software based on the data extracted from 12 testing points on the chassis using Inertial Measurement Unit (IMU). The graphs shown the acceleration of the vibration that illustrated as g, having the magnitude of gravitational acceleration, g of 9.81m/s ? The graphs for all points are benchmarked using the graphs obtained from [18] related to a vibration testing on an engine of 500cc while the engine of this project is petrol engine of 80cc. The graphs obtained are shown in Figure 4.32 below

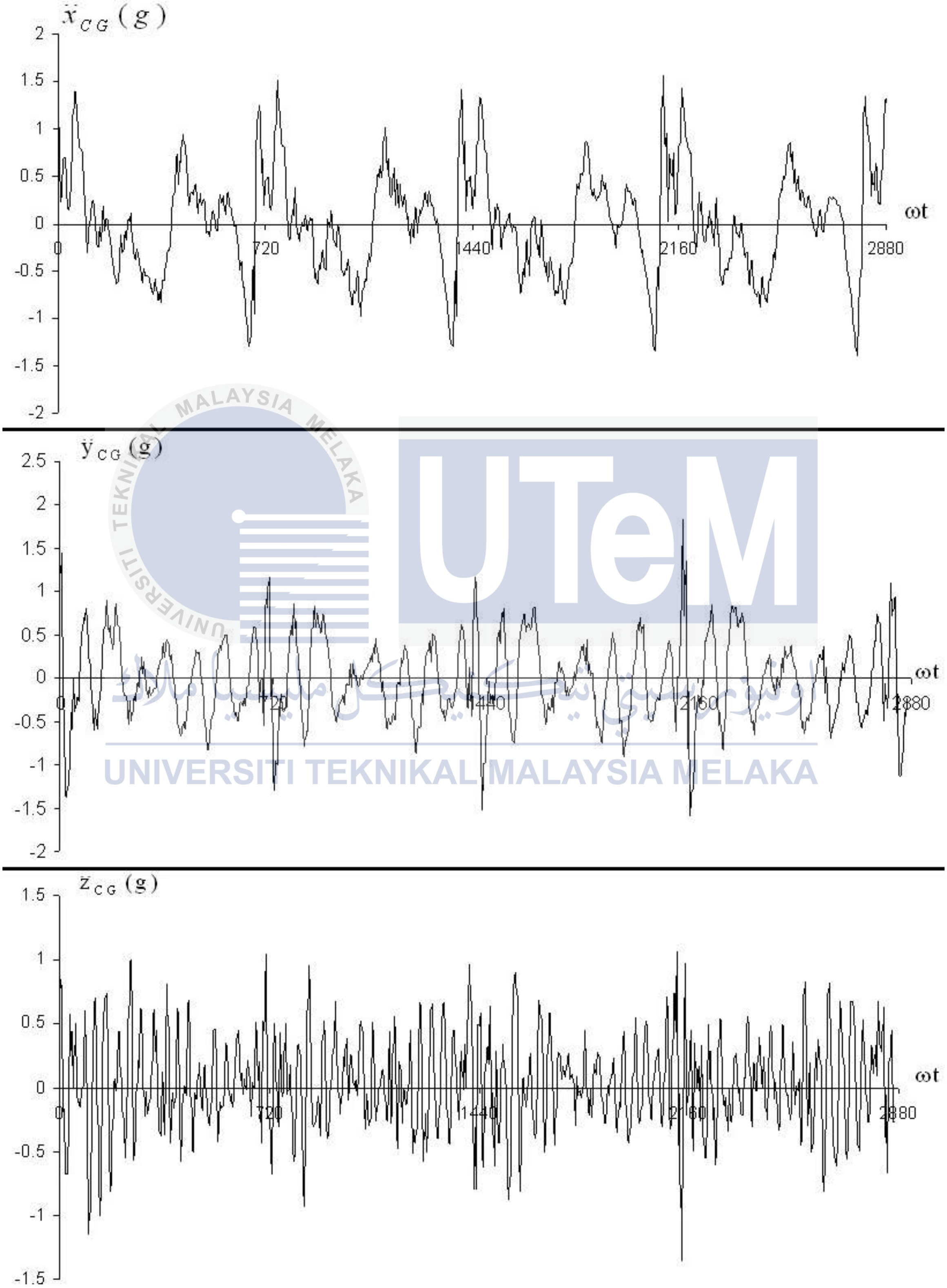

Figure 4.32: Benchmark

The information of the benchmark graph is extracted and tabulated in the Table 4.7 below.

Table 4.7: Benchmark Graph Information

Vibration In X-direction	-1.5g to 1.5g
Vibration In Y-direction	-1.5g to 1.5g
Vibration In Z-direction	-1.5g to 1.0g

4.10.1 Vibration Analysis In Rear Part Of The Chassis For Free Gear And First Gear

Based on the graphs for point 1, point 2, point 3 and point 4 from part 4.8 which located at the rear part of the chassis, the range of the vibrations of both free gear and first gear are stated in the Table 4.8, Table 4.9, Table 4.10 and Table 4.11 respectively.

Table 4.8: Vibration At Point 1

	Point 1 (Free Gear)	Point 1 (First Gear)
Vibration In X-direction	-0.2g to 0.8g	-0.3g to 0.6g
Vibration In Y-direction	-0.3g to 0.8g	-0.4g to 0.9g
Vibration In Z-direction	-0.5g to 0.8g	0.3g to 1.0g

Table 4.9: Vibration At Point 2

	Point 2 (Free Gear)	Point 2 (First Gear)
Vibration In X-direction	-0.2g to 0.2g	-0.2g to 0.2g
Vibration In Y-direction	-0.4g to 0.6g	-0.4g to 0.6g
Vibration In Z-direction	0.8g to 1.0g	0.8g to 1.0g

Table 4.10: Vibration At Point 3

	Point 3 (Free Gear)	Point 3 (First Gear)
Vibration In X-direction	0.0g to 0.7g	0.0g to 0.4g
Vibration In Y-direction	-0.4g to 0.8g	-0.4g to 0.8g
Vibration In Z-direction	0.4g to 1.0g	0.6g to 1.0g

Table 4.11: Vibration At Point 4

	Point 4 (Free Gear)	Point 4 (First Gear)
Vibration In X-direction	-0.2g to 0.3g	-0.1g to 0.2g
Vibration In Y-direction	-0.5g to 0.6g	-0.6g to 0.8g
Vibration In Z-direction	0.8g to 1.0g	0.6g to 1.0g

Based on the Table 4.8, Table 4.9, Table 4.10 and Table 4.11 above, The analysis of the points are as follows. During free gear at point 1, the vibration at X-direction has the range of -0.2g to 0.8g and the vibration at Y-direction has the range of -0.3g to 0.8g while the vibration at Z-direction has the range of -0.5g to 0.8g. From the data obtained in the experiment during the engine is in free gear, the vibration from at the Z-direction has the greater magnitude compared to X-direction and Y-direction. During first gear at point 1, the vibration at X-direction has the range of -0.3g to 0.6g and the vibration at Y-direction has the range of -0.4g to 0.9g while the vibration at the Z-direction has the range of 0.3g to 1.0g. From the data obtained in the experiment during the engine is in first gear, the data shown a similar trend as in free gear where the vibration at Z-direction has the greatest magnitude among the other axes.

During free gear at point 2, the vibration at X-direction has the range of -0.2g to 0.2g and the vibration at Y-direction has the range of -0.4g to 0.6g while the vibration at Z-direction has the range of 0.8g to 1.0g. From the data obtained in the experiment during the engine is in free gear, the vibration from at the Z-direction has the greater magnitude followed by Y-direction and X-direction. During first gear at point 2, the vibration at X-direction has the range of -0.2g to 0.2g and the vibration at Y-direction has the range of -0.4g to 0.6g while the vibration at the Z-direction has the range of 0.8g to 1.0g. From the data obtained in the experiment during the engine is in first gear, the data shown a similar trend as in free gear where the vibration at Z-direction has the greatest magnitude among the other axes.

During free gear at point 3, the vibration at X-direction has the range of 0.0g to 0.7g and the vibration at Y-direction has the range of -0.4g to 0.8g while the vibration at Z-direction has the range of 0.4g to 1.0g. From the data obtained in the experiment during the engine is in free gear, the vibration from at the Z-direction has the greater magnitude followed by Y-direction and X-direction. During first gear at point 3, the vibration at X-direction has the range of 0.0g to 0.4g and the vibration at Y-direction has the range of -0.4g to 0.8g while the vibration at the Z-direction has the range of 0.6g to 1.0g. From the data obtained in the experiment during the engine is in first gear, the data shown a similar trend as in free gear where the vibration at Z-direction has the greatest magnitude among the other axes.

During free gear at point 4, the vibration at X-direction has the range of -0.2g to 0.3g and the vibration at Y-direction has the range of -0.5g to 0.6g while the vibration at Z-direction has the range of 0.8g to 1.0g. From the data obtained in the experiment during the engine is in free gear, the vibration from at the Z-direction has the greater magnitude compared to X-direction and Y-direction. During first gear at point 4, the vibration at X-direction has the range of -0.1g to 0.2g and the vibration at Y-direction has the range of -0.6g to 0.8g while the vibration at the Z-direction has the range of 0.6g to 1.0g. From the data obtained in the experiment during the engine is in first gear, the data shown a similar trend as in free gear where the vibration at Z-direction has the greatest magnitude among the other axes.

After obtaining the vibration at each point both from free gear and first gear, the average vibrations for the rear part of the chassis are calculated and tabulated. The average vibration is shown is Table 4.12 below.

Table 4.12: Vibration At Rear Part

	Rear Part (Free Gear)	Rear Part (First Gear)
Vibration In X-direction	-0.2g to 0.5g	-0.2g to 0.4g
Vibration In Y-direction	-0.4g to 0.7g	-0.4g to 0.8g
Vibration In Z-direction	0.4g to 1.0g	0.5g to 1.0g

Based on the tabulated data in Table 4.12, the average vibration of the rear part of the chassis is as follows. The vibration in the X-direction during free gear has the range of -0.2g to 0.5g and the vibration in the Y-direction during free gear has the range of -0.4g to 0.7g. Then the vibration during free gear in the Z-direction is between 0.4g and 1.0g. Furthermore, the vibration in the X-direction during first gear has the range of -0.2g to 0.4g and the vibration in the Y-direction during first gear has the range of -0.4g to 0.8g. Then the vibration during first gear in the Z-direction is between 0.5g and 1.0g. From the Table

4.12 shown, the amplitude of vibrations are almost similar for both free gear and first gear. Besides that, the data also has shown the similar trend of having the highest magnitude of vibration at the Z-direction and lowest magnitude of vibration at the X-direction. Moreover, the highest fluctuation happened along the Y-direction. Compared with the benchmark graph and graph information shown in Figure 4.32 and Table 4.7 respectively, the vibrations at all axes in the rear part of the chassis has the similar pattern as the benchmark graph and the magnitude of vibrations are lesser than the benchmark value. However, the value obtained from the experiment should be lesser than the benchmark value because the benchmark magnitude of vibration obtained is from a 550cc engine while the vibration for this project experiment is obtained from a 80cc engine.

4.10.2 Vibration Analysis In Middle Part Of The Chassis For Free Gear And First Gear

Based on the graphs for point 5, point 6, point 7 and point 8 from part 4.8 which located at the middle part of the chassis, the range of the vibrations of both free gear and first gear are stated in the Table 4.13, Table 4.14, Table 4.15 and Table 4.16 respectively.

Table 4.13: Vibration At Point 5

	Point 5 (Free Gear)	Point 5 (First Gear)
Vibration In X-direction	-0.5g to 0.3g	0.0g to 0.7g
Vibration In Y-direction	-0.2g to 0.2g	-0.4g to 0.2g
Vibration In Z-direction	-0.3g to 0.7g	0.7g to 1.0g

Table 4.14: Vibration At Point 6

	Point 6 (Free Gear)	Point 6 (First Gear)
Vibration In X-direction	-0.4g to 0.7g	-0.6g to 0.5g
Vibration In Y-direction	-0.4g to 0.7g	-0.6g to 0.0g
Vibration In Z-direction	0.4g to 1.0g	0.6g to 1.0g

Table 4.15: Vibration At Point 7

	Point 7 (Free Gear)	Point 7 (First Gear)
Vibration In X-direction	-0.2g to 0.2g	-0.2g to 0.1g
Vibration In Y-direction	-0.3g to 0.5g	-0.2g to 0.6g
Vibration In Z-direction	0.6g to 0.9g	0.8g to 1.0g

Table 4.16: Vibration At Point 8

	Point 8 (Free Gear)	Point 8 (First Gear)
Vibration In X-direction	-0.6g to 0.2g	-0.1g to 0.7g
Vibration In Y-direction	-0.6g to 0.6g	-0.6g to 0.1g
Vibration In Z-direction	-0.6g to 1.0g	0.5g to 0.9g

Based on the Table 4.13, Table 4.14, Table 4.15 and Table 4.16 above, The analysis of the points are as follows. During free gear at point 5, the vibration at X-direction has the range of -0.5g to 0.3g and the vibration at Y-direction has the range of -0.2g to 0.2g while the vibration at Z-direction has the range of -0.3g to 0.7g. From the data obtained in the experiment during the engine is in free gear, the vibration from at the Z-direction has the greater magnitude compared to X-direction and Y-direction. During first gear at point 5, the vibration at X-direction has the range of 0.0g to 0.7g and the vibration at Y-direction has the range of -0.4g to 0.2g while the vibration at the Z-direction has the range of 0.7g to 1.0g. From the data obtained in the experiment during the engine is in first gear, the data shown a similar trend as in free gear where the vibration at Z-direction has the greatest magnitude among the other axes.

During free gear at point 6, the vibration at X-direction has the range of -0.4g to 0.7g and the vibration at Y-direction has the range of -0.4 g to 0.7g while the vibration at Z-direction has the range of 0.4g to 1.0g. From the data obtained in the experiment during the engine is in free gear, the vibration from at the Z-direction has the greater magnitude followed by X-direction and Y-direction. During first gear at point 6, the vibration at X-direction has the range of -0.6g to 0.5g and the vibration at Y-direction has the range of -0.6g to 0.0g while the vibration at the Z-direction has the range of 0.6g to 1.0g. From the data obtained in the experiment during the engine is in first gear, the data shown a similar trend as in free gear where the vibration at Z-direction has the greatest magnitude among the other axes and has the similar pattern as during free gear where the vibration at X-axis is greater than the vibration in Y-direction but smaller than the vibration is Z-direction.

During free gear at point 7, the vibration at X-direction has the range of -0.2g to 0.2g and the vibration at Y-direction has the range of -0.3g to 0.5g while the vibration at Z-direction has the range of 0.6g to 0.9g. From the data obtained in the experiment during the engine is in free gear, the vibration from at the Z-direction has the greater magnitude followed by Y-direction and X-direction. During first gear at point 7, the vibration at X-direction has the range of -0.2g to 0.1g and the vibration at Y-direction has the range of -0.2g to 0.6g while the vibration at the Z-direction has the range of 0.8g to 1.0g. From the data obtained in the experiment during the engine is in first gear, the data shown a similar trend as in free gear where the vibration at Z-direction has the greatest magnitude among the other axes.

During free gear at point 8, the vibration at X-direction has the range of -0.6g to 0.2g and the vibration at Y-direction has the range of -0.6g to 0.6g while the vibration at Z-direction has the range of -0.6g to 1.0g. From the data obtained in the experiment during the engine is in free gear, the vibration from at the Z-direction has the greater magnitude compared to X-direction and Y-direction. During first gear at point 8, the vibration at X-direction has the range of -0.1g to 0.7g and the vibration at Y-direction has the range of -0.6g to 0.1g while the vibration at the Z-direction has the range of 0.5g to 0.9g. From the data obtained in the experiment during the engine is in first gear, the data shown a similar trend as in free gear where the vibration at Z-direction has the greatest magnitude among the other axes. However, the sudden declination appeared in the graph shown in Figure 4.27 (b) is expected to be caused by the incomplete combustion of the engine and causing choking to the engine. Hence, the magnitude of the minimum value of the vibration during free gear at all the 3 axes should be different from the data obtained.

After obtaining the vibration at each point both from free gear and first gear, the average vibrations for the middle part of the chassis are calculated and tabulated. The average vibration is shown is Table 4.17 below.

Table 4.17: Vibration At Middle Part

	Middle Part (Free Gear)	Middle Part (First Gear)
Vibration In X-direction	-0.4g to 0.3g	-0.2g to 0.5g
Vibration In Y-direction	-0.4g to 0.5g	-0.4g to 0.3g
Vibration In Z-direction	0.0g to 0.9g	0.7g to 1.0g

Based on the tabulated data in Table 4.17, the average vibration of the middle part of the chassis is as follows. The vibration in the X-direction during free gear has the range of -0.4g to 0.3g and the vibration in the Y-direction during free gear has the range of -0.4g to 0.5g. Then the vibration during free gear in the Z-direction is between 0.0g and 0.9g. Furthermore, the vibration in the X-direction during first gear has the range of -0.2g to 0.5g and the vibration in the Y-direction during first gear has the range of -0.4g to 0.3g. Then the vibration during first gear in the Z-direction is between 0.7g and 1.0g. From the Table 4.17 shown, the amplitude of vibrations are almost similar for both free gear and first gear in the X-direction and Y-direction. However in Z-direction, the vibration during free gear has the wider range than during first gear. Besides that, the data also has shown the similar trend of having the highest magnitude of vibration at the Z-direction and lowest magnitude of vibration at the X-direction. Moreover, the fluctuation happened is consistent except in the Z-direction during first gear where the data only fluctuated between 0.7g and 1.0g. Compared with the benchmark graph and graph information shown in Figure 4.32 and Table 4.7 respectively, the vibrations at all axes in the middle part of the chassis has the similar pattern as the benchmark graph and the magnitude of vibrations are lesser than the benchmark value. However, the value obtained from the experiment should be lesser than the benchmark value because the benchmark magnitude of vibration obtained is from a 550cc engine while the vibration for this project experiment is obtained from a 80cc engine.

4.10.3 Vibration Analysis In Front Part Of The Chassis For Free Gear And First Gear

Based on the graphs for point 9, point 10, point 11 and point 12 from part 4.8 which located at the front part of the chassis, the range of the vibrations of both free gear and first gear are stated in the Table 4.18, Table 4.19, Table 4.20 and Table 4.21 respectively.

Table 4.18: Vibration At Point 9

	Point 9 (Free Gear)	Point 9 (First Gear)
Vibration In X-direction	-0.2g to 0.4g	-0.1g to 0.2g
Vibration In Y-direction	-0.8g to 0.6g	-0.8g to 0.6g
Vibration In Z-direction	0.6g to 1.0g	0.6g to 1.0g

Table 4.19: Vibration At Point 10

	Point 10 (Free Gear)	Point 10 (First Gear)
Vibration In X-direction	0.0g to 0.3g	-0.2g to 0.2g
Vibration In Y-direction	-0.2g to 0.3g	-0.8g to 0.8g
Vibration In Z-direction	0.5g to 0.8g	0.6g to 1.0g

Table 4.20: Vibration At Point 11

	Point 11 (Free Gear)	Point 11 (First Gear)
Vibration In X-direction	-0.1g to 0.3g	-0.2g to 0.2g
Vibration In Y-direction	-0.2g to 0.4g	-0.9g to 0.5g
Vibration In Z-direction	0.0g to 0.6g	0.5g to 1.0g

Table 4.21: Vibration At Point 12

	Point 12 (Free Gear)	Point 12 (First Gear)
Vibration In X-direction	-0.2g to 0.2g	-0.2g to 0.0g
Vibration In Y-direction	-0.4g to 0.5g	-0.7g to 0.2g
Vibration In Z-direction	0.4g to 0.8g	0.6g to 1.0g

Based on the Table 4.18, Table 4.19, Table 4.20 and Table 4.21 above, The analysis of the points are as follows. During free gear at point 9, the vibration at X-direction has the range of -0.2g to 0.4g and the vibration at Y-direction has the range of -0.8g to 0.6g while the vibration at Z-direction has the range of 0.6g to 1.0g. From the data obtained in the experiment during the engine is in free gear, the vibration from at the Z-direction has the greater magnitude compared to X-direction and Y-direction. During first gear at point 9, the vibration at X-direction has the range of -0.1g to 0.2g and the vibration at Y-direction has the range of -0.8g to 0.6g while the vibration at the Z-direction has the range of 0.6g to 1.0g. From the data obtained in the experiment during the engine is in first gear, the data shown a similar trend as in free gear where the vibration at Z-direction has the greatest magnitude among the other axes.

During free gear at point 10, the vibration at X-direction has the range of 0.0g to 0.3g and the vibration at Y-direction has the range of -0.2g to 0.3g while the vibration at Z-direction has the range of 0.5g to 0.8g. From the data obtained in the experiment during the engine is in free gear, the vibration from at the Z-direction has the greater magnitude followed by Y-direction and X-direction. During first gear at point 10, the vibration at X-direction has the range of -0.2g to 0.2g and the vibration at Y-direction has the range of -0.8g to 0.8g while the vibration at the Z-direction has the range of 0.6g to 1.0g. From the data obtained in the experiment during the engine is in first gear, the data shown a similar trend as in free gear where the vibration at Z-direction has the greatest magnitude among the other axes. However in the graph shown in Figure 4.29 (d), the sudden increment of the vibration during first gear is believed to be caused by the incomplete combustion of fuel and caused choking to the engine. Hence, the magnitude of the maximum vibration along Y-direction during first gear should be in the range of 0.0g to 0.5g.

During free gear at point 11, the vibration at X-direction has the range of -0.1g to 0.3g and the vibration at Y-direction has the range of -0.2g to 0.4g while the vibration at Z-direction has the range of 0.0g to 0.6g. From the data obtained in the experiment during the engine is in free gear, the vibration from at the Z-direction has the greater magnitude followed by Y-direction and X-direction. During first gear at point 11, the vibration at X-direction has the range of -0.2g to 0.2g and the vibration at Y-direction has the range of -0.9g to 0.5g while the vibration at the Z-direction has the range of 0.5g to 1.0g. From the data obtained in the experiment during the engine is in first gear, the data shown a similar trend as in free gear where the vibration at Z-direction has the greatest magnitude among the other axes.

During free gear at point 12, the vibration at X-direction has the range of -0.2g to 0.2g and the vibration at Y-direction has the range of -0.4g to 0.4g while the vibration at Z-direction has the range of 0.4g to 0.8g. From the data obtained in the experiment during the engine is in free gear, the vibration from at the Z-direction has the greater magnitude compared to X-direction and Y-direction. During first gear at point 12, the vibration at X-direction has the range of -0.2g to 0.0g and the vibration at Y-direction has the range of -

0.7g to 0.2g while the vibration at the Z-direction has the range of 0.6g to 1.0g. From the data obtained in the experiment during the engine is in first gear, the data shown a similar trend as in free gear where the vibration at Z-direction has the greatest magnitude among the other axes. Furthermore along Z-direction during first gear, the magnitude of vibration has the most at 1.0g showing that the magnitude of vibration at that particular point is high.

After obtaining the vibration at each point both from free gear and first gear, the average vibrations for the front part of the chassis are calculated and tabulated. The average vibration is shown is Table 4.22 below.

Table 4.22 Vibration At Front Part

	Front Part (Free Gear)	Front Part (First Gear)
Vibration In X-direction	-0.1g to 0.3g	-0.2g to 0.2g
Vibration In Y-direction	-0.4g to 0.5g	-0.8g to 0.6g
Vibration In Z-direction	0.3g to 0.8g	0.6g to 1.0g

Based on the tabulated data in Table 4.22, the average vibration of the front part of the chassis is as follows. The vibration in the X-direction during free gear has the range of -0.1g to 0.3g and the vibration in the Y-direction during free gear has the range of -0.4g to 0.5g. Then the vibration during free gear in the Z-direction is between 0.3g and 0.8g. Furthermore, the vibration in the X-direction during first gear has the range of -0.2g to 0.2g and the vibration in the Y-direction during first gear has the range of -0.8g to 0.6g. Then the vibration during first gear in the Z-direction is between 0.6g and 1.0g. From the Table 4.22 shown, the amplitude of vibrations are almost similar for both free gear and first gear in the direction of X while in direction of Y and Z, the magnitude of vibration during first gear is slightly greater than the magnitude of vibration during free gear. Besides that, the data also has shown the similar trend of having the highest magnitude of vibration at the Z-direction and lowest magnitude of vibration at the X-direction. Moreover, the highest fluctuation happened along the Y-direction. Compared with the benchmark graph and graph information shown in Figure 4.32 and Table 4.7 respectively, the vibrations at all axes in the rear part of the chassis has the similar pattern as the benchmark graph and the magnitude of vibrations are lesser than the benchmark value. However, the value obtained from the experiment should be lesser than the benchmark value because the benchmark magnitude of vibration obtained is from a 550cc engine while the vibration for this project experiment is obtained from a 80cc engine.

4.10.4 Discussion

By comparing the Table 4.12, Table 4.17 and Table 4.22 regarding the vibrations at each part of the chassis, there are several observations can be seen. First and foremost during the free gear and first gear, the vibrations along the X-direction have the similar trend where vibrations at the X-direction have the least in vibration magnitude compared to other 2 axes. For the vibration in Y-direction, greatest fluctuations can be seen from the data obtained. This can be happened due to the piston cylinder of the two strokes engine installed at the chassis is moving in the direction along Y-direction. Then for the vibration along Z-direction showed the highest magnitude of vibration. The highest magnitude of vibration is caused by the inlet and outlet of the fuel and exhaust are located along the Z-direction. During the combustion of fuel and the release of unwanted gas, pressure could be generated and the pressure generated are in the direction of Z. Therefore, the vibration in the Z-direction would be increased.

Secondly, the comparison of the 3 tables also can seen that the part having the greatest magnitude of vibration located at the rear part of the chassis where the engine located. The engine is the main source of vibration during the experiment testing process due to the whole chassis is jacked up and not moving. In this project, a Suzuki RC80 is used. Suzuki RC80 is a two stroke petrol engine of 80cc capacity with a single piston cylinder. The vibration caused by the engine is due to there is no counter moving piston available in the design of the engine. This has caused imbalance in force distribution during the crankshaft is rotating. Besides that, the moving of piston during combustion also caused reciprocating vibration. Furthermore, the engine installed at the chassis is not exactly at the centre of the chassis in X-direction due to the development of drivetrain of the chassis. The chain and sprocket of the drivetrain need to be at the middle of the chassis, therefore the engine need to be shifted.

By comparing the data obtained in this project with the data obtained by [18], the engine that [18] used was Kubota RT100DI diesel engine of 550cc capacity. The installed engine has the axis of rotation of the crankshaft similar to this project which was along X-axis and the piston moving in Y-direction. Based on the data shown in Table 4.7, compared with the data obtained in this project having the similar trend of vibrations. Although the experiment done by [18] was measuring the vibration at the engine and this project was measuring the vibration at the chassis, but the source of the vibrations are similar which is the engine. Besides that, the difference in capacity of the engine could only affect the magnitude of the vibration obtained by accelerometer due to the power generated by higher capacity engine is higher.

It is expected to obtain result that shows the vibrations of chassis during first gear are greater than the vibration during free gear since vehicles could have higher magnitude of vibration due to several factors such as the road condition and moving parts of the vehicles. However due to some development constraint that faced which is the incomplete of braking system by other team member, the vibration test during first gear can only be done during the go-kart in static condition and having only the rear wheels moving but not the whole go-kart in moving. Therefore, this can explained that the results obtained during free gear and first gear has almost the similar trend and magnitude of vibrations.

In conducting vibration test on the chassis, it is impossible to eliminate all the errors that has the potential to be appeared during the experiment. Error such as equipment error which is the IMU could has slight tolerance in the reading obtained. In order to reduce the error, the experiment is done twice at each point to obtain the average of value from two values and thus reduce the error of the IMU. Besides that, environmental factor is hard to avoid. In order to reduce the error, the fans in the laboratory are closed and a atmosphere with minimum air flow is created during the experiments are conducted. Furthermore, the data obtained by the accelerometer of IMU was having a lot of noise and makes analysis process of the data very difficult. In this case, the graphs plotted based on the data obtained in the experiments are filtered using MATLAB low pass Butterworth filter. The smoothing of graph using filter in MATLAB software could have eliminate the unwanted noise but it may also reduce the actual reading of the data. Therefore, this is the error that impossible to prevent during the analysis process.

4.11 Summary

In this chapter, the results from the static test and vibration test conducted are analyzed and discussed. Besides that, the fabricated chassis structure with all the combining parts to develop the Go-Kart are also been shown in this chapter. The analysis and discussion of the static test involve the Von Mises stress, resultant displacement and also the equivalent strain while the analysis and discussion of the vibration test using IMU involve the vibration experienced by the chassis during engine in free gear and first gear. The discussion about the result obtained from the static test and vibration test are explained in this chapter.

CHAPTER 5

CONCLUSION AND RECOMMENDATIONS

5.1 Introduction

In previous chapter discussed about the result obtained during conducted experiments which is the static test using Solidworks software and the vibration test using IMU. The results obtained is analyzed and discussed in previous chapter. In this chapter, explanation about the conclusion obtained from the experiment done on the chassis is included. Besides that, the summary of entire work from final year project one is also explained in this chapter. Lastly, the recommendation of the future work to be done is also explained in this chapter.

5.2 Conclusion

During the final year project one, the three dimensional chassis frame structure combining with parts based on the requirements from Formula UniMAP 2013 and Shell Eco-Marathon competitions are designed using Solidworks software. The chassis structure selected is the space frame type chassis. Static test is also performed on the chassis design using the simulation function in the Solidworks software. Then, the basic chassis frame structure is fabricated using the materials selected which is the 25mm x 25mm square mild steel tube with the thickness of 1.6mm.

The static test conducted using simulation function in Solidwork software determines the Von Mises stress, resultant displacement and equivalent strain experienced by the chassis frame structure. In the static test, the finest available mesh is chosen in order to increase the accuracy of the result obtained. Then, the result obtained are analyzed and discussed. Based on the result obtained from the static test, the factor of safety (FOS) of the chassis frame structure has the minimum value of 3 at most of the parts, calculated based on the Von Mises Stress contour. However, there are also location where the factor of safety (FOS) is less than 2 which located at the joint of the chassis frame structure. Therefore, improvement has to be made on the structure to increase the factor of safety value. While for the resultant displacement result, it can clearly seen that at the middle part of the chassis experienced the most significant displacement which is approximately 2mm compared to the front part and the rear part of the chassis frame. Furthermore, the equivalent strain experienced by the chassis frame structure has the same characteristics as the Von Mises stress contour where the highest strain is concentrated at the joint of the chassis frame. The value of the strain determine and directly affect the displacement of the chassis frame structure.

The vibration test is conducted physically using Inertial Measurement Unit (IMU) to determine the vibration in acceleration experienced by the chassis body. In the vibration test, 12 points which consist of 4 points for each front part, middle part and rear part of the chassis are tested. The vibration test is done twice for both condition where the engine is in free gear condition and first gear condition. The data obtained from the test is transferred to Microsoft Excel software to calculate the average before the data is transferred to MATLAB software to perform graph plotting. Butterworth low pass filter is used in MATLAB software in order to smooth the graph and ease the analysis process. The graph for all the points are analyzed and discussed. Based on the results obtained, the rear part of the chassis where the engine is located had the greatest magnitude of vibration compared with the middle part and front part of the chassis. Besides that, the results obtained from free gear condition and first gear condition had almost similar trend of vibration as well as magnitude of vibration due to several constraints that has been discussed in the discussion part. Based on the data obtained and benchmarked with the data from [18], the vibration from the experiments done have the similar characteristics.

As a conclusion, the chassis frame developed based on the simulation result obtained from Solidworks software could probably withstand the applied load on the chassis. Although the vibration experienced by the chassis is around -1g and 1g, but it can be considered that the vibration is still acceptable due to the chassis structure can be improved by installing the bushings that act as a damping to the vibration. However, the chassis structure has to be further improved to increase the performance as well as the safety of the chassis.

5.3 Recommendation

In this final year project, the chassis structure can be analyzed and modified further in order to obtain a better and stronger chassis with low Von Mises stress concentration and low strain concentration. By having low stress and strain concentration, the displacement of the chassis structure can also be reduced. For the vibration experienced on the chassis, bushings can be added to the engine mounting part in order to act as a damping that produce damping effect to the vibration.

5.4 Summary

In this chapter, the summary of work done in final year project is explained and the conclusion drawn from the results obtained during final year project is also included. Furthermore, the future works that could to be done is also been explained briefly in this chapter.

REFERENCES

[1] S.Chignola, M.Gadola, L.Leoni and M.Resentera, On The Design Of A Low Cost Racing Car Chassis. International Design Conference - Design 2002, pp. 1035-1040, 2002

[2] J.Hirsch, Aluminium In Innovative Light-Weight Car Design. Material Transactions, vol.2, No. 5, pp. 818-824, 2011.

[3] J.Reimpell, H.Stoll and J.W. Betzler, The Automotive Chassis: Engineering Principles: Chassis And Vehicle Overall, Wheel Suspensions And Types Of Drive Axle Kinematics And Elastokinematics, Steering, Springing, Tyres Construction And Calculation Advice, 2nd ed..USA: Butterworth-Heinemann, 2001.

[4] S.Y.Pang, X.Guan, J.Zhan, Research Of Chassis Torsional Stiffness On Vehicle Handling Performance. 2010 WASE International Conference On Information Engineering, pp. 253-255, 2010.

[5] R.Rajappan and M.Vivekanandhan, Static And Modal Analysis Of Chassis By Using FEA. The International Journal Of Engineering (IJES), vol. 2: Issue 2, pp.63-73, 2013.

[6] Y.S.Rajput, V.Sharma, S.Sharma and G.Saxena, A Vibration Analysis Of Vehicle Frame. International Journals Of Engineering Research And Application (IJERA), vol. 3: Issue 2, pp. 348-350, 2013.

[7] G.Solasa, N.SD Saradeep, T.R.K.Prasad, G.S.Babu, Modal Analysis Of Chassis. International Journal Of Engineering And Advanced Technology (IJEAT), vol. 2: Issue 4, pp. 789-795, 2013

[8] W.L.Wang, S.Y.Cheng, M.J.Luo, Experimental Modal Test For Structure Refinement Of An Automotive Chassis. 2010 International Conference On Measuring Technology And Mechatronics Automation, 2010.

[9] M.S.M.Sani, M.T.Arbain, M.M.Noor, G.L.Ming, M.H.Zohari, C.K.E Nizwan, T.T.Mon, Stress Analysis And Modal Transient Response Of Car Chassis. International Conference On Advanced Mechanical Engineering (ICAME09), 2009.

[10] V.V.Patel and R.I.Patel, Structural Analysis Of A Ladder Chassis Frame. World Journal Of Science And Technology 2012, vol. 2, Issue 4, pp. 5-9, 2012.

[11] H.C.Davies, M.Bryant, M.Hopeand C. Meiller, Design, Development, And Manufacture Of An Aluminium Honeycomb Sandwich Panel Monocoque Chassis For Formula Student Competition. Journal Of Automobile Engineering 2012, [online]. Available at: http://pid.sagepub.com/content/226/3/325(SAGE) [Accessed: 23 September 2013]

[12] M.A.Abdullah, M.R.Mansor, M.M.Tahir, S.I.A.Kudus, M.Z.Hassan, M.N.Ngadiman, Design, Analysis And Fabrication Of Chassis Frame For UTeM Formula Varsity Race Car. International Journal Of Mining, Metallurgy, Mechanical Engineering (IJMMME) vol. 1, Issue 1, pp. 75-77, 2013.

[13] Formula UniMAP 2013, Part 3: Technical Requirements, 2013

[14] Shell Eco-Marathon, Official Rules 2013, Chapter 1, 2013

[15] IMU 5 Degrees Of Freedom. Cytron Technologies. [online]. Available at: http://www.cytron.com.my/viewProduct.php?pcode=SN-IMU5 [Accessed: 10 May 2014]

[16] Signal Processing Toolbox-Analog and Digital Filters-Analog Filters-Butterworth Filters Design. [online]. Available at: http://www.mathworks.com/help/signal/ref/butter.html [Accessed: 15 May 2014]

[17] C.Thomas, B.Sarah. Accelerometer Based Localization For Distributed Off-The-Shelf Robot(Cots-Bots), 2001.

[18] B.Wongchai, P.Visuwan, S Chuepeng, The Vibration Analysis Of Diesel Engine With Hydrogen-Diesel Duel Fuel. American Journal of Applied Sciences, 10 (1): pp8-14, 2013.

APPENDIX I

```
#define INPUT_COUNT 5     //number of analog inputs
#define VDD 5000.0f       //Analog reference voltage in milivolts
#define PI 3.14159265358979f
int an[INPUT_COUNT];      //analog inputs
char firstSample;         //marks first sample
struct {
 char inpInvert[INPUT_COUNT];    // bits 0..5 invert input
 int zeroLevel[INPUT_COUNT];     // 0..2 accelerometer zero level (mV) @ 0 G
 int inpSens[INPUT_COUNT];       // 0..2 acceleromter input sensitivity (mv/g)
 float wGyro;                    // gyro weight/smooting factor
} config;
unsigned long interval; //interval since previous analog samples
float RwAcc[3];         //projection of normalized gravitation force vector on x/y/z axis, as
measured by accelerometer
void setup() {
  static int i;
  Serial.begin(9600);
  //Setup parameters for Acc_Gyro board, see http://www.gadgetgangster.com/213
  for(i=0;i<=2;i++){                  // X,Y,Z axis
    config.zeroLevel[i] = 1650;       // Accelerometer zero level (mV) @ 0 G
    config.inpSens[i] = 500;          // Accelerometer Sensisitivity mV/g
  }

  for(i=3;i<=4;i++){
    config.inpSens[i] = 2000;         // Gyro Sensitivity mV/deg/ms
    config.zeroLevel[i] = 1230;       // Gyro Zero Level (mV) @ 0 deg/s
  }}
void loop() {
  getEstimatedInclination();
```

```
  Serial.print(RwAcc[0]);  //Inclination X axis (as measured by accelerometer)
  Serial.print(",");
  Serial.print(RwAcc[1]);  //Inclination Y axis (as measured by accelerometer)
  Serial.print(",");
  Serial.print(RwAcc[2]);  //Inclination Z axis (as measured by accelerometer)
  Serial.println("");
}
void getEstimatedInclination(){
  static int i,w;
  static float tmpf,tmpf2;
  static unsigned long newMicros; //new timestamp
  static char signRzGyro;
  //get raw adc readings
  newMicros = micros();       //save the time when sample is taken
  for(i=0;i<INPUT_COUNT;i++) an[i]= analogRead(i);
 interval = newMicros - lastMicros;    //please note that overflows are ok, since for example
0x0001 - 0x00FE will be equal to 2
  lastMicros = newMicros;              //save for next loop, please note interval will be invalid
in first sample but we don't use it
  //get accelerometer readings in g, gives us RwAcc vector
  for(w=0;w<=2;w++) RwAcc[w] = getInput(w);
  //normalize vector (convert to a vector with same direction and with length 1)
  normalize3DVector(RwAcc);
  if (firstSample){
    for(w=0;w<=2;w++) RwEst[w] = RwAcc[w];    //initialize with accelerometer readings
  }else{
    //evaluate RwGyro vector
    if(abs(RwEst[2]) < 0.1){
      //Rz is too small and because it is used as reference for computing Axz, Ayz it's error
fluctuations will amplify leading to bad results
      //in this case skip the gyro data and just use previous estimate
      for(w=0;w<=2;w++) RwGyro[w] = RwEst[w];
    }else{
      for(w=0;w<=1;w++){
```

```
      tmpf = getInput(3 + w);                    //get current gyro rate in deg/ms
      tmpf *= interval / 1000.0f;                //get angle change in deg
      Awz[w] = atan2(RwEst[w],RwEst[2]) * 180 / PI;   //get angle and convert to degrees
      Awz[w] += tmpf;                             //get updated angle according to gyro movement
     }

        signRzGyro = ( cos(Awz[0] * PI / 180) >=0 ) ? 1 : -1;
     for(w=0;w<=1;w++){
      RwGyro[w] = sin(Awz[w] * PI / 180);
      RwGyro[w] /= sqrt( 1 + squared(cos(Awz[w] * PI / 180)) * squared(tan(Awz[1-w] * PI / 180)) );  }
     RwGyro[2] = signRzGyro * sqrt(1 - squared(RwGyro[0]) - squared(RwGyro[1])); }
      for(w=0;w<=2;w++) RwEst[w] = (RwAcc[w] + config.wGyro* RwGyro[w]) / (1 + config.wGyro);
    normalize3DVector(RwEst); }
  firstSample = 0;}
void normalize3DVector(float* vector)
{
  static float R;
  R = sqrt(vector[0]*vector[0] + vector[1]*vector[1] + vector[2]*vector[2]);
  vector[0] /= R; vector[1] /= R; vector[2] /= R;
}
float squared(float x)
{
  return x*x;
}
float getInput(char i){
  static float tmpf;              //temporary variable
  tmpf = an[i] * VDD / 1023.0f;  //voltage (mV)
  tmpf -= config.zeroLevel[i];  //voltage relative to zero level (mV)
  tmpf /= config.inpSens[i];    //input sensitivity in mV/G(acc) or mV/deg/ms(gyro)
  tmpf *= config.inpInvert[i];  //invert axis value according to configuration
  return tmpf;}
```